Three-dimensional Librational Dynamics and Control of Multi-body Tethered Satellite Systems

by

Nasrollah Monshi

Department of Mechanical Engineering
McGill University
Montreal, Canada

Thesis submitted to the Faculty of Graduate Studies and Research
in partial fulfillment of the requirements for the degree of
Master of Engineering

shortened version of the thesis title:

3D Librational Dyn. & Control of Multi-body Tethered Satellite Systems

to my beloved parents,

Badri Nabati and Abolghasem Monshi

Abstract

This thesis concentrates on studying the three-dimensional dynamics and control of librational motion in the large for multi-body tethered satellite systems. Easy to-implement, reel rate control laws have been chosen for controlling the retrieval phase, the critical phase of the motion. The study is based on both numerical and analytical approaches.

The Lagrangian approach is used to develop the equations of motion. In this work, the vibrational motions of the tethers are ignored and the tethers are considered massless. The tethered bodies are modelled as point masses. Since the principles are the same for two-body and multi-body systems, for the sake of simplicity, the analysis starts with two-body systems and is subsequently extended to multi-body systems. The method of formulation makes this extension quite easy. The set of second order nonlinear coupled equations is solved using the Bulirsch-Stoer extrapolation method from $IMSL$ libraries.

The first analytical method that is used for the development of reel rate laws is the Liapunov's second method. In this work it is shown that the Hamiltonian can be used as a Liapunov function. A reel rate law is devised that stabilizes the in-plane and out-of-plane librations at the same time, for two body systems. However, since the resulting motion has some deficiencies, this reel rate law is not extended to multi-body systems.

For overcoming these deficiencies, two new reel rate laws are proposed and their performances are examined through the energy dissipation approach together with the averaging method. The resulting motions with all the reel rate laws, including the one from Liapunov approach, are limit cycle oscillations. The reel rate laws obtained from the energy dissipation approach perform efficient retrievals with sufficiently small out-of-plane limit cycle amplitudes. These reel rate laws are extended to multi-body systems and lead to acceptable results. For multi-body systems a station-keeping stage is added that brings the system to a final desired configuration. An analysis on the effects of different parameters and gains on the resulting motion has also been performed. Hence, one has the general information for selecting the gains to obtain a desired motion

Sommaire

Dans cette thèse, nous nous intéressons à la dynamique tridimensionnelle des mouvements de grandes amplitudes et au contrôle de systèmes à satellite composés de plusieurs éléments reliés par des fils. Des lois de contrôle par taux de déroulement des fils –Facile à implanter– sont proposées, afin de contrôler l'étape de récupération qui correspond à la phase critique. L'étude est basée sur une approche numérique et analytique.

L'approche Lagrangienne est utilisée pour dériver les équations du mouvement. Dans cette étude, les mouvements vibratoires des fils, considérés sans masse, ne sont pas pris en compte. De plus, les mouvements de corps rigides des éléments sont négligés. Puisque les principes sont les mêmes dans les deux cas, dans un but de simplification, l'analyse est appliquée tout d'abord à des systèmes à deux éléments puis étendue ensuite à des systèmes à plusieurs éléments. La formulation de la méthode permet facilement cette extension. Le système de second ordre d'équations nonlinéaires couplées est résolu en utilisant la méthode d'extrapolation de type Bulirsch-Stoer que l'on trouve parmi les sous-programmes IMSL.

La première méthode analytique utilisée pour développer les lois du taux de déroulement est la seconde méthode de Liapunov. Cette méthode est particulièrement intéressante puisqu'elle s'applique dans le cas de mouvements larges, bien qu'il soit d'ordinaire difficile de construire une telle fonction de Liapunov. Ici, on démontre que la fonction d'Hamilton peut être utilisée comme fonction de Liapunov. Une loi du taux de déroulement a été déterminée, stabilisant à la fois les mouvements dans le plan et hors-plan, dans le cas de systèmes à deux éléments. Mais, puisque le mouvement résultant exigeait des améliorations, cette loi n'a pas été étendue aux cas de systèmes à plusieurs éléments.

Pour surmonter les problèmes sus-mentionnés, deux nouvelles lois du taux de déroulement sont proposées et leurs performances examinées par une approche de dissipation d'énergie et une méthode de type KB (Krylov-Bogoliubov). Pour toutes les lois, incluant celle obtenue par l'approche de Liapunov, les mouvements résultants ont été des oscillations de type cycle limite. Les lois du taux de déroulement obtenue par l'approche de dissipation d'énergie engendrent des récupérations efficaces avec des amplitudes de cycle limite hors-plan suffisamment petites. Elles ont été appliquées aux systèmes à plusieurs éléments et conduisent à des résultats acceptables. Dans ce dernier cas, une étape supplémentaire ("station-keeping stage") est ajoutée qui permet de placer le système dans la configuration finale désirée. Une analyse des effets des différents paramètres et des gains sur les mouvements résultants a également été effectuée. Des informations générales permettant de sélectionner les valeurs des gains pour obtenir un certain mouvement est ainsi mise à la disposition du lecteur.

Acknowledgements

I would like to express my sincere gratitude to Prof. A.K. Misra for his constant guidance, encouragement, kindness, and caring throughout the course of this research. His precise and critical reviews, patience and financial support during the period of writing this dissertation are gratefully appreciated.

I would like to thank Dr.Vinhson B. Nguyen for his great help in familiarizing me with the document preparation software, Latex, and his genuine offering of all the necessary files in this respect. His careful proofreading of some parts of this thesis is also appreciated. I am also grateful to Christian Semler for translating the abstract of this thesis. His efforts for finding French equivalents for specialized technical terms used in this work are highly regarded.

All the staff of the Department of Mechanical Engineering have made my stay at McGill a pleasant one. Among them I would like to make special mention of Ms. Helga Symington and Prof. B.R. Baliga. Besides his kindness and caring, I would like to thank Prof. Baliga for use of some of his equipment which has been very helpful and valuable.

During my graduate studies, I have had the opportunity to familiarize myself with different cultures, especially because of the characteristics of Canada and Montreal in this respect. I have made numerous friends whose friendship is a real honour for me. Among them I would like to express special thanks to Nathalie Boudreault, Stéphane Cyr, Nabil Elkouh, Wadood Hamad, Josiane Joannon, Christian Masson, Daniel Rousse, Simone Sebben and Victor Storm; in brief, they were my family here during my Master's studies.

Finally, I would like to express my best regards to people who are very special to me — my sister Mina, my brother Navid, my aunts, or better be said my second and third mothers, Shamsi Nabati and Ghamar Monshi— for their long distance moral support.

Table of Contents

List of Figures

Nomenclature

A, A'	amplitude of quasi-harmonic response of the system (in the averaging method) and its derivative with respect to τ
$A')_{av.}$	approximation for A' based on the averaging method
$A)_{lim.}$	the value of limit cycle amplitude
A_θ, A_ϕ	A associated with θ and ϕ motions, respectively
A_{ji}	a mass parameter, defined in Eq. 2.10
c	retrieval constant in a nominal exponential retrieval
c_i	the i^{th} nominal exponential retrieval constant in a multi-body system
C, C_1	constant factors, used in Liapunov function
D_h	spherical domain
E	the center of the Earth
$E_\theta, \dot{E}_\theta$	norm representing the energy related to θ motion and its time derivative
$E_\phi, \dot{E}_\phi$	norm representing the energy related to ϕ motion and its time derivative
f	the function that comprises the part of the reel rate law that controls the motion
f_l	the function that comprises the LHS of the l^{th} constraint equation
$\hat{F}$	the nondimensional thruster force
F_c	the centrifugal force
F_{c_i}	the centrifugal force on the i^{th} body
F_g	the gravitational force

F_{g_i}	the gravitational force on the i^{th} body
$F_{\theta_{ki}}, F_{\phi_{ki}}, F_{\ell_{ki}}$	functions comprising the main part of the equations of motion, respectively; expressed in Eqs. 2.46–2.48
g	the function in the general representation of the RHS of a nonlinear equation (in the averaging method)
g_i	the i^{th} function of state variables in Eq. 3.7
G	universal gravitational constant
G_{ki}	a mass parameter, defined in Eq. 2.45
h	radius of the spherical domain
H	Hamiltonian
$\hat{H}$	nondimensional Hamiltonian
$\mathbf{i}, \mathbf{j}, \mathbf{k}$	the unit vectors along the x, y, z axes
i	the inclination of the orbital plane
K, K_2	gains in reel rate control laws
K_1	retrieval constant in one of the reel rate control laws
K_3	thruster gain
K_θ, K_ϕ	gains of the reel rate control laws in a two-body system
K_{θ_i}, K_{ϕ_i}	gains of the reel rate control laws in a multi-body system
$\ell, \dot{\ell}, \ddot{\ell}$	the length of the tether in a two-body system and its time derivatives
ℓ_f	the final value of ℓ
ℓ_{ref}	the reference length
$\ell(0)$	the initial value of ℓ
$\ell_i, \dot{\ell}_i, \ddot{\ell}_i$	the length of the i^{th} tether in a multi-body system and its time derivatives
ℓ_i', ℓ_i''	derivatives of ℓ_i with respect to τ
$\ell_i(0), \dot{\ell}_i(0)$	initial values for ℓ_i and $\dot{\ell}_i$
L	the Lagrangian of the system
m	the total mass of the end bodies
m_i	example of a single point mass orbiting at a radius of R_a
m_i	the mass of the i^{th} body

M	a mass ratio for two-body systems (see Eq. 3.1)
M_e	mass of the Earth
n	number of constraint equations
N	number of end bodies
p	number of degrees of freedom
P	number of state variables = $2p$
$q_K, \dot{q}_K$	the K^{th} generalized coordinate and its time derivative
Q_K	the K^{th} generalized force
$Q_{\theta_k}, Q_{\phi_k}, Q_{\ell_k}$	the generalized force corresponding to θ_k, ϕ_k, ℓ_k, respectively
$\mathbf{r}_i, \dot{\mathbf{r}}_i, \ddot{\mathbf{r}}_i$	the position vector of the i^{th} mass in the orbital reference frame and its time derivatives
r_i	magnitude of the $\mathbf{r}_i$ vector
$\mathbf{R_C}$	the position vector of the origin of the reference frame relative to the center of the Earth
R_C	magnitude of $\mathbf{R_C}$
$R_{O.C.}$	radial distance of the orbital center from the center of the Earth
$R_{C.M.}$	radial distance of the center of mass from the center of the Earth
$S(a)$	unit step function
t	time
T	magnitude of the tether tension force in a two-body system
$\hat{\mathrm{T}}$	nondimensional T
$\mathbf{T}_k$	the vector representing the tension force in the k^{th} tether of a multi-body system
T_k	the magnitude of $\mathbf{T}_k$
T	kinetic energy
T_{orb}	orbital kinetic energy
$\hat{T}$	nondimensional kinetic energy
$\hat{T}_o$	the zero order terms in $\hat{T}$

$\hat{T}_2$	the second order terms in $\hat{T}$
u_i, v_i, w_i	velocity-like functions defining $\dot{\mathbf{r}}_j$ (see Eqs. 2.31–2.33)
U	potential energy
$\hat{U}$	nondimensional potential energy
U_{orb}	orbital potential energy
$\mathbf{V}_c$	orbital velocity
$\mathbf{v}_j$	the absolute velocity of the j^{th} body
$V(\mathbf{x})$ or V	Liapunov function
$\dot{V}$	time derivative of V
$W(\mathbf{x})$	representing a general form for a function of state variables
$\mathbf{x}$	the state vector (only in Chapter 3)
$x_i, \dot{x}_i$	the i^{th} element of the state vector and its time derivative (only in Chapter 3)
x, y, z	axes of the orbital reference frame
x_i, y_i, z_i	Cartesian coordinates of the i^{th} mass in the orbital reference frame
$\dot{x}_i, \dot{y}_i, \dot{z}_i$	the time derivatives of x_i, y_i, z_i respectively

Greek Letters

α, α'	the phase angle in the quasi-harmonic response of the system (in the averaging method)
$\alpha')_{av}$	approximation for α' based on the averaging method
$\alpha_\theta, \alpha_\phi$	α associated with θ and ϕ motions, respectively
β	the total angle in the quasi-harmonic response of the system (in the averaging method)
δ	virtual displacement
$\Delta R_{O.C.}$	the distance between O.C. and C.M.
ϵ	the coefficient in the general representation of the RHS of a nonlinear equation (in the averaging method)
$\theta, \dot{\theta}, \ddot{\theta}$	in-plane rotation of the tether in a two-body system and its time derivatives

$\theta(0)$, $\dot{\theta}(0)$	initial values for θ, $\dot{\theta}$
θ', θ''	derivatives of θ with respect to τ
θ_e	the equilibrium value of θ
$\bar{\theta}$	average value of θ over a period
$\tilde{\theta}, \tilde{\theta}', \tilde{\theta}''$	$\theta - \theta_e$ and its derivatives with respect to τ
$\theta_i, \dot{\theta}_i, \ddot{\theta}_i$	in-plane rotation of the i^{th} tether in a multi-body system and its time derivatives
θ_i', θ_i''	derivatives of θ_i with respect to τ
$\theta_i(0), \dot{\theta}_i(0)$	initial values for θ_i and $\dot{\theta}_i(0)$
λ	nondimensional length
λ_f	nondimensional final length
Λ_l	the l^{th} Lagrangian multiplier
μ_i	mass ratio, defined in Eq. 2.5
τ	nondimensional time
τ_i	an arbitrary instant in the limit cycle phase
$\phi, \dot{\phi}, \ddot{\phi}$	out-of-plane rotation of the tether in a two-body system and its time derivatives
ϕ', ϕ''	derivatives of ϕ with respect to τ
ϕ_e	the equilibrium value of ϕ
$\phi(0)$	the initial value of ϕ
$\phi_i, \dot{\phi}_i, \ddot{\phi}_i$	out-of-plane rotation of the i^{th} tether in a multi-body system and its derivatives
ϕ_i', ϕ_i''	derivatives of ϕ with respect to τ
$\phi_i(0), \dot{\phi}_i(0)$	initial values for ϕ_i and $\dot{\phi}_i(0)$
ψ	true anomaly
ψ_o	argument of perigee
ω	frequency in the quasi-harmonic response of the system (in the averaging method)
$\omega_\theta, \omega_\phi$	ω associated with θ and ϕ motions, respectively
Ω	orbital angular velocity
$\dot{\Omega}$	time rate of orbital angular velocity

Other Symbols

$\dot{}$	differentiation with respect to time
$'$	differentiation with respect to nondimensional time, τ
$\vert \;\; \vert$	absolute value
$\Vert \;\; \Vert$	magnitude of a vector
$\hat{}$	denotes nondimensionality
	denotes the average value over a period of oscillation
$\tilde{}$	used only in $\tilde{\theta}$ representing $\theta - \theta_e$
$_{av}$	as a subscript, represents the approximate value according to the averaging method
$_{lim}$	as a subscript, represents the value corresponding to the limit cycle phase
^{o}	as a superscript, denotes that the value of the angle is in degrees

Abbreviations

C.M.	center of mass
IMSL	International Mathematical and Statistical Libraries
KB	Krylov-Bogoliubov (name of a method)
LHS	left-hand side
NASA	National Aeronautics and Space Administration
MTL	Materials Technology Lab
O.C.	orbital center
RHS	right-hand side
SAO	Smithsonian Astrophysical Observatory
SCOWT	Shuttle Continuous Open Wind Tunnel
STARFAC	Shuttle Tethered Aerothermodynamics Research Facility
TSS-2	the second specific mission of NASA for Tethered Satellites Systems

Chapter 1

Introduction

1.1 Outline of the Chapter

In this chapter we first briefly discuss the historical background of the tethered satellite systems in general. The application of multi-body tethered systems, whose dynamics and control are the main concerns of this thesis, is the subject of the third section. The aims of the thesis comes next. The last section of this chapter presents the outline of the thesis.

1.2 Historical Background

The initial idea of using tethers in space goes back to the previous century. In 1895 Tsiolkovsky suggested connecting large masses in space by a long thin string [1,2] to take advantage of weak gravity-gradient forces for stabilization purposes. Gravity-gradient stabilization has been applied to satellites since the beginning of the space program, but only with short rigid booms rather than long strings. As described by von Tiesenhausen [3], sixty-five years later in 1960, the Russian engineer Artsutanov [4] conceived the futuristic idea of anchoring a geostationary satellite to the Earth's surface by a long cable (tether). A ballast would be deployed from the satellite by another cable in the opposite direction. so the center of gravity can be maintained in the geostationary orbit.

Two other ideas involving long tethers were also suggested in the past, but they have not been given any serious consideration by the succeeding researchers, since they do not seem to be feasible at present. They are mentioned here only because of the historical significance. The first was a low altitude geostationary satellite proposed by Collar and Flower [5] in 1969. The second was a wheel tether proposed by Artsutanov [6] in the same year.

Actual application of tethers was considered in the early sixties by Starly and Adlhoch for finding a way of retrieving stranded astronauts [7,8]. Successful experiments during Gemini *XI*, *XII* in September and November of 1966, respectively, established the feasibility of using tethered systems [9]. But in these experiments only a short tether was used for connecting an unmanned vehicle to a manned space vehicle. Subsequently, some long-antenna-wire experiments were conducted, but only small end-masses were used.

In the early seventies, a proposal by Colombo et al. [10] to use the Shuttle-based tethered systems with large subsatellites and very long tethers gave birth to the modern era of tethered satellite systems. As a matter of fact, Bekey [1] considers Colombo to be the father of space tethers. The details of the proposal involved deploying a 500 kg subsatellite from the Space Shuttle into the atmosphere using a 100 km long tether. Considerable research activities have been conducted by NASA, Smithsonian Astrophysical Observatory (SAO), and other researchers on the dynamics, control, design and scientific applications of this concept. Since the planning of the Space Station has been in progress for some time, possible applications of tethered systems in conjunction with the Space Station have also been studied. Some applications not involving either the Shuttle or the Space Station have also been suggested [11].

Sending scientific platforms or any research probe to different altitudes by tethering them, as subsatellites, to the Shuttle Orbiter or Space Station has many advantages. The subsatellites can be retrieved at the end of the mission and instead of just being left in space, most of the parts may be re-used for subsequent missions. Another advantage is that the subsatellite is always under the control of the Shuttle or Space Station crew and in case any reparation is necessary it can be performed by the crew. The tether can also be utilized as a means of transferring data or power.

In some of the applications, there are more than two bodies that are connected together by tethers. In this thesis, we have concentrated on the investigation of this kind of tethered systems. Generally we call these systems multi-body or N-body tethered systems. Therefore in the next section we present the applications of multi-body tethered systems. Other applications of the tethered systems are explained in Appendix A.

1.3 Some Applications of the Multi-body Tethered Satellite Systems

The applications of the tethered satellite systems in general is the subject of Appendix A. Here we only consider applications concerning multi-body systems.

1.3.1 Upper atmosphere measurements

An on-going study concerning the application of multi-body tethered satellites in upper atmospheric measurements is to lower a constellation of probes, which are located at different altitudes, into the atmosphere. The first is tethered to the Shuttle while the others are connected together by tethers (see page 36 of Ref. [11]). In this way it will be possible to *collect data at different locations simultaneously* which is a valuable capability in atmospheric measurements.

1.3.2 Gravity related applications

Microgravity laboratory

For this application a laboratory facility on board the Space Station is situated in the proximity of its vertical center of gravity. Two opposing tethers with end masses are deployed vertically from the Space Station (one above and one below, refer to the figure on page 76 of [11]). The length of the tethers is varied to control the center of gravity of the system, placing it on the microgravity modules to minimize their gravity gradient acceleration and set it in the microgravity level (10^{-4} g and less). The tethered end masses are also useful for reducing the disturbances mainly caused by the crew activities, and enhancing overall system attitude control. Some microgravity laboratories are currently under study, one of them is MTL (Materials Technology Lab) and the other one a Biological laboratory. Some biological processes to be studied would be animal and plant growth, and human performance.

Variable low-gravity laboratory

In this application a tether with an end mass is deployed upward from the Space Station and the laboratory can be positioned at different points along this tether (page 88 of [11] demonstrates the arrangement). The gravity gradient between the center of gravity of the system and the laboratory gives rise to an artificial gravity at the laboratory. The laboratory gravity level is varied by changing its distance from the system center of gravity. Since the system gravity characteristics change with orbital variations, the gravity level inside the laboratory varies with time even if it is located at a constant distance relative to the Space Station. Therefore, for maintaining a constant gravity level in the laboratory, its position should be adjusted in accordance with the orbital variations. This configuration allows performance of experiments under conditions of constant or variable low gravity for extended periods of time. The laboratory can attain microgravity levels if it can move to the center of gravity. In comparison with the previous configuration for microgravity this has the disadvantage of reducing the human access. On the other hand it has the advantages of isolating the laboratory from the disturbances present in the Space Station itself, and minimizing the gravity gradient inside the laboratory. It can also attain higher gravity. It has been calculated that the laboratory could attain g-levels of $10^{-6}, 10^{-4}, 10^{-2}$, and 10^{-1} at the distances above the center of gravity of about (the accurate values depend on the subsatellite mass) 2 m, 200 m, 20 km, 200 km, respectively.

Gravity wave detector

Because of the seismic noises, an Earth-based detector cannot detect gravitational waves in the 10–100 MHz band. An orbiting gravity wave detector would solve the problem. A tethered system has been suggested for this purpose The system would consist of a spring which is connected to two end masses by tethers (refer to the figure on page 39 of [11]). As this tethered system orbits the Earth, gravitational waves from supernovas, stars, pulsars or any other gravity sources would make the masses to oscillate. The oscillations would be transmitted to the spring, which could be recorded by a sensing device.

1.3.3 Tether communications antenna

An insulated conducting tether, with plasma contactors at both ends, may be connected to a spacecraft in the middle. Variations in the tether current can be produced to generate ULF, ELF, or VLF waves for communications. Waves are emitted by a loop antenna composed of the tether, magnetic field lines, and the ionosphere (page 61 of [11] presents a general view of this application).

Although there are many more proposed applications for the multi-body tethered systems, the ones referred to in this section provides sufficient motivation for undertaking this thesis.

1.4 Aims of the Study and the Related Literature

A wide range of potential applications, only some of which were presented in the previous section and in Appendix A, has created quite a good interest in tethered satellite systems in recent years. Hence, there is a rich literature available on the dynamics and control of such systems, but most of the previous works have been concentrated on two-body systems. *Our main goal is to contribute to the studies on the dynamics and control of multi-body tethered systems* Therefore, in this section, the available literature on the dynamics and control of multi-body tethered systems is reviewed. In the introductions of some of the ensuing chapters, the literature related to the subject of the chapter will also be presented.

Liu [12], in 1985, formulated the dynamics of three-body tethered systems. The tethers were assumed to be straight and massless. Even though he considered only the in-plane motion of a cargo transportation, the equations of motion were very complicated. This was caused by his selection of coordinates which happened to be subjected to constraints. Pointing out this complexity, he did not present any numerical result for his set of combined algebraic and differential equations.

For performing the microgravity experiments, Lorenzini [13] proposed the idea of tethering the g-laboratory to the Space-Station. In 1987, the same author [14] discussed the control strategies for deployment of the system and damping of the oscillations in station-keeping stage. The system is a three-body tethered system consisting of the Space-Station, the micro-g/variable-g laboratory and another scientific platform. The g-laboratory is in between the other two bodies and crawls along a 10-km-long, 2-mm-diameter kevlar tether. The analysis was concentrated on the in-plane motion. The tethers were assumed massless but their longitudinal vibrations have been included. The orbital motion is considered to be circular and a spherical Earth is assumed. Two mathematical models were used, one using the Lagrangian approach and the other one Newtonian.

In 1987, Misra, Amier and Modi [15] used the Lagrangian approach to analyze the in-plane motion of the three-body systems for fixed-length as well as variable-length tethers. The tethers were assumed to have negligible mass The coordinates used were different from those of Lorenzini. In the case of fixed length tethers, they investigated the stability of the equilibrium configurations. The equilibrium along the local vertical was found to be the only stable one (for small motion). The variable-length cases included deployment of a constellation as well as cargo transportation. Among the results the most significant one was that large librations could occur in the cargo transportation case.

The 4-mass tethered system of the Space Station-based Elevator/Crawler micro and variable-gravity facility, consisting of two platforms, Space Station, and an elevator, was studied by Lorenzini et al. [16] and by Cosmo et al. [17] The former study [16] mainly demonstrates the accelerations and the g-level of the Space Station and the Elevator. The latter analysis [17] considered the dy namics and control of two-dimensional motion of the system. The degrees of freedom included lengths of the tethers, in-plane libration, longitudinal elastic oscillations and in-plane lateral deflections (these are the lateral deflections of the point masses not the lateral elastic vibrations of the tethers). They formulated the problem with the Lagrangian approach and found the eigenvalues and eigenvectors of the system. It was noticed that the longitudinal oscillations are highly coupled to the in-plane librational and lateral motions. A tether length control law was suggested for controlling the in-plane librational and lateral deflections. The longitudinal oscillations of the tether were damped out by longitudinal dampers tuned to the longitudinal frequencies.

All the bodies were considered as point masses in all of the above studies. On the other hand, Bachmann et al. [18] included the rigid-body rotational motion of the Space Station in a three-body Space Station-based Tethered Elevator System; they also considered the offset of the tether attachment point from the Station center of mass. The equations of motion were derived using the Lagrangian approach. Tethers were assumed massless and elastic in the formulation stage, but rigid in numerical computations. An optimization was carried out on two control schemes: thruster control and hybrid offset-thruster control.

Misra and Modi [19] formulated the general three-dimensional dynamics of N-body tethered systems using a multiple-pendulum model. The tethers were assumed massless and straight. The equations obtained are valid for large motion as well as for variable-length tethers and any arbitrary orbit. A study on librational frequencies was carried out by considering small angle motion in the neighbourhood of the local vertical equilibrium configuration for the special case of a circular orbit. Based on the linearized equations of motion, a general discussion was presented on the acceptable range of control gains in a particular reel rate control law for controlling the in-plane and out-of-plane librations at the same time.

The well-known control methods for tethered satellites are tension control laws, length rate or reel rate control laws, thruster control laws and, offset control laws. In the case of the tension control law one modulates the tension in the tether using the feedback of appropriate generalized coordinates or their derivatives. The tension control law is the first standard method that had been used for controlling the motion of tethered satellite systems, therefore a rich literature is available for this control method. Among them one can highlight the References [20] by Rupp, [21] by Kulla, [22] by Bainum and Kumar, and [23] by Liangdong and Bainum. In length rate or reel rate control laws the tether reel rate or the tether length is fed back with appropriate form. As examples of the earliest works on the reel rate control laws, one can refer to Reference [24] by Kohler et al. Thruster control laws are implemented by firing thrusters at an appropriate point of the system and modulating the magnitude of the thrust by suitable feedbacks. Thruster control laws have been used for obtaining a better performance in out-of-plane motion; Reference [25] by Banerjee and Kane can be referred in this regard. As a recent reference one can consider Reference [26] by Fleurisson et al. Offset control laws have been proposed recently as an alternative to thruster controller. Offset control laws function generally by changing the offset of the point of attachment of the tether to the main satellite, which must be treated as a rigid body (Reference [27] by Modi et al. can be mentioned as an example). The first three, which are compatible with our model, have been augmented to the simulation of the motion in this thesis, but the offset control method does not fit with a model that considers the bodies as point masses.

The thruster augmented and offset control schemes have some restrictions in their implementation. For benefiting from the thruster forces one should include some fuel in one or more elements of the system. The other problem with thrusters is that they cannot be fired in the proximity of the Shuttle. On the other hand, for the offset controllers, moving the point of attachment of the tether is not always possible. However, the tension control laws and length or reel rate control laws are easy-to-implement.

Here, in this thesis, a simulation package is developed for studying both the in-plane and out-of-plane motions of the multi-body systems. The formulation is valid for motion in the large. Bodies are treated as point masses and the emphasis is on the librational motion of the tethers; i.e. the elastic vibrations of the tethers are assumed to be negligible. The formulation and simulation consider for the general case of N number of bodies.

The code developed in the thesis is used to study the three-dimensional motion of the system. There have been very few studies on three-dimensional motion of multi-body systems. Besides analyzing the three-dimensional dynamics of the multi-body tethered satellites, the purpose of the thesis is also to develop easy-to-implement control schemes to stabilize the in-plane and out-of-plane motions at the same time. Even for the two-body systems, in the available literature that consider controlling the in-plane and out-of-plane motions simultaneously, the suggested control systems are comprised, completely or partially, of the thruster and/or offset control laws that have difficulty in implementation. The reel rate and tension control laws have been used extensively in the past for controlling the in-plane motion, but they could be very useful to control the out-of-plane motion as well. One of the objectives of this thesis is to do this for multi-body systems with reel rate control laws. There is no work available that offers a pure reel rate control law for stabilizing the in-plane and out-of-plane librations of multi-body systems.

Xu et al. [28] and Xu [29], using the energy dissipation method, proposed a reel rate control law for two-body tethered systems to control the in-plane librations together with the out-of-plane librations. As a logical approach, here we start with two-body systems and then extend the results to multi-body systems.

It should also be mentioned that it is well known that the deployment of the tethered systems can be performed even without a feedback control system but, during the retrieval the presence of a feedback control system is indispensable. This is due to the sign of $\dot{\ell}/\ell$ term which acts as a damping coefficient in the second order equations for in-plane and out-of-plane librations. For the deployment, $\dot{\ell}/\ell$ is positive and we have positive damping. For the retrieval $\dot{\ell}/\ell$ is negative and we have negative damping; i.e. it will add energy to the system. Due to the criticality of the retrieval phase, most of the attention in this thesis will be focused on that phase.

1.5 Outline of the Thesis

The aims of the thesis were discussed in the previous section. In the following chapters, the formulation of the problem, the proposal of the control laws by analytical methods and the results of the simulation of motion are presented.

Chapter 2 contains the development of the equations of motion for N-body tethered systems. The Lagrangian approach is used. The center of mass is assumed to have a prescribed Keplerian orbit. The bodies are considered as point masses and three-dimensional motion of straight tethers is considered. The nonlinear terms are retained in the equations; hence, they hold for motion in the large. Explanation of the developed computer code closes the chapter.

Chapter 3 deals with the development of a reel rate law by using Liapunov's second method. The method, which is also called Liapunov's direct method is described in detail first, and its advantages and disadvantages are pointed out. Based on the Hamiltonian of the system, which is often a good candidate for the Liapunov function of dynamical systems, a proper reel rate law for controlling the retrieval phase is obtained. The resulting motion with this reel rate law is presented at the end of the chapter.

Chapter 4 introduces an alternative analytical method, called the energy dissipation approach. This approach is also applicable to the nonlinear equations of motion, but the complexity of the mathematics behind it obliges us to apply the method to linearized equations. However, the effectiveness of the control laws developed is validated by simulation of the system dynamics with nonlinear equations. Two reel rate control laws for the retrieval motion are obtained, one with quadratic roll rate feedback and another with absolute value roll rate feedback. The comparison of the performances of the system with different reel rate laws is done next. Then the superior reel rate laws are extended to multi-body systems and the results of simulation of motion for some three-body cases are presented. A discussion on the effects of different parameters and gains on the resulting motion terminates the chapter.

Conclusions and comments are the contents of Chapter 5, the final chapter of the thesis.

There are also two appendices to these chapters. Appendix A presents the applications of tethered satellites. Appendix B is on the definition and exact location of the orbital center.

Chapter 2

Dynamical Formulation for N-body Tethered Systems

2.1 Introduction

This chapter contains the formulation of the problem for a general system consisting of N bodies which will be treated as point masses, connected by $N - 1$ tethers. It starts with the description of the system and the assumptions made, which as a matter of fact is an illustration of the model that is going to be used in our study. The third section discusses the generalized coordinates and the kinematics of the system. The Lagrangian approach is used next for developing the equations of motion. A brief explanation of the computer code terminates the chapter.

2.2 General Description of the System and Assumptions Made

The entire system is orbiting around the Earth mainly under the action of the gravitational attraction of the Earth, which is assumed to be spherical. There may be some other external forces like aerodynamic forces, solar radiation pressure, electromagnetic forces, etc. acting as perturbations. Depending on the situation the significance of these different forces varies, for example aerodynamic forces are not important at higher altitudes.

The system, consisting of N bodies and $N-1$ tethers is shown in Fig. 2.1, where $m_i, i = 1, 2, \ldots, N$ represent the mass the bodies. These bodies can include the Space Station, the Shuttle, scientific platforms, and/or elevators, etc. The center of mass of the system (C.M.) is assumed to have a prescribed Keplerian orbit. As a matter of fact the best point for representing the orbital motion of the system is the *orbital center* (O.C.) and not the center of mass. The orbital center is the point where the sum of the gravitational and centrifugal forces is zero and is discussed in more detail in Appendix B. In this thesis it is assumed that the O.C. coincides with C.M. and the degree of validity of this assumption will be discussed shortly. The inclination of the orbital plane to the equatorial plane is represented by the angle i, the argument of perigee by ψ_o, and the true anomaly by ψ. The coordinate system used here is the rotating orbital coordinate system x, y, z shown in Fig.2.1, with its origin situated at the center of mass of the system (C.M.). The center of the Earth is indicated by E, and R_C represents the instantaneous radial distance of the C.M. with respect to the center of the Earth. The x axis is along the local vertical pointing outwards, the z axis is normal to the orbital plane, and y axis is perpendicular to both of them, completing the triad.

The orbital motion of the system is assumed to be unaffected by the librations of the tethers and the attitude motion of the end bodies. If the masses are considered as rigid bodies, the attitude motion of these bodies will be coupled with the librational (rotational) motion of the tethers. The effect of attitude motion of the bodies is significant if either the size of the bodies is comparable to the lengths of the tethers, or the aerodynamic forces are considerable. Here we study the cases where the lengths of the tethers are much larger than the sizes of the bodies, and the altitude is high enough for not having any significant aerodynamic effect (200 km or more). Hence, we may consider the bodies as point masses.

Since the tethers are long, their mass as well as their transverse and longitudinal vibrations should be considered. But for the sake of simplicity the tethers are considered massless and straight. As was discussed in Chapter 1 and Appendix A, most of the applications of the tethered satellites are in conjunction with the Shuttle or the Space Station. In practice, the mass of the tethers is of the order of 10^2 kg, while that of the Orbiter or the Space Station is of the order of $10^4 - 10^5$ kg. Therefore ignoring the mass of the tethers is not a severe approximation. As will be later demonstrated, even after these assumptions, the equations of motion are very complicated. In the later stages of research on N body systems these assumptions could be relaxed, as in the case of investigations on two-body systems where the studies started with simplified models and were later improved upon.

The effect of the electrodynamic field of the Earth is negligible except for the cases of electrodynamic applications which need a separate study. The other source of perturbation is the solar radiation; it does affect the temperature of the tethers. By being exposed to the solar radiation and being in the shadow of the Earth periodically while orbiting around the Earth, the tethers have a time-dependent temperature and consequently time-varying elongation. Kalaghan et al. [30] have demonstrated that for a stainless steel tether there is a change in elongation of 0.09 % for a temperature fluctuation of 60° K. We do not consider this effect since we are not considering the longitudinal vibrations of the tethers. In addition, we plan to control the motion solely by reel rate laws and without the assistance of any thruster. Therefore no thrust will appear in the equations either.

As it was mentioned before, another assumption here is that the orbital center coincides with the center of mass. The validity of this approximation is very high, and for showing it we perform a comparison between the positions of the O.C. and center of mass. Employing Eq. B.9 from Appendix B, the distance between O.C. and C.M., relative to the radius of C.M., can be written as

$$\Delta R_{O.C.} = \frac{R_{C.M.} - R_{O.C.}}{R_{C.M.}} = 1 - \frac{\sum_{i=1}^{N} m_i}{\left[\left(\sum_{i=1}^{N} m_i r_i\right)^2 \left(\sum_{i=1}^{N} m_i / r_i^2\right)\right]^{1/3}} \quad . \tag{2.1}$$

For the systems with short tethers, basically there is no sensible difference between the positions of the two points. Even for the systems with moderately long tethers, the two points are very close. In order to give an idea about this difference we consider an example of a two-body system with a 100 km long tether. From Eq. 2.1 one can show that for any tether length, the distance between the positions of the C.M. and O.C. is maximum if the bodies have equal masses, therefore we consider examples with equal masses for the two bodies. For a system with characteristics of $m_1 = m_2$, tether length=100 km, $r_1 = 6870$ km, $r_2 = 6970$ km, the offset between C.M. and O.C. is about 0.005 percent radius of C.M.

For having a relatively significant difference in the positions of O.C. and C.M., the tether should be very long. For example in another system with

$m_1 = m_2$, tether length=1000 km, $r_1 = 6870$ km, $r_2 = 7870$ km, this offset is about 0.46 percent. It can be seen that even in the case of such a long tether the difference in positions of the two points is not much. Therefore, in this thesis we neglect the difference in positions of C.M. and O.C.; in Fig 2.1 the point C, the origin of the orbital reference frame, represents their assumed common position. Having the center of mass at the origin simplifies the kinematical relations significantly.

In summary the assumptions made here are:

1. The gravitational field is assumed to be that of a spherical Earth and the effects of the Sun and the Moon on this field are ignored.
2. The bodies are treated as point masses.
3. The orbital motion is assumed to be based on the central force motion , and independent of the librational motion.
4. Longitudinal and transverse vibrations, and mass of the tethers are ignored.
5. The effects of the aerodynamic forces, electrodynamic field of the Earth and solar radiations are negligible.
6. The center of mass is considered to be coincident with orbital center.

2.3 Kinematics of the System

Since the origin of the orbital coordinate system x, y, z coincides with the center of mass, from the definition of the C.M. we get

$$\sum_{i=1}^{N} m_i x_i = 0, \quad \sum_{i=1}^{N} m_i y_i = 0, \quad \sum_{i=1}^{N} m_i z_i = 0 \quad . \tag{2.2}$$

Because of these three constraint equations, the N-body system which can potentially have $3N$ degrees of freedom, will have only $3N - 3$ degrees of freedom. These $3N - 3$ degrees of freedom are relative to the orbital coordinate axes. In order to have a complete representation of the motion, one should add the orbital motion of the axes to these degrees of freedom. In this thesis, the orbital motion is assumed to be prescribed, and can be described in terms of the radial distance R_C and true anomaly ψ. True anomaly is an indication of time and enters the equations as the independent variable.

Let us now discuss the choice of the generalized coordinates. Of course, the dynamics of the system can be described by the Cartesian coordinates, x_i, y_i, z_i, $i = 1, 2, \ldots, N$. This set consists of $3N$ coordinates, but since the generalized coordinates are supposed to be independent, their number should be equal to the degrees of freedom of the system, i.e. $3N - 3$. Hence for choosing the generalized coordinates one should take out three coordinates from this set, say x_N, y_N, z_N. However, the resulting set is not convenient and will not be used here. Instead, another set of coordinates will be considered as generalized coordinates which is comprised of the length of the tethers, ℓ_i, and two rotations for each tether, θ_i and ϕ_i, $i = 1, 2, \ldots, N - 1$. As is shown in Fig. 2.1(b), the angle θ_i is measured in the orbital plane, so it is called the *in-plane* rotation; it is also known as the *pitch* angle. The angle ϕ_i indicates the amount of deviation of the tether from this plane so it is called the *out-of-plane* rotation. This angle is also known with another name, the *roll* angle.

Using Fig. 2.1 the Cartesian coordinates of the masses can be related to the generalized coordinates in the following manner

$$
\begin{aligned}
x_2 &= x_1 + \ell_1 \cos\theta_1 \cos\phi_1 \quad , \\
x_3 &= x_2 + \ell_2 \cos\theta_2 \cos\phi_2 &&= x_1 + \sum_{i=1}^{2} \ell_i \cos\theta_i \cos\phi_i \quad , \\
&\vdots \\
x_j &= x_{j-1} + \ell_{j-1} \cos\theta_{j-1} \cos\phi_{j-1} &&= x_1 + \sum_{i=1}^{j-1} \ell_i \cos\theta_i \cos\phi_i \quad , \\
&\vdots \\
x_N &= x_{N-1} + \ell_{N-1} \cos\theta_{N-1} \cos\phi_{N-1} &&= x_1 + \sum_{i=1}^{N-1} \ell_i \cos\theta_i \cos\phi_i \quad .
\end{aligned}
\tag{2.3}
$$

Now by substituting Eq. 2.3 into Eq. 2.2 one arrives at

$$
\begin{aligned}
x_1 & \left[\sum_{i=1}^{N} m_i\right] + \ell_1 \cos\theta_1 \cos\phi_1 \left[\sum_{i=2}^{N} m_i\right] + \cdots \\
+ & \ \ell_{j-1} \cos(\theta_{j-1}) \cos(\phi_{j-1}) \left[\sum_{i=j}^{N} m_i\right] + \cdots \\
+ & \ \ell_{N-1} \cos(\theta_{N-1}) \cos(\phi_{N-1}) [m_N] = 0 \quad .
\end{aligned}
\tag{2.4}
$$

Defining the mass ratio μ_i as

$$
\mu_i = m_i/m, \quad i = 1, 2, \ldots, N \quad , \tag{2.5}
$$

where

$$
m = \sum_{i=1}^{N} m_i = \text{total mass of the end bodies} \quad , \tag{2.6}
$$

one can solve Eq. 2.4 to obtain x_1

$$x_1 = -\left[\sum_{i=2}^{N}\mu_i\right]\ell_1\ \cos\theta_1\ \cos\phi_1 - \cdots$$
$$- \left[\sum_{i=j}^{N}\mu_i\right]\ell_{j-1}\ \cos(\theta_{j-1})\ \cos(\phi_{j-1}) \tag{2.7}$$
$$- \cdots - [\mu_N]\,\ell_{N-1}\ \cos(\theta_{N-1})\ \cos(\phi_{N-1}) \quad .$$

From the expression in Eq. 2.3 for x_j, and using Eq. 2.7 for x_1 one gets

$$\begin{aligned} x_j &= x_1 + \sum_{i=1}^{j-1}\ell_i\ \cos\theta_i\ \cos\phi_i \\ &= \left[1 - \sum_{i=2}^{N}\mu_i\right]\ell_1\ \cos\theta_1\ \cos\phi_1 + \cdots \\ &\quad + \left[1 - \sum_{i=j}^{N}\mu_i\right]\ell_{j-1}\ \cos(\theta_{j-1})\ \cos(\phi_{j-1}) \\ &\quad - \left[\sum_{i=j+1}^{N}\mu_i\right]\ell_j\ \cos(\theta_j)\ \cos(\phi_j) - \cdots \\ &\quad - [\mu_N]\,\ell_{N-1}\ \cos(\theta_{N-1})\ \cos(\phi_{N-1}) \quad . \end{aligned} \tag{2.8}$$

Since $\sum_{i=1}^{N}\ \mu_i = 1$, Eq. 2.8 reduces to

$$\begin{aligned} x_j = &+ [\mu_1]\,\ell_1\ \cos\theta_1\ \cos\phi_1 + \cdots \\ &+ \left[\sum_{i=1}^{j-1}\mu_i\right]\ell_{j-1}\ \cos(\theta_{j-1})\ \cos(\phi_{j-1}) \\ &+ \left[-1 + \sum_{i=1}^{j}\mu_i\right]\ell_j\ \cos(\theta_j)\ \cos(\phi_j) + \cdots \\ &+ \left[-1 + \sum_{i=1}^{N-1}\mu_i\right]\ell_{N-1}\ \cos(\theta_{N-1})\ \cos(\phi_{N-1}) \quad . \end{aligned} \tag{2.9}$$

By defining the coefficients A_{ji}'s as

$$A_{ji} = \left[\sum_{k=1}^{i} \mu_k\right] - S(i-j) \quad , \tag{2.10}$$

where $S(a)$ represents the *unit step function* with the following properties:

$$\begin{aligned} S(a) &= 1 \quad , \qquad \text{for} \quad a \geq 0 \quad , \\ &= 0 \quad , \qquad \text{for} \quad a < 0 \quad , \end{aligned} \tag{2.11}$$

Eq. 2.9 can be represented in the compact form

$$x_j = \sum_{i=1}^{N-1} A_{ji}\ \ell_i\ \cos\theta_i\ \cos\phi_i \quad . \tag{2.12}$$

Similarly for y and z coordinates of the j^{th} mass one obtains

$$y_j = \sum_{i=1}^{N-1} A_{ji}\ \ell_i\ \sin\theta_i \cos\phi_i \quad , \tag{2.13}$$

$$z_j = \sum_{i=1}^{N-1} A_{ji}\ \ell_i\ \sin\phi_i \quad . \tag{2.14}$$

2.4 Governing Equations of Motion

For obtaining the equations of motion of tethered systems different approaches have been used by different investigators, depending on the nature of the system and method of modelling. For the model that we have used, i.e. straight, massless tethers, and specially for our system consisting of the N bodies, the best approach seems to be the *Lagrangian approach*. The Lagrangian approach is a powerful and effective method when the number of internal elements of the system is relatively high. As opposed to the Newtonian approach, which is a force approach, this is an energy approach and is based on the energy expressions for the whole system. In the Lagrangian approach the dynamics is governed by a set of scalar second order partial differential equations as

$$\frac{d}{dt}\left(\frac{\partial L}{\partial \dot{q}_K}\right) - \frac{\partial L}{\partial q_K} = Q_K \quad , \qquad K = 1, 2, \ldots, 3N-3 \quad , \tag{2.15}$$

where $q_K = \theta_k, \phi_k, \ell_k$, $k = 1, 2, \ldots, N-1$, are the generalized coordinates, L is the system's Lagrangian defined as the difference between the kinetic energy (T) and potential energy (U) of the system, i.e.,

$$L = T - U \quad , \tag{2.16}$$

and Q_K, $K = 1, 2, \ldots, 3N-3$, are the *generalized forces.*

If the number of q_K's is more than the degrees of freedom they will not be independent, and they cannot be considered as generalized coordinates anymore[1]. In these cases there are some constraint equations, usually algebraic, which must be solved simultaneously with Lagrange's equations, and on the right-hand side (RHS) of the Lagrange's equations (Eq. 2.15) an extra term must be added as follows:

$$\frac{d}{dt}\left(\frac{\partial L}{\partial \dot{q}_K}\right) - \frac{\partial L}{\partial q_K} = Q_K + \sum_{l=1}^{n} \Lambda_l \frac{\partial f_l}{\partial q_K} \quad , \qquad K = 1, 2, \ldots, 3N-3 \quad , \tag{2.17}$$

where n represents the number of constraints, and Λ_l, $l = 1, 2, \ldots, n$ are extra un-

[1] An example is the tethered elevator problem The lengths of the two tether elements on two sides of the elevator add up to a constant value.

known coefficients called *Lagrange's multipliers*. The functions f_l, $l = 1, 2, \ldots, n$ in this case represent the left-hand side (LHS) of the constraint equations of the form

$$f_l(q_1, q_2, \ldots, q_K, t) = 0 \quad , \qquad\qquad l = 1, 2, \ldots, n \quad . \tag{2.18}$$

In the following two subsections we develop the expressions for kinetic and potential energies of the tethered satellite systems. Substitution of these expressions into Lagrange's equations comes next.

2.4.1 Kinetic energy of the system

Since the tethers are assumed massless and the bodies are considered as point masses the kinetic energy of the system is simply equal to:

$$T = \frac{1}{2} \sum_{j=1}^{N} m_j \, (\mathbf{v}_j \cdot \mathbf{v}_j) \quad , \tag{2.19}$$

where m_j is the mass of the j^{th} body, and $\mathbf{v}_j$ is the corresponding absolute velocity, and it can be expressed in the following manner

$$\mathbf{v}_j = \mathbf{v}_c + \dot{\mathbf{r}}_j \quad , \qquad\qquad j = 1, 2, \ldots, N \tag{2.20}$$

Here $\mathbf{v}_c$ represents the velocity of the C.M. (or O.C.) which is known as the *orbital velocity*, and $\dot{\mathbf{r}}_j$ is the relative velocity of the j^{th} body with respect to the x, y, z axes, i.e. $\mathbf{r}_j$ is the position vector of the j^{th} mass relative to this reference frame. Substituting Eq. 2.20 into Eq. 2.19 the kinetic energy becomes

$$
\begin{aligned}
T &= \frac{1}{2}\sum_{j=1}^{N} m_j\,(\mathbf{v}_c + \dot{\mathbf{r}}_j)\cdot(\mathbf{v}_c + \dot{\mathbf{r}}_j) \\
&= \frac{1}{2}\,m\,(\mathbf{v}_c\cdot\mathbf{v}_c) + \mathbf{v}_c\cdot\sum_{j=1}^{N} m_j\dot{\mathbf{r}}_j + \frac{1}{2}\sum_{j=1}^{N} m_j(\dot{\mathbf{r}}_j\cdot\dot{\mathbf{r}}_j) \quad .
\end{aligned}
\tag{2.21}
$$

The first term indicates the amount of the kinetic energy that all of the bodies have because of the orbital motion and it is called *orbital kinetic energy* (T_{orb}). The third term will be the non-orbital or librational kinetic energy. The second term will be zero since the origin of the reference frame is at the center of mass; i.e., $\sum_{j=1}^{N} m_j\mathbf{r}_j = 0$, and in the second term we have

$$
\sum_{j=1}^{N} m_j\dot{\mathbf{r}}_j = \sum_{j=1}^{N} \frac{d}{dt}(m_j\mathbf{r}_j) = \frac{d}{dt}(\sum_{j=1}^{N} m_j\mathbf{r}_j) = 0 \quad . \tag{2.22}
$$

Then the expression for the kinetic energy reduces to

$$
T = T_{orb} + \frac{1}{2}\sum_{j=1}^{N} m_j\,(\dot{\mathbf{r}}_j)\cdot(\dot{\mathbf{r}}_j) \quad . \tag{2.23}
$$

If $\mathbf{i},\mathbf{j},\mathbf{k}$ indicate the unit vectors along the x, y, z axes respectively, $\dot{\mathbf{r}}_j$ can be found by differentiating

$$
\mathbf{r}_j = x_j\,\mathbf{i} + y_j\,\mathbf{j} + z_j\,\mathbf{k} \quad . \tag{2.24}
$$

Since x, y, z frame is not an inertial one but is rotating with the angular velocity of Ω, $\dot{\mathbf{r}}_j$ is equal to

$$
\dot{\mathbf{r}}_j = (\dot{x}_j\,\mathbf{i} + \dot{y}_j\,\mathbf{j} + \dot{z}_j\,\mathbf{k}) + \Omega\,\mathbf{k}\times(x_j\,\mathbf{i} + y_j\,\mathbf{j} + z_j\,\mathbf{k}) \quad , \tag{2.25}
$$

or

$$\dot{\mathbf{r}}_j = (\dot{x}_j - \Omega y_j)\,\mathbf{i} + (\dot{y}_j + \Omega x_j)\,\mathbf{j} + \dot{z}_j\,\mathbf{k} \quad . \tag{2.26}$$

Differentiating Eqs. 2.12–2.14 one obtains

$$\dot{x}_j = \sum_{i=1}^{N-1} A_{ji}\,(\dot{\ell}_i \cos\theta_i \cos\phi_i - \ell_i\dot{\theta}_i \sin\theta_i \cos\phi_i - \ell_i\dot{\phi}_i \cos\theta_i \sin\phi_i) \quad , \tag{2.27}$$

$$\dot{y}_j = \sum_{i=1}^{N-1} A_{ji}\,(\dot{\ell}_i \sin\theta_i \cos\phi_i + \ell_i\dot{\theta}_i \cos\theta_i \cos\phi_i - \ell_i\dot{\phi}_i \sin\theta_i \sin\phi_i) \quad , \tag{2.28}$$

$$\dot{z}_j = \sum_{i=1}^{N-1} A_{ji}\,(\dot{\ell}_i \sin\phi_i + \ell_i\dot{\phi}_i \cos\phi_i) \quad , \tag{2.29}$$

consequently $\dot{\mathbf{r}}_j$ can be expressed in the following compact form

$$\dot{\mathbf{r}}_j = \sum_{i=1}^{N-1} A_{ji}\,(u_i\,\mathbf{i} + v_i\,\mathbf{j} + w_i\,\mathbf{k}) \quad , \tag{2.30}$$

where

$$u_i = \dot{\ell}_i \cos\theta_i \cos\phi_i - \ell_i(\dot{\theta}_i + \Omega)\sin\theta_i \cos\phi_i - \ell_i\dot{\phi}_i \cos\theta_i \sin\phi_i \quad , \tag{2.31}$$

$$v_i = \dot{\ell}_i \sin\theta_i \cos\phi_i + \ell_i(\dot{\theta}_i + \Omega)\cos\theta_i \cos\phi_i - \ell_i\dot{\phi}_i \sin\theta_i \sin\phi_i \quad , \tag{2.32}$$

$$w_i = \dot{\ell}_i \sin\phi_i + \ell_i\dot{\phi}_i \cos\phi_i \quad . \tag{2.33}$$

Equations 2.30–2.33 can be substituted into Eq. 2.23 to determine the kinetic energy.

2.4.2 Potential energy of the system

For a tethered satellite system the major potential energy is the gravitational potential energy. In case of a single particle with mass m_a, orbiting around the Earth with the distance from the center of the Earth equal to R_a the gravitational potential energy is equal to

$$U = -\mathrm{GM}_e \; m_a / \left| R_a \right| \quad , \tag{2.34}$$

where G is the universal gravitational constant and M_e is the mass of the Earth. For a system consisting of N bodies the gravitational potential energy will be equal to

$$U = -\mathrm{GM}_e \sum_{j=1}^{N} m_j / \left| \mathbf{R}_C + \mathbf{r}_j \right| \quad , \tag{2.35}$$

where $\mathbf{R}_C$ is the position vector of C.M. or O.C., and $\mathbf{R}_C + \mathbf{r}_j$ will be the position vector of the j^{th} mass relative to the center of the Earth. This equation can be re-written as

$$\begin{aligned} U &= -\mathrm{GM}_e \sum_{j=1}^{N} m_j / \left[\left(\mathbf{R}_C + \mathbf{r}_j \right) \cdot \left(\mathbf{R}_C + \mathbf{r}_j \right) \right]^{1/2} \\ &= -\mathrm{GM}_e \sum_{j=1}^{N} m_j \left[\mathbf{R}_C \cdot \mathbf{R}_C + 2\mathbf{R}_C \cdot \mathbf{r}_j + \mathbf{r}_j \cdot \mathbf{r}_j \right]^{-1/2} \\ &= -\left(\mathrm{GM}_e / R_C \right) \sum_{j=1}^{N} m_j \left[1 + \frac{2\mathbf{R}_C \cdot \mathbf{r}_j}{R_C^2} + \frac{\mathbf{r}_j \cdot \mathbf{r}_j}{R_C^2} \right]^{-1/2} \quad ; \end{aligned}$$

using the binomial expansion one gets

$$U = -\left(\frac{\mathrm{GM}_e m}{R_C}\right) - \left(\frac{\mathrm{GM}_e}{R_C}\right) \sum_{j=1}^{N} m_j \Bigg[- \frac{\mathbf{R}_C \cdot \mathbf{r}_j}{R_C^2} - \frac{1}{2}\frac{\mathbf{r}_j \cdot \mathbf{r}_j}{R_C^2} + + \frac{3}{2}\left(\frac{\mathbf{R}_C \cdot \mathbf{r}_j}{R_C^2}\right)^2 + O\left(\frac{|\mathbf{r}_j|^3}{R_C^3}\right)\Bigg] \quad . \tag{2.36}$$

The first term in RHS represents the potential energy of the system, if the mass of the whole system was concentrated at the orbital center and it is called U_{orb}. Inside the square bracket the leading term can be rewritten as

$$\left(\frac{\mathrm{GM}_e}{R_C^3}\right) \mathbf{R}_C \cdot \sum_{j=1}^{N} m_j \mathbf{r}_j \quad ,$$

Since the origin is assumed to be located at the center of mass, this term vanishes. $\mathbf{r}_j$'s have the same order of magnitudes as the tether lengths, and they are much smaller than the orbital radius R_C. Therefore we neglect the terms consisting of the third and higher order of $\frac{|\mathbf{r}_j|}{R_C}$ and Eq. 2.36 changes to

$$U = U_{orb} + \left(\mathrm{GM}_e/2R_C^3\right) \sum_{j=1}^{N} m_j \left[\mathbf{r}_j \cdot \mathbf{r}_j - 3\left(\mathbf{i} \cdot \mathbf{r}_j\right)^2\right] \quad . \tag{2.37}$$

2.4.3 Substitution of T and U into the Lagrange's equations

Now by utilizing Eqs. 2.23 and 2.37, equations of motion can be found from Eq. 2.17. Our generalized coordinates consist of only the attitude dynamics parameters; thus, T_{orb} and U_{orb} are independent of them. Moreover, the potential energy, U, does not depend on $\dot{q}_K$'s, i.e. $\frac{\partial L}{\partial \dot{q}_K} = \frac{\partial T}{\partial \dot{q}_K}$. Therefore one gets:

$$\frac{\partial L}{\partial q_K} = \sum_{j=1}^{N} m_j \frac{\partial \dot{\mathbf{r}}_j}{\partial q_K} \cdot \dot{\mathbf{r}}_j - \left(\mathrm{GM}_e/2R_C^3\right) \frac{\partial}{\partial q_K} \left(\sum_{j=1}^{N} m_j \left[\mathbf{r}_j \cdot \mathbf{r}_j - 3\left(\mathbf{i} \cdot \mathbf{r}_j\right)^2 \right] \right) \quad ,$$

$$\frac{d}{dt}\left(\frac{\partial L}{\partial \dot{q}_K}\right) = \frac{d}{dt}\left(\sum_{j=1}^{N} m_j \frac{\partial \dot{\mathbf{r}}_j}{\partial \dot{q}_K} \cdot \dot{\mathbf{r}}_j \right) = \sum_{j=1}^{N} m_j \left[\frac{d}{dt}\left(\frac{\partial \dot{\mathbf{r}}_j}{\partial \dot{q}_K}\right) \cdot \dot{\mathbf{r}}_j + \frac{\partial \dot{\mathbf{r}}_j}{\partial \dot{q}_K} \cdot \ddot{\mathbf{r}}_j \right] \quad .$$

The unit vector $\mathbf{i}$ is in the direction of local vertical at each instant, and it is independent of q_K's which are all attitude dynamics parameters. Consequently Eq. 2.17 reduces to

$$\left(\sum_{j=1}^{N} m_j \left[\frac{d}{dt}\left(\frac{\partial \dot{\mathbf{r}}_j}{\partial \dot{q}_K}\right) \cdot \dot{\mathbf{r}}_j + \frac{\partial \dot{\mathbf{r}}_j}{\partial \dot{q}_K} \cdot \ddot{\mathbf{r}}_j \right] \right) - \left(\sum_{j=1}^{N} m_j \frac{\partial \dot{\mathbf{r}}_j}{\partial q_K} \cdot \dot{\mathbf{r}}_j \right) +$$
$$\left(\left(\mathrm{GM}_e/R_C^3\right) \sum_{j=1}^{N} m_j \left[\mathbf{r}_j - 3\left(\mathbf{i} \cdot \mathbf{r}_j\right) \mathbf{i} \right] \cdot \frac{\partial \mathbf{r}_j}{\partial q_K} \right) = Q_K + \sum_{l=1}^{n} \Lambda_l \frac{\partial f_l}{\partial q_K} \quad , \tag{2.38}$$

where $K = 1, 2, \ldots, 3N-3$.

Employing the following two mathematical relations [31]

$$\frac{\partial \dot{\mathbf{r}}_j}{\partial \dot{q}_K} = \frac{\partial \mathbf{r}_j}{\partial q_K} \quad , \qquad \frac{d}{dt}\left(\frac{\partial \dot{\mathbf{r}}_j}{\partial \dot{q}_K}\right) = \frac{\partial \dot{\mathbf{r}}_j}{\partial q_K} \quad , \tag{2.39}$$

Eq. 2.38 simplifies to

$$\sum_{j=1}^{N} m_j \frac{\partial \mathbf{r}_j}{\partial q_K} \cdot \left\{ \ddot{\mathbf{r}}_j + \left(\mathrm{GM}_e/R_C^3\right) \left[\mathbf{r}_j - 3\left(\mathbf{i} \cdot \mathbf{r}_j\right) \mathbf{i} \right] \right\} = Q_K + \sum_{l=1}^{n} \Lambda_l \frac{\partial f_l}{\partial q_K} \; ,$$
$$K = 1, 2, \ldots, 3N-3 \quad . \tag{2.40}$$

Eqs. 2.12–2.14 and 2.21 define $\mathbf{r}_j$, in addition, $\frac{\partial \mathbf{r}_j}{\partial q_k}$'s can be obtained from them. $\ddot{\mathbf{r}}_j$ is equal to the total time derivative of Eq. 2.30

$$\ddot{\mathbf{r}}_j = \sum_{i=1}^{N-1} A_{ji} \left[(\dot{u}_i - \Omega v_i)\,\mathbf{i} + (\dot{v}_i + \Omega u_i)\,\mathbf{j} + \dot{w}_i\,\mathbf{k}\right] \quad . \tag{2.41}$$

u_i, v_i, w_i are presented in Eqs. 2.31–2.33, and $\dot{u}_i, \dot{v}_i, \dot{w}_i$ can be found by differentiating them with respect to time. Using all the above-mentioned relations, after some algebraic manipulations, equations of motion, Eq. 2.40, can be written as

$$\sum_{i=1}^{N-1} G_{ki}\, \ell_k \ell_i\, F_{\theta_{ki}} = (Q_{\theta_k} + \sum_{l=1}^{n} \Lambda_l \frac{\partial f_l}{\partial \theta_k})/m\,, \tag{2.42}$$

$$\sum_{i=1}^{N-1} G_{ki}\, \ell_k \ell_i\, F_{\phi_{ki}} = (Q_{\phi_k} + \sum_{l=1}^{n} \Lambda_l \frac{\partial f_l}{\partial \phi_k})/m\,, \tag{2.43}$$

$$\sum_{i=1}^{N-1} G_{ki}\, F_{\ell_{ki}} = (Q_{\ell_k} + \sum_{l=1}^{n} \Lambda_l \frac{\partial f_l}{\partial \ell_k})/m\,, \tag{2.44}$$

$$k = 1, 2, \ldots, N-1\,.$$

where the parameters G_{ki}'s are given by

$$G_{ki} = \sum_{j=1}^{N} \mu_j\, A_{jk}\, A_{ji} \quad . \tag{2.45}$$

μ_j, A_{jk}, A_{ji} are the mass parameters as defined before in Eqs. 2.5 and 2.10, respectively. $F_{\theta_{ki}}, F_{\phi_{ki}}, F_{\ell_{ki}}$ are functions of the generalized coordinates and their derivatives, given in the following expressions

$$\begin{aligned} F_{\theta_{ki}} = & \Big[\{(\ddot{\theta}_i + \dot{\Omega}) + 2\,(\dot{\ell}_i/\ell_i)\,(\dot{\theta}_i + \Omega)\} \cos(\theta_k - \theta_i) + 3\,(\mathrm{GM}_e/R_C^3) \sin\theta_k \cos\theta_i \\ & - \{(\mathrm{GM}_e/R_C^3) + (\ddot{\ell}_i/\ell_i) - (\dot{\theta}_i + \Omega)^2 - \dot{\phi}_i^2\} \sin(\theta_k - \theta_i) \Big] \cos\phi_k \cos\phi_i \\ & + \Big[\{\ddot{\phi}_i + 2\,(\dot{\ell}_i/\ell_i)\,\dot{\phi}_i\} \sin(\theta_k - \theta_i) \\ & - 2\,\dot{\phi}_i\,(\dot{\theta}_i + \Omega)\cos(\theta_k - \theta_i)\Big] \cos\phi_k \sin\phi_i \quad . \end{aligned} \tag{2.46}$$

$$
\begin{aligned}
F_{\phi_{ki}} = \; & \Big[\ddot{\phi}_i + 2\,(\dot{\ell}_i/\ell_i)\,\dot{\phi}_i\Big] \\
& \Big[\cos\phi_k \;\cos\phi_i + \sin\phi_k \;\sin\phi_i \;\cos(\theta_k - \theta_i)\Big] \\
& + 3\;(\mathrm{GM}_e/R_C^3)\,\sin\phi_k \;\cos\phi_i \;\cos\theta_k \;\cos\theta_i \\
& + \Big[(\mathrm{GM}_e/R_C^3) + (\ddot{\ell}_i/\ell_i) - \dot{\phi}_i^2\Big] \\
& \Big[\cos\phi_k \;\sin\phi_i - \cos\phi_i \;\sin\phi_k \;\cos(\theta_k - \theta_i)\Big] \\
& - \Big[\{(\ddot{\theta}_i + \dot{\Omega}) + 2(\dot{\ell}_i/\ell_i)(\dot{\theta}_i + \Omega)\}\sin(\theta_k - \theta_i) \\
& - (\dot{\theta}_i + \Omega)^2 \;\cos(\theta_k - \theta_i)\Big]\;\sin\phi_k \;\cos\phi_i \\
& + 2\,(\dot{\theta}_i + \Omega)\,\dot{\phi}_i\,\sin(\theta_k - \theta_i)\;\sin\phi_k \;\sin\phi_i \quad ,
\end{aligned}
\tag{2.47}
$$

$$
\begin{aligned}
F_{\ell_{ki}} = \; & \Big[\ddot{\ell}_i - \ell_i\,(\dot{\theta}_i + \Omega)^2 - \ell_i\dot{\phi}_i^2 + (\mathrm{GM}_e/R_C^3)\,\ell_i\Big] \\
& \Big[\cos\phi_k \;\cos\phi_i \;\cos(\theta_k - \theta_i) + \sin\phi_k \;\sin\phi_i\Big] \\
& + \ell_i\,(\dot{\theta}_i + \Omega)^2 \;\sin\phi_k \;\sin\phi_i - 3\,(\mathrm{GM}_e/R_C^3)\,\ell_i \\
& \cos\phi_k \;\cos\phi_i \;\cos\theta_k \;\cos\theta_i \\
& + \Big[\{(\ddot{\theta}_i + \dot{\Omega}) + 2(\dot{\ell}_i/\ell_i)(\dot{\theta}_i + \Omega)\}\sin(\theta_k - \theta_i)\Big] \\
& \ell_i \;\cos\phi_k \;\cos\phi_i + \Big[\ddot{\phi}_i + 2\,(\dot{\ell}_i/\ell_i)\,\dot{\phi}_i\Big] \\
& \Big[\sin\phi_k \cos\phi_i - \cos\phi_k \sin\phi_i \cos(\theta_k - \theta_i)\Big]\ell_i \\
& - 2\ell_i(\dot{\theta}_i + \Omega)\dot{\phi}_i \cos\phi_k \sin\phi_i \sin(\theta_k - \theta_i) \quad .
\end{aligned}
\tag{2.48}
$$

These expressions reveal that even with the assumptions made here the equations are quite complicated. Degree of complexity grows with a rate much higher than proportional to the number of bodies.

We have not discussed about the RHS's of the equations until now. Analyzing different terms of each equation from the point of view of the forces represented by them, is helpful in having a clear understanding of the RHS's roles. The LHS's include the effect of inertial forces, through the kinetic energy, T, as well as the effect of the conservative active forces, through the potential energy, U. An active or driving force is a force that performs work when the system undergoes a virtual displacement compatible and in conformity with the constraints. In the RHS's the generalized forces, Q_{θ_k}'s, Q_{ϕ_k}'s and Q_{ℓ_k}'s account for the effect of all the driving forces that are not considered in the LHS's, i.e. the nonconservative driving forces. The second terms in the RHS's are due to the constraint forces. In summary we have divided the forces into three kinds; inertial, constraint and driving. The driving forces could be conservative or nonconservative.

The exact definition of the generalized force Q_K, corresponding to the generalized coordinate q_K, $K = 1, 2, \ldots, 3N-3$, is that, it is a scalar quantity such that for a virtual displacement in q_K alone (all other coordinates held fixed) $Q_K \delta q_K$ is equal to the work done by all driving nonconservative forces[2] acting on the system. As explained in the beginning of the chapter, in this study we neglect the perturbing effect of the solar radiation. In addition we concentrate on the cases where aerodynamic and electrodynamic perturbations are negligible, and we do not plan to employ any thruster for controlling the motion. Therefore, there are no external driving forces. However, there are internal driving forces, tensions inside the tethers. The tension forces will perform work when virtual displacements occur in length degrees of freedom ($\delta\ell_k$'s), but they do not perform work when the system undergoes virtual displacements in angular degrees of freedom ($\delta\theta_k$'s and $\delta\phi_k$'s). Therefore the Q_{θ_k}'s and Q_{ϕ_k}'s are zero and we also do not plan to impose any constraints on these degrees of freedom, i.e. the RHS's of the θ_k's and ϕ_k's equations, the Eqs. 2.42 and 2.43, are zero

[2]or possibly driving conservative forces that are not taken into account in potential energy at the LHS of the equation.

For a virtual displacement in ℓ_k, $k = 1, 2, \ldots, N-1$, the work performed is equal to $-\ \mathrm{T}_k\ \delta\ell_k$, where T_k represents the magnitude of the tension force in the k^{th} tether ($\mathbf{T}_k$). The minus sign indicates that the tension force acts in the opposite direction of a positive $\delta\ell_k$ (increase in length). Thus one obtains

$$Q_{\ell_k} = -\mathrm{T}_k \quad , \qquad\qquad k = 1, 2, \ldots, N-1 \quad . \tag{2.49}$$

One should notice a special case, where the lengths of some or all of the tethers are given as specified functions of time, $\ell_k = \ell_k(t)$ (this includes the case of a constant length). The length corresponding to each of these tethers will not be a generalized coordinate anymore and the equations $\ell_k = \ell_k(t)$ will be constraint equations. The tensions in these tethers will not be a driving force anymore, but a constraint force [32]. Q_{ℓ_k} will be zero, but tension will appear in the RHS with the same form as before, $-\mathrm{T}_k$. This time the appearance of the tension will be through the term $\sum_{l=1}^{n} \Lambda_l \frac{\partial f_l}{\partial \ell_k}$ as the constraint force. Eq. 2.44 will not describe the motion of the system anymore, but will be used to find the necessary constraint force, the tension force. Therefore, the equations of motion for a multi-body tethered satellite system under consideration are

$$\sum_{i=1}^{N-1} G_{ki}\ \ell_k \ell_i\ F_{\theta_{ki}} = 0 \quad , \tag{2.50}$$

$$\sum_{i=1}^{N-1} G_{ki}\ \ell_k \ell_i\ F_{\phi_{ki}} = 0 \quad , \qquad\qquad k = 1, 2, \ldots, N-1 \tag{2.51}$$

$$\sum_{i=1}^{N-1} G_{ki}\ F_{\ell_{ki}} = -\mathrm{T}_k/m \quad . \tag{2.52}$$

Now after obtaining the equations of motion we will present a brief explanation of the computer code that is used for numerical solution of these equations.

2.5 The Computer Code

Based on the equations of motion presented in Eqs. 2.50–2.52, together with relations 2.5, 2.10 and 2.45–2.48, a simulation code is developed for the general case with the possibility of having N number of bodies. The code is in FORTRAN language. The equations are all of the second order; hence, each of them is changed to two first order equations. Then with $N-1$ tethers and 3 second order equations for each tether, there will be altogether $6(N-1)$ first order nonlinear, coupled, ordinary differential equations. These are solved using the IMSL library. Our problem is an initial-value problem, therefore we choose the subroutine that uses the Bulirsch-Stoer extrapolation method[3].

This method is efficient for nonstiff problems where the accuracy requirements are high and/or the derivative evaluations are inexpensive, which is our case. The subroutine (DIVPBS, D indicates that the routine is double precision) keeps an estimated global error proportional to a user-specified tolerance. It uses rational functional extrapolation and is based on the midpoint rule in a slightly modified form [33]. The algorithm is described in detail by Bulirsch and Stoer [34] and was translated into FORTRAN by Clark [35]; it was further modified by Fox [36].

The program is debugged and its correctness is justified, by comparing its outputs for the small angles with the results of approximate analytical solutions, which are valid only for small angles. These test cases include the pure in-plane and out-of-plane motions for the small, with a specified length rate, exponential or linear, for two-body and three-body systems. For each case the values for the angles, the 1^{st} and 2^{nd} derivatives of the angles and the tension in the tether (or tethers) are compared. Naturally the initial values for the angles are chosen to

[3]See the "MATH/LIBRARY, FORTRAN Subroutines for Mathematical Applications" manual from IMSL, Inc., Version 1.0, April 1987.

be zero or very small, and they are allowed to increase up to a certain value that keeps the smallness of the problem valid. In the final version of the program there is good agreement between the numerical and approximate analytical results up to angles of the order of 20^o for two-body examples. This is a relatively large value and gives us reasonable confidence in the code. In three-body systems, where the accumulation of difference between the approximate analytical and numerical solutions is much faster, this value is about 8.5^c, which is still in the upper limits of what one usually considers as small angle. In addition, the program was run for some cases available in the literature and comparison of the results was performed and complete agreement was obtained.

Chapter 3

The Liapunov Approach

3.1 Introduction

As we will see shortly, an uncontrolled retrieval motion is not stable. A control scheme can be considered successful only if it can lead to a stable retrieval motion. Because of the advantages of the reel rate control scheme, mentioned in Chapter 1, here we concentrate on this method of control. Normally the first ideas of a control law are obtained from an approximate analytical method, then the numerical solution of the exact equations are carried out for verification and possible trial and error type modifications. In this chapter the aim is to use Liapunov's direct or second method for this purpose. The first method of Liapunov is based on the linearization of the system. On the contrary the second method is applicable to the stability in the large motion and it is a very powerful method, but as will be discussed in this chapter, it is a rather difficult and tricky method to apply.

There are countless number of references available on the general theory of the Liapunov's direct method, among which Reference [37] is widely used. The application of the method to the space systems has been extensive in the past. As far as spacecraft attitude control is concerned, in 1968 Mortenson [38] applied the method for attitude control of an arbitrary rigid body. Since then many investigators have used this method for analyzing the control problems associated with the spacecraft attitude maneuvers, among which we can mention References [39]–[45]. Fujii and Ishijima [46] used the method for controlling the deployment and retrieval of a Shuttle-based two-body tethered system. Recently, Vadali and Kim [47] used a Liapunov function based on the integrals of motion to perform a rather broader and more complete study on the control of **two-body** tethered systems. They developed tension control laws as well as various combinations of tension control, reel rate control and thruster control laws. As will be seen in this chapter, the proposed reel rate law have certain weaknesses to be employed unaided and these weaknesses must be removed.

One of the main objectives of this thesis is to develop a reel rate control law for stabilizing the retrieval of a **multi-body** tethered satellite system. Since the principles are the same for two-body and multi-body systems, normally the primary developments should be done on the simpler case, i.e., two-body systems, and the outcomes be extended to multi-body systems. The method of formulation expressed in Chapter 2 makes this extension very easy. This is specially so because of representing the equations of motion, Eqs. 2.50–2.52, in the form of summations over the entire set of tethers (or bodies in the G_{k_i}'s) of the system.

3.2 Comments on the Effects of Reel Rate on the Motion

The general form of the equations of motion for a multi-body tethered system was presented in Eqs. 2.50–2.52 together with relations 2.5, 2.10 and 2.45–2.48. These equations for two-body systems take the form of

$$\ddot{\theta} + 2\left[(\dot{\ell}/\ell) - \dot{\phi}\tan\phi\right](\dot{\theta}+\Omega) + 3\Omega^2\cos\theta\ \sin\theta = 0 \ , \tag{3.1}$$

$$\ddot{\phi} + 2(\dot{\ell}/\ell)\dot{\phi} + \left[(\dot{\theta}+\Omega)^2 + 3\Omega^2\cos^2\theta\right]\cos\phi\ \sin\phi = 0 \ , \tag{3.2}$$

$$\ddot{\ell} - \ell\left[\dot{\phi}^2 + (\dot{\theta}+\Omega)^2\cos^2\phi + 3\Omega^2\ \cos^2\phi\ \cos^2\theta - \Omega^2\right] = -\mathrm{T}/M \ , \tag{3.3}$$

where $M = m_1\, m_2/(m_1+m_2)$ and it has been assumed that the orbit is circular with an orbital rate Ω ($\dot{\Omega}$ is set to zero). It is convenient to define a nondimensional time $\tau = \Omega t$. Since the orbit is circular, τ is nothing but the true anomaly. If prime denotes differentiation with respect to τ, then Eqs. 3.1-3.3 transform to

$$\theta'' + 2\left[(\ell'/\ell) - \phi'\tan\phi\right](\theta'+1) + 3\cos\theta\ \sin\theta = 0 \ , \tag{3.4}$$

$$\phi'' + 2(\ell'/\ell)\phi' + \left[(\theta'+1)^2 + 3\cos^2\theta\right]\cos\phi\ \sin\phi = 0 \ , \tag{3.5}$$

$$\ell''/\ell - \left[\phi'^2 + (\theta'+1)^2\cos^2\phi + 3\ \cos^2\phi\ \cos^2\theta - 1\right] = -\hat{\mathrm{T}} \ , \tag{3.6}$$

where $\hat{\mathrm{T}} = \mathrm{T}/\,(M\,\ell\,\Omega^2)$. Here ℓ'/ℓ, is not exactly the nondimensional reel rate since ℓ is varying with time, but it can be considered as some sort of an indicator of the nondimensional reel rate.

By examining these equations, one can get some general ideas. Among the most relevant to our study is that the behaviour of both in-plane and out-of-plane rotations depends to a great extent on ℓ'/ℓ. Normally θ' and ϕ' are much smaller than 1, thus $(1+\theta')$ is much larger than ϕ'. This means that the effect of ℓ'/ℓ on the in-plane motion, θ, is considerably higher than its effect on the out-of-plane motion, ϕ.

One of the major effects of the ℓ'/ℓ on the librational motion is its differing role during the deployment and retrieval. In the θ and ϕ equations, ℓ'/ℓ appears in the coefficients of θ' and ϕ', respectively. Consider the cases of uncontrolled deployment and retrieval, i.e. having specific variations of length with time without a feedback control system. The specified variation of length must be somehow imposed by the reeling system, but the hardware design of the problem is not of interest to this thesis. For deployment, ℓ'/ℓ is positive, and it will act as a damping factor; thus it damps out the motion of θ and ϕ and stabilizes the motion. For retrieval ℓ'/ℓ is negative, then it will not act as a damping factor; on the contrary, it will add energy to the system and it has a destabilizing effect.

In other words, the deployment can be performed without a feedback control system, but we do not expect a possible retrieval without a feedback control system. Figs. 3.1 and 3.2 show the numerical simulation results for uncontrolled exponential retrieval ($\ell'/\ell = -c$) for two different values of c. They reveal that in-plane angle grows dramatically fast. However, in this very short period of time one can hardly feel any growth in the out-of-plane angle. ℓ'/ℓ destabilizes the in-plane motion much faster; this is in accordance with the previously mentioned fact that ℓ'/ℓ affects the in-plane libration with a much higher degree than out-of-plane motion.

Therefore retrieval is the critical phase of the motion and that is why we concentrate in this thesis on controlling the retrieval phase. As was discussed in the introductory Chapter, the thruster and offset control laws have difficulty in implementation and among the tension and reel rate control laws we would prefer reel rate laws for controlling the librational motion. The presence of a reeling system is inevitable in a tethered satellite system, thus by designing a reel rate control law one do not add that much of the hardware to the system for controlling librational motion.

Since ℓ'/ℓ affects the in-plane motion with a much higher degree, it is expected that controlling the in-plane motion solely by a reel rate law (i.e., by varying ℓ'/ℓ) will be remarkably simpler than the out-of-plane motion. This is very evident in the previous works on reel late (or length rate) control laws [13, 14,16,17,29]. The in-plane motion has been controlled by these laws but not the out-of-plane motion, except in [29] where a reel rate law that controls the in-plane and out-of-plane librations of a two-body system at the same time, has been presented.

Another observation that can be made from these equations is that the coupling between θ and ϕ motions is a nonlinear one. If the reel rate law is supposed to control the out-of-plane motion along with the in-plane motion, it seems logical to expect a nonlinear dependence on the out-of-plane librational motion, in the reel rate expression.

3.3 Liapunov's Second Method

Before expressing the stability criteria according to this method we discuss some related terms.

For a dynamical system, the state of the system is described in terms of a set of *state variables*, represented here by; $x_1(t), x_2(t), \ldots, x_P(t)$ (the components of the state vector, $\mathbf{x}$). The state variables are those which determine the future behavior of a system when its present state and excitation signals are known [48, 49]. Even though not the only possible one, the generalized coordinates and their derivatives comprise a good candidate for the set of state variables. In terms of the state variables, the equations of motion are usually expressed in the form of first-order differential equations as

$$\dot{x}_i = g_i(x_1, x_2, \ldots, x_P, Q_1, Q_2, \ldots, Q_p, t) \ , \qquad i = 1, 2, \ldots, P \ . \tag{3.7}$$

Here p is the system's degrees of freedom, and $P = 2p$, Q's are the generalized forces, and the state variables will be equalized with the generalized coordinates and their derivatives; $q_1, q_2, \ldots, q_p, \dot{q}_1, \dot{q}_2, \ldots, \dot{q}_p$.

Another term that must be defined is *positive (negative) definiteness* of a function. Consider a real continuous function of state variables, $W(\mathbf{x})$, possessing continuous first partial derivatives with respect to state variables, x_i , $i = 1, 2, \ldots, P$, inside a spherical domain D_h, where h represents the radius of the sphere i.e. : $\|\mathbf{x}\| \leq h$. The following definitions can be expressed for this function [37]:

1. The function $W(\mathbf{x})$ is called *positive (negative) definite* in the domain D_h if $W(\mathbf{x}) > 0 (< 0)$ for all $\mathbf{x} \neq \mathbf{0}$ and $W(\mathbf{0}) = 0$.

2. The function $W(\mathbf{x})$ is called *positive (negative) semidefinite* in the domain D_h if $W(\mathbf{x}) \geq 0 (\leq 0)$, i.e. it can vanish for some $\mathbf{x} \neq \mathbf{0}$ in D_h. The positive (negative) definite and semidefinite functions are also referred to as *sign-constant.*

3. The function $W(\mathbf{x})$ is called *indefinite* if it can assume both positive and negative values in the in the domain D_h, no matter how small is the value of h.

Now *the Stability Criterion* according to Liapunov's second method is:

"If there exists a positive definite scalar function of the state variables, $V(\mathbf{x})$, whose total time derivative $\dot{V}(\mathbf{x})$ is negative definite or semidefinite along every system's trajectory Eq. 3.7, then the trivial solution $\mathbf{x} = \mathbf{0}$ is stable, i.e. the system is stable at the origin of the state space."

The function $V(\mathbf{x})$ mentioned in this theorem is called *Liapunov function.* This method is very powerful and has two main features: 1. The method can examine the stability of the nonlinear systems for motion in the large. 2. It can reveal the stability of the system only by utilizing the differential equations of the system without actually solving them. On the other hand, the main disadvantage of this method is its complexity of applying. It requires creating a Liapunov function which may not be always possible. Since at present there are no established criteria for the selection of Liapunov function except for linear autonomous systems, Liapunov's direct method should be regarded as more of a philosophy of approach than a method. The fact that for a given system a proper Liapunov function cannot be found gives no indication of the system's instability or stability.

3.4 Liapunov's Approach for Tethered Satellite Systems

For mechanical systems the situation is not altogether that bad. In these systems there are some good candidates for the Liapunov function: motion integrals or momentum integrals such as the Jacobi integral, the Hamiltonian, etc. Here, for tethered satellite systems we investigate the possibility of a proper Liapunov function from the Hamiltonian. The Hamiltonian of a dynamical system is defined as

$$H = \left(\sum_{i=1}^{K} \dot{q}_i \frac{\partial L}{\partial \dot{q}_i} \right) - L \quad , \tag{3.8}$$

where K is the number of degrees of freedom, q_i's are the generalized coordinates, L is the system's Lagrangian. $\dfrac{\partial L}{\partial \dot{q}_i}$ is called *generalized momentum*, and as explained in Chapter 2 it is equal to $\dfrac{\partial T}{\partial \dot{q}_i}$, where T represents the kinetic energy of the system. As discussed in the introduction of this chapter, we start with the investigation on two-body systems.

Eqs. 2.23 and 2.37 represent the general expressions for the kinetic and potential energies of multi-body tethered systems. In a two-body system they take the form of [50]

$$T = \frac{1}{2} M \left\{ \ell^2 \left[(\dot{\theta} + \Omega)^2 \cos^2\phi + \dot{\phi}^2 \right] + \dot{\ell}^2 \right\} \quad , \tag{3.9}$$

$$U = \frac{1}{2} M \, \ell^2 \, \Omega^2 \left[1 - 3 \cos^2\theta \cos^2\phi \right] \quad , \tag{3.10}$$

or in the nondimensional form

$$\hat{T} = \frac{T}{M \, \ell^2 \, \Omega^2} = \frac{1}{2} \left\{ \left[(\theta' + 1)^2 \cos^2\phi + \phi'^2 \right] + (\ell'/\ell)^2 \right\} \quad , \tag{3.11}$$

$$\hat{U} = \frac{U}{M \, \ell^2 \, \Omega^2} = \frac{1}{2} \left[1 - 3 \cos^2\theta \cos^2\phi \right] \quad . \tag{3.12}$$

From the expressions for $\hat{T}$ and $\hat{U}$ we can determine the nondimensional Hamiltonian, $\hat{H} = H/(M \, \Omega^2 \, \ell^2)$ as

$$\hat{H} = \frac{1}{2} \left\{ \left[\phi'^2 + \theta'^2 \cos^2\phi + 3 \sin^2\theta \cos^2\phi + 4 \sin^2\phi - 3 \right] + (\ell'/\ell)^2 \right\} \quad . \tag{3.13}$$

As was mentioned before, we believe that the Hamiltonian is a good candidate for a Liapunov function. Therefore, we plan to use the part in the square bracket, the part related to librational motion, in the Liapunov function.

The Liapunov function used by Vadali and Kim [47] for the case of combined reel rate and thruster control laws was

$$V = C_1\left[\phi'^2 + \theta'^2 \cos^2\phi + 3\sin^2\theta\cos^2\phi + 4\sin^2\phi\right] + \frac{K_1}{2}(\lambda - \lambda_f)^2 \,. \quad (3.14)$$

Here λ is a nondimensional length equal to ℓ/ℓ_{ref}, where ℓ_{ref} is a reference length and λ_f is the final value of λ. As can be observed, this is intimately related to the nondimensional Hamiltonian, but they obtained it from the integrals of motion. It is clear that it could also be found from the Hamiltonian of the system. For reasons to be discussed later, the reel rate law obtained from this Liapunov function has certain weaknesses, and it must be accompanied by a thruster controller.

Here we propose to modify the length dependence part in the Liapunov function, to a logarithmic function in order to eliminate the necessity of a thruster:

$$V = C\left[\phi'^2 + \theta'^2 \cos^2\phi + 3\sin^2\theta\cos^2\phi + 4\sin^2\phi\right] + \ln(\ell/\ell_f)\,. \quad (3.15)$$

It will be shown that a reel rate law which makes this function satisfy all of the conditions for a proper Liapunov function, guaranteeing the system's stability, will have a much better performance than the reel rate based on the Liapunov function given by Eq. 3.14. Here ℓ_f is the final tether length and C is a positive constant. This function is clearly positive definite during the retrieval, since during the retrieval stage of the motion $\ell \geq \ell_f$, making the last term positive with the final value of zero. Of course, the terms within the square bracket are positive definite for all stages, with the exception of the equilibrium value of zero. The derivative of this function with respect to the nondimensional time τ, is

$$\begin{aligned} V' &= C\left[2\,\theta'\,\theta''\cos^2\phi - 2\,\theta'^2\phi'\cos\phi\sin\phi + 6\,\theta'\sin\theta\cos\theta\cos^2\phi\right.\\ &\quad \left.-\ 6\,\phi'\sin^2\theta\cos\phi\sin\phi + 2\,\phi'\phi'' + 8\,\phi'\sin\phi\cos\phi\right] + \ell'/\ell\,. \quad (3.16)\end{aligned}$$

in this relation θ'' and ϕ'' must be substituted from the equations of motion, i.e. along the system's trajectory. Using Eqs. 3.4 and 3.5, after some simplification one gets

$$V' = -(\ell'/\ell)\left\{-1 + 4C\left[\theta'(1+\theta')\cos^2\phi + \phi'^2\right]\right\} \quad . \tag{3.17}$$

Now let us consider the following reel rate law for stabilizing the motion

$$\ell'/\ell = c\left\{-1 + \mathrm{K}\left[\theta'(1+\theta')\cos^2\phi + \phi'^2\right]\right\} \quad , \tag{3.18}$$

where c is a positive constant and $\ell'/\ell = -c$ gives rise to an exponential retrieval. If K is chosen as $4C$, one gets

$$V' = -c\left\{-1 + \mathrm{K}\left[\theta'(1+\theta')\cos^2\phi + \phi'^2\right]\right\}^2 \quad . \tag{3.19}$$

As one can see, the reel rate law of the Eq. 3.18 makes V' negative semi-definite (since we can have $V' = 0$ while $\phi,\ \theta \neq 0$) and stabilizes the system in the sense of Liapunov, but not asymptotically. Here $K = 4C$ is the common constant gain for both the pitch and roll motions.

The reel rate law proposed by Vadali and Kim [47] is

$$\ell'/\ell = \mathrm{K}_1(-1 + \ell_f/\ell) + \mathrm{K}_2\left[\theta'(1+\theta')\cos^2\phi + \phi'^2\right](\ell_{ref}/\ell)^2 \quad , \tag{3.20}$$

where K_1 is the retrieval constant, and K_2 is the control gain. The reference length, ℓ_{ref}, is chosen as the initial tether length by them. This reel rate law must be accompanied by an additional thruster control law

$$\hat{F} = -K_3 (\ell/\ell_{ref}) \phi' \, . \tag{3.21}$$

The difficulty with the control law given by Eq. 3.20 is the presence of the factor $(\ell_{ref}/\ell)^2$, which increases to as high as 10^8 (for an example with $\ell_{ref} = \ell(0) =$ 100.0 km and $\ell_f = 10.0$ m) as retrieval progresses, i.e., as length ℓ becomes smaller. Hence, either the gain K_2 must be chosen very small, implying that there is hardly any control (especially on out-of-plane motion) or if K_2 is not small, the retrieval process becomes very slow; in fact, there may not be any retrieval after some time. Thus, there is a need for the additional thruster control in their control scheme.

On the other, hand in the Liapunov function used here, i.e. Eq. 3.15, the quadratic length dependence is replaced by a logarithmic one. This has eliminated the necessity of having the length in the denominator in the reel rate law, in order to make V' negative semi-definite. Then it can extract energy from the system to stabilize the in-plane and out-of-plane motions without the help of any out-of-plane thruster and at the same time perform a retrieval operation.

For a certain set of initial conditions, we have numerically simulated the resulting motion using the proposed reel rate law (Eq. 3.18) and that using Vadali and Kim's reel rate law of Eq. 3.20 without the presence of thrusters ($\hat{F} = 0$). The analysis is performed for a wide range of c, K, K_1, K_2 ($c = K_1$ varying from 0.05 to 0.6; K from 0.05 to 20, K_2, equivalent to c K from 0.0025 to 12). The results show that the reel rate law proposed here can control the retrieval motion for a wide range of c and K, but the reel rate law of Eq. 3.20, alone and without the thruster, does not lead to any acceptable retrieval because after a short while ℓ starts to oscillate. Only one example of each case is presented in Figs. 3.3 and 3.4 respectively. Fig. 3.3 shows the results for $c = 0.34$ and K$= 5.0$ with reel rate law of Eq. 3.18, while Fig. 3.4 presents the resulting motion for the corresponding values of the coefficients ($K_1 = 0.34$ and $K_2 = 0.34 \times 5.0 = 1.7$)

with reel rate of Eq. 3.20. (Fig. 3.4 c) shows the oscillations in the magnitude of the tether length while one employs the reel rate law of Eq. 3.20.

Comparing the resulting motion for the reel rate law given by Eq. 3.18 (Fig. 3.3) with the uncontrolled exponential retrievals (Figs. 3.1 and 3.2), one can notice the remarkable improvement. The reel rate law performs an acceptable retrieval; however, it still has to be improved since the retrieval time is rather high. The reel rate presented in Eq. 3.18 satisfies the presence of the nonlinear dependence on the out-of-plane motion in the control law. However, there is also a quadratic, nonlinear term from the in-plane motion. If a linear in-plane feedback is sufficient for controlling the motion, it is definitely better to replace the linear plus quadratic in-plane terms with just a linear one. This is because a quadratic term is always positive and will decrease the average value of the retrieving rate. Furthermore, the possibility of decreasing the out-of-plane limit cycle amplitude should be examined. In the present reel rate law, the in-plane and out-of-plane motions have a common control gain. The out-of-plane amplitude can be decreased by assigning different control gains to the in-plane and out-of-plane feedbacks, and choosing a higher value for out-of-plane gain

In the next chapter we will investigate the effectiveness of the two new reel rate laws which are in conformity with the above-mentioned corrective points. For this purpose, we will use the energy dissipation approach together with the averaging method. The reason we are choosing another approach for verifying the effectiveness of the succeeding reel rate laws is the difficulty involved in finding a proper Liapunov function. Since the reel rate laws for the two-body systems presented in the next chapter are superior to the present one, only the former are extended to multi-body systems.

Chapter 4

The Energy Dissipation Approach and Averaging Method

4.1 Introduction

As mentioned in the previous chapter, it seems necessary to develop a reel rate law for the retrieval phase superior to the one obtained from the Liapunov approach. The averaging method and the so-called energy dissipation approach are chosen in this chapter for analyzing the performance of the alternate reel rate laws. Among the available literature on tethered satellites, the energy dissipation approach has been used by Xu [29] and Lorenzini [14]. The former was concentrated on two-body systems while the latter studied the in-plane motion of three-body systems. Here we are after finding reel rate laws to stabilize the in-plane as well as out-of-plane librations, for multi-body systems.

In contrast to the previous chapter where we considered the motion in the large through the powerful Liapunov's direct method, in this chapter we perform approximate analyses based on the equations for small motion. The averaging method basically presents a linearized model to find an approximate response for a nonlinear system. On the other hand, even though the concept of the energy dissipation approach holds for nonlinear equations as well, this approach will be also applied to a linearized approximate model. The reason for not using the nonlinear exact equations of motion with the energy dissipation approach is that the mathematics involved in the analysis would be too complicated to give any information about an appropriate reel rate law with a reasonable effort. It should also be noticed that when the nonlinear equations are used, the analysis may get more tedious and time consuming than for the Liapunov approach. Then the whole point of switching from the Liapunov approach to another one will be lost.

Therefore, the procedure which will be followed here is that the analytical part will be based on the simplified linearized equations, but the numerical simulation, which is the final verification of the control law, will be based on the exact nonlinear equations. For the reasons already mentioned in this thesis, this chapter starts with developing satisfactory control laws for two-body systems and then they will be extended to multi-body systems. The averaging method is a well established method and is discussed in any textbook concerning the dynamical analysis of nonlinear systems. But the ideas behind the energy dissipation approach must be explained here; this is the subject of the next section.

4.2 Energy Dissipation Approach for Two-body Tethered Satellite Systems

The nondimensional equations for the motion in the large of a two-body tethered system, with the assumptions made in this thesis, were presented in Eqs. 3.4–3.6.

With the usual approximation of the trigonometric functions for small angles, the equations governing small in-plane and out-of-plane motions can be written as

$$\theta'' + 2(\ell'/\ell)(\theta' + 1) + 3\theta = 0 \quad , \tag{4.1}$$

$$\phi'' + 2(\ell'/\ell)\phi' + 4\phi = 0 \quad . \tag{4.2}$$

Because of the dependence of the final steady state of the retrieval process on the nature of the reel rate law, one would have to specify first the nominal form of the reel rate law that one is interested in. Here we concentrate on the reel rate laws that have a nominal exponential variation, i.e.,

$$\ell'/\ell = -c + f(\theta, \theta', \phi, \phi') \quad , \tag{4.3}$$

where c is a positive constant so that $\ell'/\ell = -c$ gives rise to an exponential retrieval. The function f contains the necessary feedback for stabilizing the in-plane and out-of-plane librations. If the control law is a successful one, it would guide the system towards a stable configuration with *constant* in-plane and out-of-plane equilibrium angles. For finding these constant values, which will be denoted here by θ_e and ϕ_e, one should set $\theta', \theta'', \phi', \phi''$ equal to zero in Eqs. 4.1 and 4.2. At this steady state, the feedback f normally vanishes, because it is a function of the deviation from this state. Thus θ_e and ϕ_e are given by

$$2(-c) + 3\theta_e = 0 \implies \theta_e = 2c/3 \qquad \text{or} \qquad c = (3/2)\theta_e \quad , \tag{4.4}$$

$$4\phi_e = 0 \implies \phi_e = 0 \quad . \tag{4.5}$$

If nonlinearities are taken into account, then the terminal phase of the motion consists of limit-cycle oscillations about θ_e and ϕ_e. In this case, θ_e and ϕ_e represent approximations for the average value of the pitch and roll angles over a period of oscillation.

Substitution of Eq. 4.3 into Eqs. 4.1 and 4.2 yields

$$\theta'' - 2c\theta' + 2f(\theta' + 1) + (3\theta - 2c) = 0 \quad , \tag{4.6}$$

$$\phi'' - 2c\phi' + 2f\phi' + 4\phi = 0 \quad . \tag{4.7}$$

These equations of motion can be re-written as

$$\theta'' + 3(\theta - \theta_e) = 2c\theta' - 2f(\theta' + 1) \quad , \tag{4.8}$$

$$\phi'' + 4\phi = 2(c - f)\phi' \quad . \tag{4.9}$$

The reason for this rearrangement lies in the role of each term according to energy considerations. Each term in Eqs. 4.8 and 4.9 represents a nondimensional force acting on the system, including the inertial forces. Multiplication of Eqs. 4.8 and 4.9 by θ' and ϕ' respectively and integration with respect to τ give us an indication of what happens to the total energy (kinetic and potential) of the system due to retrieval and control actions, as discussed below. We have

$$\int_o^T [\theta'' + 3(\theta - \theta_e)]\,\theta' \mathrm{d}\tau \;=\; \int_o^T [2c\theta' - 2f(\theta' + 1)]\,\theta' \mathrm{d}\tau \quad , \tag{4.10}$$

$$\int_o^T [\phi'' + 4\phi]\,\phi' \mathrm{d}\tau \;=\; \int_o^T [2(c - f)\phi']\,\phi' \mathrm{d}\tau \quad . \tag{4.11}$$

Carrying out integrations of the left-hand sides results in

$$\int_o^\tau \left[\theta'' + 3(\theta - \theta_e)\right]\theta' \, d\tau = \left[\frac{1}{2}(\theta')^2 - \frac{1}{2}(\theta'_o)^2\right] + \left[\frac{3}{2}(\theta - \theta_e)^2 - \frac{3}{2}(\theta_o - \theta_e)^2\right] \quad , \tag{4.12}$$

$$\int_o^\tau \left[\phi'' + 4\,\phi\right]\phi' \, d\tau = \left[\frac{1}{2}(\phi')^2 - \frac{1}{2}(\phi'_o)^2\right] + \left[2\,\phi^2 - 2\,\phi_o^2\right] \quad . \tag{4.13}$$

We now define the following two energy norms for the in-plane and out-of-plane librations

$$E_\theta = \frac{1}{2}\left[(\theta')^2 + 3\,(\theta - \theta_e)^2\right] \quad , \tag{4.14}$$

$$E_\phi = \frac{1}{2}\left[(\phi')^2 + 4\,\phi^2\right] \quad . \tag{4.15}$$

Then one can notice that the integrals of the LHS's of the Eqs. 4.10 and 4.11, carried out in Eqs. 4.12 and 4.13, represent the changes in these norms. These norms may be interpreted as the total energy (strictly speaking, Hamiltonian) related to small θ and ϕ motions, respectively. This can be understood by examining Eqs. 3.11 and 3.12 from Chapter 3, expressions for the kinetic and gravitational potential energy of a two-body tethered satellite system. For small angle motion, $\cos^2\theta$ and $\cos^2\phi$ can be replaced by $(1 - \theta^2)$ and $(1 - \phi^2)$, respectively. Then neglecting the third and higher order terms, the expressions for nondimensional kinetic and potential energies change to

$$\hat{T} = \frac{1}{2}\left[\theta'^2 + 2\theta' + 1 - \phi^2 + \phi'^2 + (\ell'/\ell)^2\right] \quad , \tag{4.16}$$

$$\hat{U} = \frac{1}{2}\left[-2 + 3\theta^2 + 3\phi^2\right] \quad , \tag{4.17}$$

while the total energy and Hamiltonian are equal to

$$\hat{T} + \hat{U} \;=\; \frac{1}{2}\left[\theta'^2 + 3\theta^2 + 2\theta' + \phi'^2 + 2\phi^2 - 1 + (\ell'/\ell)^2\right] \quad , \tag{4.18}$$

$$\hat{H} = \hat{T}_2 - \hat{T}_o + \hat{U} \;=\; \frac{1}{2}\left[\theta'^2 + 3\theta^2 + \phi'^2 + 4\phi^2 - 3\right] + \text{contribution of}(\ell'/\ell)^2 \quad . \tag{4.19}$$

It can be seen that the norms E_θ and E_ϕ do not quite represent the total energy related to θ and ϕ. For θ motion there is an extra θ' term and instead of $(\theta - \theta_e)^2$ there is a θ^2 term. For ϕ motion instead of $4\,\phi^2$ in E_ϕ, there is a $2\,\phi^2$ term in total energy. In addition, in the total energy there exists a ℓ'/ℓ term that usually includes feedbacks from in-plane and out-of-plane librations. In case of the Hamiltonian the situation is somewhat different. The deviation is only due to the θ_e and ℓ'/ℓ terms. But for a case where the length is constant (e.g. a station keeping stage but not for the retrieval that is the case of our study) θ_e is also zero hence, E_θ and E_ϕ represent exactly the parts of the Hamiltonian related to θ and ϕ motions.

As an outcome of the above discussions, one can state that the E_θ and E_ϕ are two energy-like norms that are related to, but not equal to either the total energy or the Hamiltonian of the system. Noticing Eqs. 4.12–4.15, Eqs. 4.10 and 4.11 can be rewritten as

$$E_\theta - E_{\theta_o} \;=\; 2\int_o^\tau \left[c\,(\theta')^2 - f(\theta'^2 + \theta')\right]\, \mathrm{d}\tau \quad , \tag{4.20}$$

$$E_\phi - E_{\phi_o} \;=\; 2\int_o^\tau \left[c\,(\phi')^2 - f(\phi')^2\right]\, \mathrm{d}\tau = 2\int_o^\tau (-\ell'/\ell)\,(\phi')^2\, \mathrm{d}\tau \quad . \tag{4.21}$$

Considering these equations, we interpret the stability criterion for a retrieval with a nominal exponential reel rate law, as follows.

The desired terminal state for a retrieval process is the quasi-equilibrium configuration. For a retrieval with a nominal exponential reel rate law, as discussed before, this configuration is when tether forms a straight line inside the plane of motion with a constant inclination with respect to the local vertical[1]. This is the condition where $\theta = \theta_e$ and $\theta' = \phi = \phi' = 0$. Since E_θ and E_ϕ are positive semi-definite functions, if the control system ensures that they approach zero, the two terms defining them in Eqs. 4.14 and 4.15 should go towards zero. This brings the system to the desired terminal state for a retrieval with a nominal exponential reel rate law. Hence, a reel rate control law will be a successful one and will guaranty the stability of the in-plane and out-of-plane librations, only if it makes the right-hand sides (RHS's) of the Eqs. 4.20 and 4.21 negative definite; or zero, in the case of marginal stability.

Often one supposes that for having a retrieval, the reel rate should be negative throughout the motion, i.e., ℓ should decrease monotonically; but this is not an obligatory condition. In fact, if the RHS of the Eq. 4.21 is to be made negative semi-definite, i.e.,

$$\left(\int_o^{\tau}(-\ell'/\ell)(\phi')^2\,\mathrm{d}\tau\right) \leq 0 \quad , \tag{4.22}$$

the reel rate must indispensably be positive in some intervals during the retrieval process. In other words, some of the reel rate effort goes for controlling the librational motion. This effort is apparently from the second term in the square bracket in Eq. 4.21, the function f, because the integral of the first term, $\int_o^{\tau} c(\phi')^2 \mathrm{d}\tau$, is always positive and its effect is to increase the system's energy. Obviously the necessary condition for having retrieval is

[1]This is true, for the cases like ours, in the absence of aerodynamic forces and other probable disturbing forces like solar radiation pressure. If the tethers are long and the system is inside the atmospheric altitudes then the aerodynamic drag on the tether and the bodies is significant Consequently the tether will not be completely straight.

$$\left(\int_o^T (\ell'/\ell)\ \mathrm{d}\tau\right) \quad < 0 \quad . \tag{4.23}$$

The two inequalities 4.22 and 4.23 must be satisfied together and this is feasible if the time variation of f be chosen in a way that the intervals where ℓ'/ℓ is positive be coincident with the periods where the absolute value of ϕ' is relatively large.

On the other hand, in selecting the time variation of f, one should consider making the RHS of Eq. 4.20 negative as well, or

$$\int_o^T \left[c(\theta')^2 - f(\theta'^2 + \theta')\right]\ \mathrm{d}\tau \quad \leq \quad 0 \quad . \tag{4.24}$$

In the above expression also, the integrand is not always negative and depending on the magnitudes and signs of θ' and f, it changes its sign. In other words, this condition is not naturally satisfied and the function f should be so chosen as to make this integral negative too, even though the integrand is not always negative.

If one compares this method with the one discussed in the last chapter, it can be seen that the energy norms E_θ and E_φ here are analogous to the Liapunov function V. The E's and V are all positive semi-definite functions; however, $\dot{E}$'s are not necessarily made to be negative semi-definite for stabilization, unlike $\dot{V}$. Although it is not a necessary condition for stability of the system, it is possible to make $\dot{E}$'s negative semi-definite too, by choosing a proper variation of f with time. In the following sections we first introduce two new reel rate laws for two-body systems and we will verify their effectiveness by the stability criterion explained in this section and by employing the averaging method. Their performances will be compared with the reel rate law introduced in Chapter 3 based on the Liapunov method. Then the new reel rate laws will be extended to multi-body systems.

4.3 Reel Rate Law with Quadratic Out-of-plane Feedback

At the end of Chapter 3 we made two remarks about the reel rate of Eq. 3.18 obtained from the Liapunov approach. First of all, there was a nonlinearity involved in the in-plane part of the reel rate that does not seem essential. Secondly the in-plane and out-of-plane librations have a common control gain. Since the amplitude of only the out-of-plane motion was rather high, one expects that by having separate control gains for in-plane and out-of-plane librations and choosing a larger out-of-plane control gain, one can overcome this problem. Using approximate approaches, we would investigate the performance of any desirable reel rate in this chapter analyticaly. The following simpler reel rate law is in conformity with the two mentioned remarks

$$\ell'/\ell = c\Big[-1 + K_\theta\theta' + K_\phi\phi'^2\Big] \quad , \tag{4.25}$$

that is, there is a linear feedback of the pitch rate and quadratic feedback of the roll rate. Each term has a distinct objective; as discussed before, the first term is for generating an exponential retrieval and c represents the magnitude of this exponent. The second term is for stabilizing the in-plane librations where K_θ is the in-plane gain, and the third term has the same role for out-of-plane librations with K_ϕ indicating the out-of-plane gain. Even though the equations for small motion of θ and ϕ, Eqs. 4.1 and 4.2, are explicitly independent, they are coupled through the (ℓ'/ℓ) term. The feedback for each motion automatically affects the other degree of freedom. Consequently an exact knowledge of the performance of the reel rate control law can be obtained only by numerical simulation, which would be done later. For being able to investigate analytically the effectiveness of this reel rate law, one should consider the in-plane and out-of-plane motions separately. So if we first consider only a purely in-plane motion the reel rate will be

$$\ell'/\ell = c\Big[-1 + K_\theta\theta'\Big] \quad , \tag{4.26}$$

or

$$f = c\,K_\theta\theta' \quad .$$

As discussed before, one way of analyzing the performance of this in-plane reel rate is by studying the sign of the integral of the RHS of Eq. 4.20 over the entire motion. The stability criterion according to the energy dissipation approach states that the in-plane motion is stable if this integral is negative semi-definite. The RHS of 4.20 with the reel rate of Eq. 4.26 is

$$2c\int_o^\tau \Big[(1-K_\theta)\theta'^2 - K_\theta\,\theta'^3\Big]\ d\tau \quad . \tag{4.27}$$

The integral here is over the retrieval time. The retrieval time will depend on the values of c and K_θ. Since θ'^2 is always positive, the integral of the first term will be negative if we have $K_\theta > 1$. The second term is sign-indefinite, but one expects a quasi-harmonic response (The existence of a quasi-harmonic response will be confirmed shortly.) for the system. Hence, the integral of the second term over a period of oscillation vanishes. In any case, it is a third order term and is small. Consequently, the energy dissipation approach predicts that the in-plane motion is stable for $K_\theta > 1$.

For confirming the prediction of this stability criterion we perform a direct analysis by finding the response of the system through an approximate analytical method. Replacing the (ℓ'/ℓ) from Eq. 4.26 in the equation of the in-plane motion for the small, Eq. 4.8, yields

$$\theta'' + 3(\theta - \theta_e) = 2c\theta' - 2(c\,K_\theta\theta')(\theta' + 1) \quad . \tag{4.28}$$

By defining $\tilde{\theta} = (\theta - \theta_e)$, one can represent the equation of in-plane motion in the alternate form

$$\tilde{\theta}'' + 3\tilde{\theta} = 2c\tilde{\theta}' - 2(c\,K_\theta\tilde{\theta}')(\tilde{\theta}' + 1) \quad . \tag{4.29}$$

This is a nonlinear equation with a small nonlinearity if c is small. It falls into the class of equations whose general form is

$$y'' + \omega^2 y = \epsilon\; g(y, y') \quad . \tag{4.30}$$

The solution to this equation can be written as

$$y = A\cos(\omega_\tau + \alpha) = A\cos\beta \quad . \tag{4.31}$$

Equation 4.30, with a small degree of nonlinearity, can be solved approximately by finding a linear equivalent to it. The two well-known analytical methods for nonlinear systems, *variation of parameters* and *harmonic balance*, reach to the same first order approximation for these kinds of systems [51]. This first order approximation is

$$A')_{av.} = -\frac{1}{2\pi\omega}\int_o^{2\pi} \epsilon\; g\; \sin\beta\, d\beta \quad , \tag{4.32}$$

$$\alpha')_{av.} = -\frac{1}{2\pi\omega A}\int_o^{2\pi} \epsilon\; g\; \cos\beta\, d\beta \quad . \tag{4.33}$$

Using relations 4.32 and 4.33 to find A and α in Eq. 4.31 is sometimes referred to as *the averaging method*, or an approximation of Krylov-Bogoliubov (KB) type. Applying these equations to Eq. 4.29, one gets

$$
\begin{aligned}
y &\equiv \tilde{\theta} = A\cos(\omega\tau + \alpha) \quad , \qquad\qquad \omega^2 = 3 \quad , \\
\epsilon\, g &\equiv 2c\tilde{\theta}' - 2(c\,K_\theta\tilde{\theta}')(\tilde{\theta}' + 1) = -2c\tilde{\theta}'\left[(K_\theta - 1) + K_\theta\,\tilde{\theta}'\right] \quad .
\end{aligned}
$$

Then

$$
\begin{aligned}
A')_{av} &= \frac{c}{\pi\omega}\int_o^{2\pi}\left[(K_\theta - 1)(-A\omega\sin\beta) + K_\theta(-A\omega\sin\beta)^2\right]\sin\beta\, d\beta \quad . \\
\alpha')_{av} &= \frac{c}{\pi\omega A}\int_o^{2\pi}\left[(K_\theta - 1)(-A\omega\sin\beta) + K_\theta(-A\omega\sin\beta)^2\right]\cos\beta\, d\beta \quad ,
\end{aligned}
\tag{4.31}
$$

which give rise to

$$
\begin{aligned}
A')_{av.} &= -cA(K_\theta - 1) \quad , \\
\alpha')_{av} &= 0 \quad .
\end{aligned}
\tag{4.35}
$$

One can see that the behaviour of α is like the linear systems i.e. it is constant. Furthermore, if we consider $A')_{av}$ as A', we get an exponential variation for the amplitude.

$$
\begin{aligned}
\frac{dA}{d\tau} &= -cA(K_\theta - 1) \\
\text{or} \qquad A &= A_o e^{-c(K_\theta - 1)\tau} \quad .
\end{aligned}
\tag{4.36}
$$

This shows that the in-plane motion will be stable if $K_\theta > 1.0$ and the higher the value of K_θ, the more stable the θ motion. Finding the system's response through the averaging method confirmed the prediction of the stability criterion and existence of the quasi-harmonic response.

These results are based on two approximations, firstly that the motion is considered to be small and, secondly by applying an equivalent linearization method which approximates our nonlinear system, a system with a small degree of nonlinearity. Hence, these results have to be verified by numerical simulation of the motion in the large. The equation of the pure in-plane motion in the large can be obtained by eliminating out-of-plane motion from the θ equation, Eq. 3.4 and employing the reel rate law of Eq. 4.26. The resulting equation of motion is

$$\theta'' + 2c\left[-1 + K_\theta \theta'\right](\theta' + 1) + 3\cos\theta\,\sin\theta = 0 \quad . \tag{4.37}$$

The results of the numerical solution to this equation, for four different sets of parameters are shown in Figs. 4.1–4.4. As we can see the results are completely in agreement with the prediction of the approximate analytical method. For $K_\theta < 1.0$, the in-plane motion is unstable. It has neutral stability in case of $K_\theta = 1.0$ and for $K_\theta > 1.0$ it is stable, approaching the equilibrium position $\theta_e = 2c/3$ rad. It can be seen also that when we choose very high values for K_θ, the motion is overdamped i.e. the control system dissipate the system's energy with such a high rate that there is no oscillation about the equilibrium situation.

Now we concentrate on the out-of-plane part of this control law. This time we consider a pure out-of-plane motion, then the control law would be

$$\begin{aligned} \ell'/\ell &= c\Big[-1 + K_\phi \phi'^2\Big] \quad , \qquad (4.38) \\ \text{or} \qquad f &= c\,K_\phi \phi'^2 \quad , \end{aligned}$$

Again the stability criterion according to energy dissipation approach expresses that the out-of-plane motion is stable if the integral in RHS of Eq. 4.21 is negative semi-definite, or zero in case of marginal stability. The RHS of Eq. 4.21 with the reel rate of Eq. 4.38 is

$$2c\int_{o}^{\tau}\left(1-K_{\phi}\,\phi'^{2}\right)\phi'^{2}\,\mathrm{d}\tau \quad . \tag{4.39}$$

A clear understanding of this integral is not possible without having the response of the system. Therefore we first obtain the approximate response of the system through the averaging method and then will study this integral.

Equation 4.9 with the reel rate of Eq. 4.38 becomes

$$\phi''+\;4\phi = 2c\phi' - 2c\,K_{\phi}\phi'^{2}\phi' \quad . \tag{4.40}$$

We investigate the performance of the out-of-plane part with the same approximate analytical method used for the in-plane part, i.e., the method for a nonlinear system with a small degree of nonlinearity. Comparing this equation with Eq. 4.30 one gets; $\omega = 2$, $\epsilon\; g = 2c\,\phi'(1-K_{\phi}\,\phi'^{2})$. Then Eqs. 4.32 and 4.33 yield

$$\begin{aligned} A')_{av.} &= cA\,(1-3\,A^{2}K_{\phi}) \quad , \\ \alpha')_{av.} &= 0 \quad , \end{aligned} \tag{4.41}$$

which show that, similar to the case of in-plane motion, the phase angle, α, is constant. Examining the expression for $A')_{av.}$, one notices that with the quadratic reel rate law, the out-of-plane motion can experience a limit cycle oscillation. This is because the $A')_{av}$ will be zero for a particular amplitude:

$$A')_{av.} = 0 \qquad \Longrightarrow \qquad A)_{lim.} = \sqrt{\frac{1}{3\,K_\phi}} \quad . \tag{4.42}$$

This is an acceptable stable motion, even though it has neutral stability. Numerical simulation must verify the existence of the limit cycle oscillation. Similarly to the in-plane motion, the numerical solution could be based on pure out-of-plane motion in the large. This equation can be found by eliminating the θ related terms in the Eq. 3.5 and employing the reel rate law given by of Eq. 4.38:

$$\phi'' + 2c\Big[-1 + K_\phi \phi'^2\Big]\phi' + 4\,\cos\phi\,\sin\phi = 0 \quad . \tag{4.43}$$

Numerical simulation of this equation for the case of $c = 0.5$ and $K_\phi = 27.0$ is presented in the Fig. 4.5. The approximate analytical method predicts the value of $A)_{lim.} = \sqrt{\frac{1}{3 \times 27.0}} = 0.111\,rad. = 6.367^{\circ}$ for the amplitude of the limit cycle and the exact numerical solution yields 6.52° for this value. This is very good agreement with a discrepancy of 2%.

Thus, according to the averaging method, the steady state of the out-of-plane motion is a limit cycle oscillation with

$$\phi' = -A\omega\sin(\omega\,\tau + \alpha) = -\sqrt{\frac{4}{3\,K_\phi}}\,\sin(2\,\tau) \quad . \tag{4.44}$$

Now we go back to the integral of Eq. 4.39 which shows the stability characteristics of the out-of-plane motion according to the energy dissipation approach. For the limit cycle oscillation phase with a constant amplitude, we expect this integral to be zero over a period of ϕ oscillations. Carrying it out for ϕ' appearing in Eq. 4.44 results in

$$\frac{8c}{3\,K_\phi}\left\{\left[\frac{\tau}{2} - \frac{\sin 4\,\tau}{8}\right] - \frac{4}{3}\left[\frac{3}{8}\tau - \frac{\sin 4\,\tau}{8} + \frac{\sin 8\,\tau}{64}\right]\right\}_{\tau_1}^{\tau_1+\pi} = 0 \quad , \tag{4.45}$$

here, τ_i can be any instant in oscillatory phase of the motion and, since ω is equal to 2, the period is equal to π. Since the integral vanishes over a period of oscillation, the stability criterion also agree with the existence of neutral stability.

At this stage, the performance of the complete coupled reel rate law of Eq. 4.25 with quadratic out-of-plane feedback will be compared with the reel rate law of Eq. 3.18, obtained from the Liapunov approach in Chapter 3. We base our final judgement on the numerical simulation of Eqs. 3.4–3.6, the *coupled nonlinear equations* of motion. Figure 3.3 shows the resulting motion for the reel rate obtained from the Liapunov approach and Fig. 4.6 represents the corresponding graphs for the reel rate of Eq. 4.25, with the same initial conditions as for Fig. 3.3 and $c = 0.5$, $K_\theta = 2.0$, $K_\phi = 9.0$. Comparing the two sets, one can observe the improvement in the retrieval time and the amplitude of the out-of-plane limit cycle oscillations. The variations of length and reel rate are basically similar for the two cases, and only because of the difference in the retrieval time, the x-axis scales are different.

It should be pointed out that the gains chosen for the two cases are not the same. For each control law, the performance of the system depends on the values of the control gains. The set of gains chosen for the reel rate law obtained from the Liapunov approach gives essentially the most acceptable performance with this reel rate law. Any effort to decrease retrieval time (or limit cycle amplitude) from the case of Fig. 3.3, i.e. by changing the value of c or K, results in an increase in the limit cycle amplitude (or retrieval time). On the other hand, the set of control gains used with the reel rate of Eq. 4.25 is just a typical one; nevertheless, it gives a better performance than the best resulting motion with the reel rate obtained from the Liapunov approach. Therefore, it is certain that the reel rate represented by Eq. 4.25 with quadratic out-of-plane feedback and linear in-plane feedback is superior to the one obtained from the Liapunov approach.

Another point that can be emphasized about these results is about the in-plane motion. By comparing the variation of θ obtained from the simulation of nonlinear coupled equations of motion in Fig. 4.6 to the variation of θ in case of a pure in-plane motion, as in Figs. 4.3 and 4.4, one can see two major differences. Firstly, there is a limit cycle oscillation for θ that did not exist in pure in-plane motion; secondly, instead of $\frac{2}{3}c$, θ approaches a much smaller equilibrium value. These are the effects of out-of-plane libration on in-plane libration. For studying the first effect, namely the induction of oscillations from ϕ to θ, we consider the coupled nonlinear θ-equation, Eq. 3.4, with reel rate of Eq. 4.25

$$\theta'' + 2\left[c(-1 + K_\theta\theta' + K_\phi\phi'^2) - \phi'\tan\phi\right](\theta' + 1) + 3\cos\theta\,\sin\theta = 0 \quad . \tag{4.46}$$

The out-of-plane motion is affecting the in-plane motion through the $\phi'\tan\phi$ and $K_\phi\phi'^2$ terms. These terms should go to the RHS as forcing functions. The products of these terms with θ' are of third order and negligible. If one approximates $\tan\phi$ by ϕ, then the forcing terms are $\phi'\phi$ and ϕ'^2. Since the value of θ is small in the oscillatory phase of the motion, $3\cos\theta\,\sin\theta$ can be replaced by 3θ. Thus Eq. 4.46 becomes

$$\theta'' + 2\left[c(-1 + K_\theta\theta')\right](\theta' + 1) + 3\theta = 2(\phi'\phi - cK_\phi\phi'^2) \quad . \tag{4.47}$$

After a short transient period in the beginning, the ϕ motion is an oscillatory one with constant amplitude that can be formulated as $\phi = A_\phi \sin\omega_\phi\tau$, and its derivative will be $\phi' = A_\phi\omega_\phi\cos\omega_\phi\tau$. These relations reveal that the forcing functions in Eq. 4.47 are oscillatory, in the form of $\sin 2\omega_\phi\tau$ (for $\phi'\phi$) and $\cos 2\omega_\phi\tau$ (for ϕ'^2). As already seen in Fig. 4.6(a), Eq. 4.47 with these forcing functions results a limit cycle oscillation in θ that can be formulated as

$$\theta = \bar{\theta} + A_\theta\sin(\omega_\theta\tau + \alpha_\theta) \quad . \tag{4.48}$$

Since, in an oscillatory motion with harmonic excitation, after a very short transient interval, the frequency of the forcing function is the dominant one, here the frequency of the θ limit cycle oscillations is equal to the forcing frequency

$$\omega_\theta = 2\omega_\phi \quad . \tag{4.49}$$

With the form of Eq. 4.48, one can also investigate the second main effect of the ϕ motion on the θ motion. The second effect was the decrease of the final approach value of θ. This approach value is the average of θ in the final oscillatory phase, called $\bar{\theta}$ in this formulation and shown in Fig. 4.6(a). For finding the value of $\bar{\theta}$, we average Eq. 4.47 over a period of θ

$$\overline{\theta''} + 2c\left[-1 + (K_\theta - 1)\,\overline{\theta'} + K_\theta\,\overline{\theta'^2}\right] + 3\bar{\theta} = 2(\,\overline{\phi'\phi} - cK_\phi\,\overline{\phi'^2}) \quad . \tag{4.50}$$

Since the derivatives of θ and ϕ have as well as ϕ itself are harmonic, $\overline{\theta''}$, $\overline{\theta'}$ and $\overline{\phi'\phi}$ are zero, thus

$$\bar{\theta} = \frac{2}{3}c\left[1 - K_\theta\,\overline{\theta'^2} - K_\phi\,\overline{\phi'^2}\right] \quad , \tag{4.51}$$

i.e. the approach value of θ is decreased from $\frac{2}{3}c$ by two terms: $K_\theta\,\overline{\theta'^2}$ and $K_\phi\,\overline{\phi'^2}$. The later usually has larger values and is the direct coupling effect of the out-of-plane motion on in-plane one. The former is the indirect effect of out-of-plane motion, since it is the effect of θ-oscillations on the average value of θ and this oscillatory motion is induced by the out-of-plane oscillations. The averages of θ'^2 and ϕ'^2 over a period of θ are

$$\overline{\theta'^2} = \frac{A_\theta^2\,\omega_\theta^2}{2} = 2A_\theta^2\,\omega_\phi^2 \quad , \qquad \overline{\phi'^2} = \frac{A_\phi^2\,\omega_\phi^2}{2} \quad ; \tag{4.52}$$

the exact numerical values for the case of Fig. 4.6 are as follows:

$$c = 0.5 \quad \Longrightarrow \tfrac{2}{3}c = 19.1^\circ \quad , \qquad K_\theta = 2.0 \quad , \qquad K_\phi = 9.0,$$

$\omega_\phi = 1.9$ (approximate pure out-of-plane motion had predicted the value of 2.0)

$$\overline{\theta'^2} = 0.024 \quad , \qquad K_\theta \overline{\theta'^2} = 0.048 \quad , \qquad \overline{\phi'^2} = 0.094 \quad , \qquad K_\phi \overline{\phi'^2} = 0.846$$

then the predicted value for $\bar{\theta}$ from Eq. 4.51 is $19.1\ [1 - 0.048 - 0.846] = 2.02^\circ$, and the graph shows the value of 2.74 for $\bar{\theta}$. By comparing these values, the improvement from the previous predicted value by the pure in-plane motion analysis, 19.1°, is evident.

The resulting motion with the reel rate law of Eq. 4.25 for another set of parameters, with a higher out-of-plane gain, $K_\phi = 27.0$, and a lower retrieval constant, $c = 0.3$, is shown in Fig. 4.7. In this figure, in addition to θ and ϕ, we present variations of the tether tension and the transferred mechanical power, which is equal to the product of the absolute value of the reel rate and tension. Checking the tension insures us that the tether does not go slack, and concentrating on the variation of power is essential for the energy considerations.

In summary, it is concluded in this section that a reel rate with linear in-plane feedback and different control gains for in-plane and out-of-plane librations has overcome the deficiencies of the reel rate law obtained from the Liapunov approach. A linear in-plane feedback is sufficient for controlling the in-plane motion. Then the presence of nonlinear quadratic term of the in-plane libration is not necessary; in fact, it has a negative effect. It increases the retrieval time, since it is always positive and decreases the average retrieval rate. In the next section, we introduce another reel rate law, a reel rate with absolute value out-of-plane feedback.

4.4 Reel Rate Law with Absolute Value Out-of-plane Feedback

As was discussed earlier, we need a nonlinear feedback for out-of-plane motion. It was noticed that, using an absolute value ϕ' feedback instead of quadratic, one can also stabilize the motion with a similar behaviour. Then the reel rate law of Eq. 4.25 will change to

$$\ell'/\ell = c\Big[-1 + K_\theta \theta' + K_\phi |\phi'|\Big] \quad . \tag{4.53}$$

Similarly to the previous case, a pure out-of-plane motion should be considered, i.e., using a reel rate of

$$\ell'/\ell = c\Big[-1 + K_\phi |\phi'|\Big] \quad . \tag{4.54}$$

or

$$f = c\, K_\phi |\phi'| \quad .$$

The integral, corresponding to the Eq. 4.39 which shows the stability characteristics of the system according to the energy dissipation approach, will be

$$2c \int_{\tau_1}^{\tau_1+\pi} (1 - K_\phi\, |\phi'|)\, \phi'^2 \, d\tau \quad . \tag{4.55}$$

Again it will be evaluated after finding the approximate response of the system; but due to the similarity to the quadratic roll rate feedback case, we expect that the response is a limit cycle oscillation and that this integral vanishes over a period of oscillations.

We apply the same approximate analytical method, namely the averaging method, for finding the response of the system. Equation 4.9 with the reel rate of Eq. 4.54 yields

$$\phi'' + 4\phi = 2c\phi' - 2c\,K_\phi|\phi'|\phi' \quad . \tag{4.56}$$

Comparing this equation with Eq. 4.30 one gets: $\omega = 2$,
$\epsilon\, g = 2c\,\phi'(1 - K_\phi\,|\phi'|)$; Eqs. 4.32 and 4.33 give

$$\begin{aligned} A')_{av.} &= \frac{c\,A}{\pi}(\pi - 16\,A\,K_\phi/3) \quad , \\ \alpha')_{av} &= 0 \quad , \end{aligned} \tag{4.57}$$

which show again that the phase angle, α, is constant. In addition, one can see that similarly to the quadratic feedback case, there is a possibility for existence of limit cycle oscillations. This can happen for the amplitude of

$$A')_{av} = 0 \qquad \Longrightarrow \qquad A)_{lim} = \frac{3\,\pi}{16\,K_\phi} \quad . \tag{4.58}$$

Numerical simulation of the equation of pure out-of-plane motion in the large must be used to verify the existence of the limit cycle oscillation. This equation can be obtained by changing the quadratic feedback to an absolute value in Eq. 4.43, i.e.

$$\phi'' + 2c\Big[-1 + K_\phi|\phi'|\Big]\phi' + 4\,\cos\phi\,\sin\phi = 0 \quad . \tag{4.59}$$

Numerical simulation of this equation for the case of $c = 0.5$ and $K_\phi = 6.0$ is presented in the Fig. 4.8. The approximate analytical method predicts the value of $A)_{lim} = \frac{3\pi}{16\times 60} = 0.098\,rad. = 5.62^\circ$ for the amplitude of the limit cycle and the exact numerical solution gives 5.67° for this value. This is a very good agreement with a difference of 0.9%.

Now we carry out the integration of Eq. 4.55. The expression for ϕ' is

$$\phi' = -\frac{3\pi}{8\,K_\phi}\sin(2\,\tau) \quad . \tag{4.60}$$

The integral adds up to zero[2] again, indicating the existence of neutral stability.

Finally, the performance of the complete coupled reel rate law of Eq. 4.53 will be compared with the other two reel rate laws discussed before. The numerical simulation is based on the *coupled nonlinear equations* of motion, Eqs. 3.4–3.6, with this reel rate law. Shown in the Figs. 4.9 and 4.10 are the results for the same sets of parameters as Figs. 4.6 and 4.7. Comparing these graphs with the case of quadratic reel rate i.e. Figs. 4.6 and 4.7 shows that, for the same set of parameters, using the reel rate with absolute value feedback results in a smaller out-of-plane limit cycle amplitude, but a larger retrieval time than the one with quadratic feedback.

In case of Fig. 4.10, like Fig. 4.7, we included the plots of θ, ϕ, tension and power. However, in Fig. 4.9, we have included all of the six outputs: θ, ϕ, length, reel rate, tension, power. For the sake of completeness, we have included all six output curves for this figure, and because of similarity, we have not presented a complete set of output curves in the other figures.

Instead of comparing the two reel rate laws for the same set of gains, another comparison can be made that perhaps gives a better understanding of the situation. By employing the two different reel rate laws, we find two different val-

[2]Regarding $|\phi'|$, since ϕ' changes sign, it is more convenient to choose the initial time τ_i as $2k\pi$ where k represents an integer number

ues for each of the three important characteristics of the motion: retrieval time, limit cycle amplitude of ϕ and the peak value of θ. By choosing proper gain sets we can make two out of the three of these characteristics the same, e.g , retrieval time and out-of-plane limit cycle amplitude. Then by comparing the values for the third characteristic, each corresponding to one of the reel rate laws, we can compare the performance of these laws. Here, we find a set of gains for the reel rate with quadratic roll rate feedback that makes the amplitude of the limit cycle of ϕ and the peak value of θ equal to those for the case of Fig. 4.9. The results are shown in Fig. 4.11. The retrieval time is less for the case of reel rate with quadratic out-of-plane feedback.

From the plots we can see that variations in length are very similar for all of the cases considered. This is because we are using the same initial conditions, nominal length change (exponential), and final retrieval lengths, for all of the cases and only a small part of the reel rate effort in each case goes to controlling the in-plane and out-of-plane librations. This part, namely the function f in Eq. 4.3, distinguishes different reel rate laws. For reel rate, tension, and power, although the general trend is similar for most of the cases, the range of variation changes from case to case. Since we normally have chosen $\theta'(0) = 0$ and $\phi'(0) = 0$ we get $\ell'(0) = c\,\ell$, i.e. the initial value of the reel rate changes by choosing different values for the retrieval constant c. Consequently, the initial values for tension and power will change too.

By concentrating on the figures that contain both length change and tension variation, one can see that after a short while from the beginning of the motion, the general trends of variation of length and tension are the same. They will reach very small values at almost the same time. This can be explained by looking at Eq. 3.6. This equation shows that when the system is in steady conditions, for the small motion, one gets T= $3M\Omega^2\ell$. Here the librational angles are small and after a short period of time the time variations are not zero, but very small. Then this relation holds approximately.

At this point after finding acceptable reel rate laws for two-body systems, we will try to extend them to multi-body systems.

4.5 Multi-body Systems

For a system with N number of bodies, the reel rate laws of Eqs. 4.25 and 4.53, i.e. reel rate laws with quadratic and absolute value roll rate feedback, respectively, will be

$$\ell_i'/\ell_i = c_i\Big[-1 + K_{\theta_i}\theta_i' + K_{\phi_i}\phi_i'^2\Big] , \tag{4.61}$$

or

$$\ell_i'/\ell_i = c_i\Big[-1 + K_{\theta_i}\theta_i' + K_{\phi_i} \mid \phi_i' \mid \Big] , \tag{4.62}$$

for $\quad i = 1, 2, \ldots N-1$.

In this thesis, numerical results are obtained for three-body systems only. Then the reel rate laws chosen are either

$$\ell_1'/\ell_1 = c_1\Big[-1+K_{\theta_1}\theta_1'+K_{\phi_1}\phi_1'^2\Big] , \qquad \ell_2'/\ell_2 = c_2\Big[-1+K_{\theta_2}\theta_2'+K_{\phi_2}\phi_2'^2\Big], \tag{4.63}$$

or

$$\ell_1'/\ell_1 = c_1\Big[-1 + K_{\theta_1}\theta_1' + K_{\phi_1} \mid \phi_1' \mid \Big] , \ \ell_2'/\ell_2 = c_2\Big[-1 + K_{\theta_2}\theta_2' + K_{\phi_2} \mid \phi_2' \mid \Big]. \tag{4.64}$$

Figures 4.12 and 4.13 show two examples for the case of quadratic roll rate feedback, with the same sets of initial conditions and retrieval constants as the uncontrolled cases and two sets of gains. Figures.4.14 and 4.15 are similar graphs for absolute value roll rate feedback law. A station-keeping control stage follows the retrieval for improving the terminal response; in the station-keeping phase the reel rate laws are as follows:

$$\ell_1'/\ell_1 = c_1\left(K_{\theta_1}\,\theta_1' + K_{\phi_1}\,\phi_1'^2\right)\,, \qquad \ell_2'/\ell_2 = c_2\,\left(K_{\theta_2}\,\theta_2' + K_{\phi_2}\,\phi_2'^2\right)\,, \quad (4.65)$$

or

$$\ell_1'/\ell_1 = c_1\left(K_{\theta_1}\,\theta_1' + K_{\phi_1}\,\mid\phi_1'\mid\right)\,, \qquad \ell_2'/\ell_2 = c_2\,\left(K_{\theta_2}\,\theta_2' + K_{\phi_2}\,\mid\phi_2'\mid\right)\,. \quad (4.66)$$

This stage can bring the system to a final desired configuration which is normally an equilibrium condition with zero in-plane and out-of-plane angles. The results reveal that the proposed reel rate laws are as equally applicable to three-body systems as they were to two-body systems.

Without presenting the graphs the results of investigating the effectiveness of these laws for large initial values of ϕ_i will be explained. This study is done for the case of $\phi_i(0) = 10^o$ with other conditions being the same as in the case of Fig.4.14, with gains $K_{\theta_1} = K_{\theta_2} = 2.0$, $K_{\phi_1} = K_{\phi_2} = 9.0$. The value of retrieval constant, c, has been changed over a wide range. In quadratic roll rate feedback case, good performance has been observed over a wide range of c, while in the case of absolute value roll rate feedback c can be increased only up to 0.43, beyond which the tethers become slack.

4.6 Effects of the Retrieval Constant and Control Gains on the Motion

Since, when we the introduced reel rate laws for multi-body systems, we observed behaviour similar to that of two-body systems, we base this section on two-body systems for the sake of simplicity.

Figure 4.16 shows the variation of retrieval time, amplitudes of out-of-plane limit cycle oscillations, the initial sharp peak of θ, and amplitudes of in-plane limit cycle oscillations, with c, K_θ, K_ϕ for quadratic roll rate law. Fig. 4.17 presents similar results for absolute value roll rate law. Most of the cases are continued until $c = 0.5$, because for $c \geq 0.6$, the tethers become slack.

Regarding the out-of-plane amplitude, one expects that increasing K_ϕ decreases this amplitude and it is so in the graphs. The approximate analytical solution based on the averaging method, as introduced before, predicted the value of $A)_{lim.} = \sqrt{\frac{1}{3K_\phi}}$ for the reel rate with quadratic roll rate feedback, and $A)_{lim.} = \frac{3\pi}{16K_\phi}$ for the absolute value roll rate feedback. With the values of 3, 9 and 27 for K_ϕ, in case of quadratic roll rate feedback, the predicted values will be $19.1^\circ, 11^\circ$ and 6.4°, respectively; in case of absolute value feedback, the corresponding values are $11.25^\circ, 3.75^\circ$ and 1.25°. These predicted values are shown in the out-of-plane limit cycle amplitude graphs as straight lines. The exact numerical results show relatively close agreement with these values, both in terms of amplitude and the independence of the amplitude from c and K_θ.

Generally retrieval time decreases with increasing c. This was expected since $\ell'/\ell = -c$ gives the main retrieving effect and increasing c will make retrieval faster. Increasing the gains K_θ and K_ϕ generally increases retrieval time, since the pitch and roll feedbacks modulate the reel rate, often decreasing the retrieval rate and sometimes even making the reel rate positive instead of negative. This makes complete sense if one notices that these feedbacks are added to extract some of the retrieving effort of the reel rate system to stabilize the in-plane and out-of-plane librations. Of course the exact effect depends on the average value of θ' and ϕ'; as we can see for quadratic roll rate feedback in one case, decreasing K_θ has increased retrieval time (compare cases 3, 6, 9 in Fig. 4.16).

The variation of the initial sharp peak of θ with c, K_θ and K_ϕ is considered next. Increasing c, increases this peak. The reason can be explained from Fig.4.3. This was a plot for pure in-plane motion. It is an oscillatory motion about the equilibrium value of $\frac{2}{3}c$. Because of having the highest deviation from this equilibrium in the beginning of the motion, the maximum value for θ occurs at that time. By choosing initial value for θ equal to zero, the initial difference from $\frac{2}{3}c$ increases with increasing c and this pushes the peak in θ to a higher value. It should be mentioned that due to the coupling effect of out-of-plane limit cycle oscillations on the in-plane motion, Eq. 4.51 gives $\bar{\theta} = \frac{2}{3}c\left[1 - K_\theta\,\overline{\theta'^2} - K_\phi\,\overline{\phi'^2}\right]$, instead of $\bar{\theta} = \frac{2}{3}c$ for the equilibrium position. However, the limit cycle oscillations start after a while and in the beginning of the motion this effect does not exist. Then the above discussion about the peak of θ in the beginning of the motion is still valid.

Now we consider the effect of K_θ and K_ϕ on this peak. As of the effect of K_ϕ, one can notice that, naturally, the out-of-plane motion does not have a significant effect on this peak value of the in-plane motion. For quadratic feedback there is almost no change with K_ϕ and for absolute value feedback the variation of the peak with K_ϕ is slightly more significant. The reason for this difference between the cases with two different out-of-plane feedbacks is that the absolute value of ϕ' is normally less than 1; i.e. $\phi'^2 < |\phi'|$. Then considering the two out-of-plane feedbacks, $K_\phi\phi'^2$ and $K_\phi|\phi'|$, one can see that for the same value of K_ϕ the effect of the absolute value feedback will be more. On the other hand K_θ has a very significant effect on the value of this peak. The reason for having a very significant variation with K_θ is that, in the reel rate law, the in-plane feedback is added to control the in-plane libration, θ; naturally increasing K_θ increases the control effect and decreases this undesired peak.

The variation of in-plane limit cycle amplitudes are very similar for two reel rate laws since the difference between the two reel rates is in out-of-plane feedbacks. They vary significantly with in-plane gain, K_θ, but not with out-of-plane gain, K_ϕ.

Chapter 5

Concluding Remarks

5.1 Review of the Thesis and Its Conclusions

Most of the previous studies on tethered satellite systems have investigated two-body systems. This thesis, on the other hand, has concentrated on furthering the knowledge on multi-body systems. Except for very few cases, the available literature on multi-body systems is limited to the study of two-dimensional in-plane motion. For the first time, a simulation code on the dynamics and control of three-dimensional librational motion in the large for a tethered satellite system, composed of N number of bodies, has been developed. A significant amount of time and effort has been spent on writing , debugging, and testing the computer program. The formulation used here is valid for any arbitrary orbit and variable-length tethers, which are assumed massless and straight.

Similar to the early studies on two-body systems, our investigation which is in early stages of research on the three-dimensional motion of multi-body systems, has made some simplifications. Even with these, the equations of motion are quite complicated. In the future stages of study on three-dimensional motion of multi-body systems, these assumptions might be relaxed. A complete list of assumptions is given at the beginning of Chapter 2, a major one being that the tethers are considered massless and straight.

There are four well-known control methods for tethered satellite systems: tension control laws, length or reel rate control laws, thruster control laws and offset control laws. Thruster augmented and offset control laws have some difficulties in their implementations. Tension control laws and reel rate laws are easy to implement. They have been considered extensively in the past for controlling the in-plane motion. The presence of a reeling system in a tethered satellite system is indispensable. Thus, in this thesis we have chosen reel rate control laws for controlling the out-of-plane and in-plane motions at the same time. There has been no previous work that presents an unaided reel rate law to control the three-dimensional librational motion of multi-body tethered satellite systems. Regarding the necessity of a control system, the retrieval phase is the critical phase of the motion; therefore, in the control part we have concentrated on this phase of the motion. Naturally, the attempts for finding suitable reel rate laws have started with a simpler case, two-body tethered systems; subsequently the reel rates are extended to multi-body systems. This extension has been done quite easily since the method of formulation is very appropriate for this purpose.

Among the in-plane and out-of-plane librations, the reel rate (ℓ'/ℓ) affects the former with a much higher degree. Therefore, controlling the out-of-plane rotation with an unaided reel rate law has been a more demanding task. Since the coupling between the in-plane and out-of-plane motions is a nonlinear one, in the reel rate law a nonlinear dependence on the out-of-plane motion is expected. Two analytical methods have been used for developing the reel rate laws and verifying the performance of the system with their presence. The first method is Liapunov's direct method, and the second one is the energy dissipation approach together with the averaging method, an approximate method for finding the response of the system.

Liapunov's direct method is a very powerful method, since it is applicable to the motion in the large and it can reveal the stability of the system just by using the equations of motion without actually solving them. However, constructing a proper Liapunov function is very challenging and strenuous. Based on the Hamiltonian of the system a reel rate law has been found that stabilizes the in-plane and out-of-plane librations in the sense of Liapunov. Although this reel rate law performs an acceptable retrieval, the retrieval time and amplitude of out-of-plane motion are rather high. The problem associated with the out-of-plane amplitude can be resolved by separating the in-plane and out-of-plane gains and choosing a larger out-of-plane gain. Regarding the retrieval time, there is a linear plus a quadratic term of the in-plane angular velocity in the reel rate. A quadratic term is always positive and reduces the average rate of retrieval. Since a linear feedback of pitch rate is sufficient for controlling the motion, this quadratic feedback is redundant. For the out-of-plane motion, however, a nonlinear feedback is necessary.

A new reel rate law has been proposed next. This reel rate law which is consistent with the above mentioned points; it possesses a linear in-plane feedback and a quadratic out-of-plane feedback with separate gains. For analyzing the behaviour of the system with this reel rate law we have not used the Liapunov approach anymore. This is due to the complexity of finding a proper Liapunov function. It should be noticed that if after spending a lot of time and effort one is confronted with lack of success in finding a suitable Liapunov function, one cannot reach any conclusion about stability or instability of the system. The energy dissipation approach together with the averaging method has been used instead. This approach revealed the effectiveness of the new reel rate law in stabilizing the in-plane and out-of-plane motions at the same time, as well as performing a retrieval sufficiently fast. Similar to this reel rate, another reel rate with its nonlinear out-of-plane feedback composed of an absolute value term, has also been proven efficient through the same approach.

The two new reel rate laws have been extended to multi-body systems and have demonstrated completely acceptable results. A station-keeping stage has been added to the motion, in multi-body systems. After reaching the final length, this phase brings the system to the final desired configuration. A study of the effects of different parameters and gains of the reel rate laws on the resulting motion wraps up the thesis. The complete discussions can be found in Section 4.6 that will not be repeated here. These can be used for selecting the values of the gains and parameters in order to achieve a desired resulting motion.

5.2 Recommendations for Future Work

The following items are recommended for further studies in continuation of this research project.

i. Preparing the facilities and performing the necessary experiments to verify the results obtained in this thesis through analytical and numerical analyses.

ii. Including the mass and three-dimensional vibrational motion of tethers for multi-body systems simulation models.

iii. Adding the three-dimensional rigid-body motion of the end bodies and investigating the effectiveness of the offset control laws in multi-body tethered systems.

iv. Studying the perturbing effects of aerodynamic forces, solar radiation pressure and electrodynamic forces on the motion of the multi-body tethered systems, for the applications in which these effects are significant.

v. Comparing the effectiveness of possible thruster or tension control laws for controlling the three-dimensional librational motion of multi-body tethered systems with those of the reel rate laws presented in this thesis.

vi. Considering the possibility of decreasing the initial sharp peak in the in-plane motion through modification of the present reel rate laws or adding another control law to the system.

vii. Replacing the nominal exponential retrieval by a proportional one ($\ell' =$ æ constant) in some parts of the motion, in order to decrease the retrieval time. This has been done previously for two-body systems; it has to be extended to multi-body systems.

Bibliography

[1] Bekey, I., "Tethers Open New Space Options," *Astronautics and Aeronautics*, Vol. 21, No. 4, 1983, pp. 32–40.

[2] Tsiolkovsky, K.E., "Grezy O. Zemie i nebe (i) Na Veste ," (Speculations between Earth and sky, and on Vesta; science fiction works), Moscow, izd-vo AN SSSR, 1959, p. 35.

[3] Von Tiesenhausen, G., "Tethers in Space: Birth and Growth of a New Avenue to Space Utilization," *NASA, TM-82571*, February 1984.

[4] Artsutanov, Y., "V kosmos na elektrovoze," *Komsomolskaya Pravda*, July 31, 1960.

[5] Collar, A.R. and Flower, J.W., "A (Relatively) Low Altitude 24-Hour Satellite," *Journal of the British Interplanetary Society*, Vol. 22, 1969, pp. 442-457.

[6] Artsutanov, Y., "V kosmos Bez Raket," (Into Space Without Rockets), *Air Force Systems Command, Wright Patterson AFB*, Ohio, Report No. ADA084507, 1969.

[7] Misra, A.K. and Modi, V.J., "A Survey on the Dynamics and Control of Tethered Satellite Systems," *Tethers in Space, Advances in Astronautical Sciences*, Vol. 62, 1987, pp. 667–720.

[8] Starley, W.H. and Adlhoch, R.W., "Study of the Retrieval of an Astronaut from an Extra-Vehicular Assignment," *The Marquardt Corporation (TMC)*, Van Nuys, California, Report No. S-356, November 1963.

[9] Lang, D.L. and Nolting, R.K., "Operations with Tethered Space Vehicles," *NASA SP-138, Gemini Summary Conference*, February 1967.

[10] Colombo, G., Gaposchkin, E.M., Grossi, M.D. and Weiffenbach, G.C., "Shuttle borne Skyhook: a new tool for low-orbital-altitude research," *Smithsonian Institution Astrophysical Observatory*, Cambridge, Massachusetts, Reports in Geoastronomy, No. 1, September 1974.

[11] Penzo, P.A. and Ammann, P.W., "Tethers In Space Handbook," -Second Edition- *NASA, Office of Space Flight, Advanced Program Development*, NASA Headquarters, Washington, DC, May 1989.

[12] Liu, F.C., "On Dynamical formulation of a Tethered Satellite System with Mass Transfer," *AIAA 23rd Aerospace Sciences Meeting*, Reno, Nevada, Paper No. 85-0117, January 1985.

[13] Lorenzini, E.C., "Analytical Investigation of the Dynamics of Tethered Constellations in Earth Orbit," *Smithsonian Institution Astrophysical Observatory*, Cambridge, Massachusetts, Final Report for NASA/MSFC under Contract NAS8-35497, Dec. 1984.

[14] Lorenzini, E.C., "A Three-Mass Tethered System for Micro-g/Variable-g Applications," *AIAA/AAS Guidance, Navigation and Control Conference*, Williamsburg, VA, Paper No. 86-1990, August 1986, appeared in *Journal of Guidance, Control, and Dynamics*, Vol. 10, No. 3, May-June 1987, pp. 242–249.

[15] Misra, A.K., Amier, Z.E. and Modi, V.J., "Attitude Dynamics of Three-Body Tethered Systems," *AIAA 25th Aerospace Sciences Meeting*, Reno, Nevada, Paper No. 87-0117, January 1987.

[16] Lorenzini, E.C., Cosmo, M., Vetrella, S. and Moccia, A., "Acceleration Levels on Board the Space Station and a Tethered Elevator for Micro and Variable-Gravity Applications," *Proceedings of the NASA/PSN/AIAA Second International Conference on Tethers in Space*, Venice, Italy, October 1987, pp. 513–522.

[17] Cosmo, M., Lorenzini, E.C., Vetrella, S. and Moccia, A., "Transient Dynamics of the Tether Elevator/Crawler System," *Proceedings of the AIAA/AAS Astrodynamics Conference*, Minneapolis, Minnesota, August 1988, pp. 480–489.

[18] Bachmann, S., Modi, V.J. and Misra, A.K., "Dynamics and Control of a Space Station Based Tethered Elevator System," *AAS/AIAA Spaceflight Mechanics Meeting*, Houston, Texas, Paper No. 91–177, February 1991.

[19] Misra, A.K. and Modi, V.J., "Three-Dimensional Dynamics and Control of Tether-Connected N-Body Systems," *AIAA 28th Aerospace Science Meeting*, Reno, Nevada, Paper No. 90-0751, January 1990.

[20] Rupp, C.C., "A Tether Tension Control Law for Tethered Subsatellites Deployed Along Local Vertical," *NASA, TMX-64963*, Marshall Space Flight Center, September 1975.

[21] Kulla, P., "Stabilization of Tethered Satellites," *ESTEC* Report TMM/78-07/PK-avs., December 1977.

[22] Bainum, P.M. and Kumar, V.K., "Optimal Control of the Shuttle-Tethered-Subsatellite System," *Acta Astronautica*, Vol. 7, No. 12, 1980, pp. 1333–1348.

[23] Liangdong, L., and Bainum, P.M., "Dynamics and Control of a Tethered Antenna/Reflector in Orbit," *The Journal of the Astronautical Science*, Vol. 38, No. 3, July-September 1990, pp. 247–268.

[24] Kohler, P., Maas, W., Wehrli, R., Weber, R. and Brauchli, H., "Dynamics of a system of Two Satellites Connected by a Deployable and Extensible Tether of Finite Mass," *ESTEC*, Contract Report, Contract No. 2992/76/NL/Ak(SC), Vols. 1 and 2, October 1978.

[25] Banerjee, A.K., and Kane, T.R., "Tethered Satellite Retrieval with Thruster Augmented Control," *Journal of Guidance, Control, and Dynamics*, Vol. 7, January–February 1984, pp. 45–50.

[26] Fleurisson, E.J., Pines, D.J. and von Flotow, A.H., "Trajectory Design, Feedforward and Feedback Stabilization of Tethered Spacecraft Retrieval," *AAS Spaceflight Mechanics 1991*, Advances in the astronautical Sciences, Vol. 75, Part II, 1991, pp. 1077–1097.

[27] Modi, V.J., Lakshmanan, P.K. and Misra, A.K., "Offset Control of Tethered Satellite Systems: Analysis and Experimental Verification," *Acta Astronautica*, Vol. 21, No. 5, 1990, pp. 283–294.

[28] Xu, D.M., Misra, A.K. and Modi, V.J., "Three dimensional control of the shuttle supported tethered satellite systems during deployment and retrieval," *Proceedings of the 3rd VPISU/AIAA Symposium on Dynamics and Control of Large Flexible Spacecraft*, Blacksburg, VA., June 1981, pp. 453–469.

[29] Xu, D.M., "The Dynamics and Control of the Shuttle Supported Tethered Subsatellite Systems," Ph.D. Thesis, Department of Mechanical Engineering, McGill University, Montreal, Canada, November 1984.

[30] Kalaghan, P.N., Arnold, D.A., Colombo, G., Grossi, M.D., Kirschener, L.R. and Orringer, O., "Study of the Dynamics of a Tethered Satellite System (Skyhook)," *Smithsonian Institution Astrophysical Observatory*, Cambridge, Massachusetts, Final report, Contract NAS8-32199, March 1978.

[31] Wells, D.A., "Theory and Problems of Lagrangian Dynamics," *Schaum Publishing Co.*, New York, New York, 1967.

[32] Baker, W.P., Dunkin, J.A., Galaboff, Z.J., Johnston, K.D., Kissel, R.R., Rheinfurth, M.H. and Siebel, M.P.L., "Tethered Subsatellite Study," *NASA, TMX-73314*, March 1976.

[33] Gragg, W.B., "On Extrapolation Algorithms for Ordinary Initial-Value Problems," *SIAM Journal on Numerical Analysis*, Series B, Vol. 2, 1965, pp. 384–403.

[34] Bulirsch, R. and Stoer, J., "Numerical Treatment of Ordinary Differential Equations by Extrapolation methods," *Numerische Mathematik*, Vol. 8, 1966, pp. 1–13.

[35] Clark, N.W., "3600 FORTRAN Program," *Argonne National Laboratories*, ANL D250-DIFSUB, 1966.

[36] Fox, P.A., "DESUB: Integration of a First-Order System of Ordinary Differential Equations," *Mathematical Software (edited by John R. Rice)*, Academic Press, New York, 1971.

[37] Meirovitch, L., "Methods of Analytical Dynamics," *McGraw-Hill*, New York, New York.

[38] Mortenson, R.E., "A Globally Stable Linear Attitude Regulator," *International Journal of Control*, Vol 8, No. 3, 1968, pp. 927-302.

[39] Vadali, S.R. and Junkins J.L., "Optimal Open loop and Stable Feedback Control of Rigid Spacecraft Attitude Maneuvers," *The Journal Of Astronautical Sciences*, Vol. 32, No. 2, April- June 1984, pp. 105–122.

[40] Vadali, S.R., "Feedback Control of Flexible Spacecraft Large-Angle Maneuvers Using Liapunov Theory," *Proceedings of the American Control Conference*, Vol. 3, 1984, pp. 1674–1678.

[41] Wie, B. and Barba, P.M., "Quaternion Feedback for Spacecraft Large Angle Maneuvers," *Journal of Guidance, Control, and Dynamics*, Vol. 8, No. 3, May-June 1985, pp. 360–365.

[42] Fujii, H. and Ishijima S., "Mission Function Control applied to Slew Maneuvers," *38th Congress of the IAF*, Brighton, U.K., paper 87–354, October 1987.

[43] Lee, B. and Grantham, W.J., "Aeroassisted Orbital Maneuvering Using Liapunov Optimal Feedback Control," *Journal of Guidance, Control and Dynamics*, Vol. 12, No. 2, March-April 1989, pp. 237–242.

[44] Oh, H.S. and Vadali, S.R., "Feedback Control and Steering Laws for Spacecraft Using Single Gimbal Control Moment Gyros," *AIAA Guidance, Navigation, and Control Conference*, Boston, paper 89–3475, 1989.

[45] Junkins, J.L., Rahman, Z., Bang, H., "Near-Minimum-Time Maneuvers of Flexible Vehicles: A Liapunov Control Design Method," *Mechanics and Control of Large Space Structures* , Published by AIAA, 1990.

[46] Fujii, H. and Ishijima S., "Mission Function Control for Deployment and Retrieval of a Subsatellite," *Journal of Guidance, Control, and Dynamics*, Vol. 12, No. 2, March-April 1989, pp. 243-247.

[47] Vadali, S.R. and Kim, E.S., "Feedback Control of Tethered Satellites Using Liapunov Stability Theory," *AIAA Dynamics Specialists Conference*, Long Beach, CA, Paper No. 90–97, April 1990.

[48] D'Souza, A.F. and Vijay, K.G., "Advanced Dynamics, Modelling and Analysis," *Prentice-Hall, Inc*, Englewood Cliffs, New Jersey, 1984.

[49] Dorf, R.C., "Modern Control Systems," *Addison-Wesley,Inc*, Philippines, 1980.

[50] Modi, V.J., Chang-Fu, G., Misra, A.K. and Xu, D.M., "On the Control of the Space Shuttle Based Tethered Systems," *Acta Astronautica*, Vol. 9, June-July 1982, pp. 437–443.

[51] Cunningham, W.J., "Introduction to Nonlinear Analysis" *McGraw-Hill*.

[52] Arnold, D.A., "The Behavior of Long Tethers in Space," *The Journal of the Astronautical Sciences*, Vol. 35, No. 1, January-march 1987, pp. 3–18.

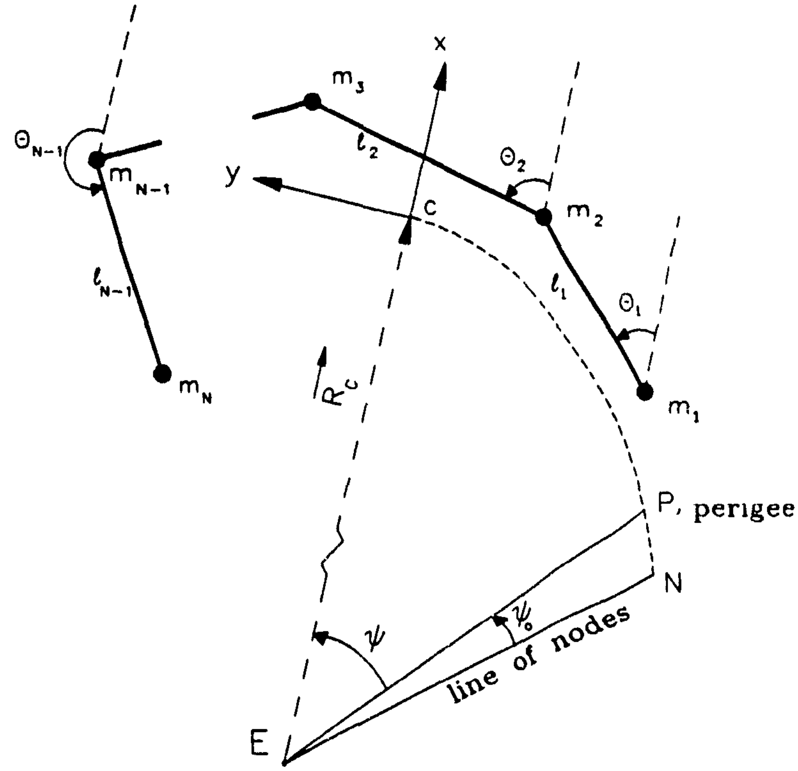

a) Projection of the N–body system in the orbital plane;

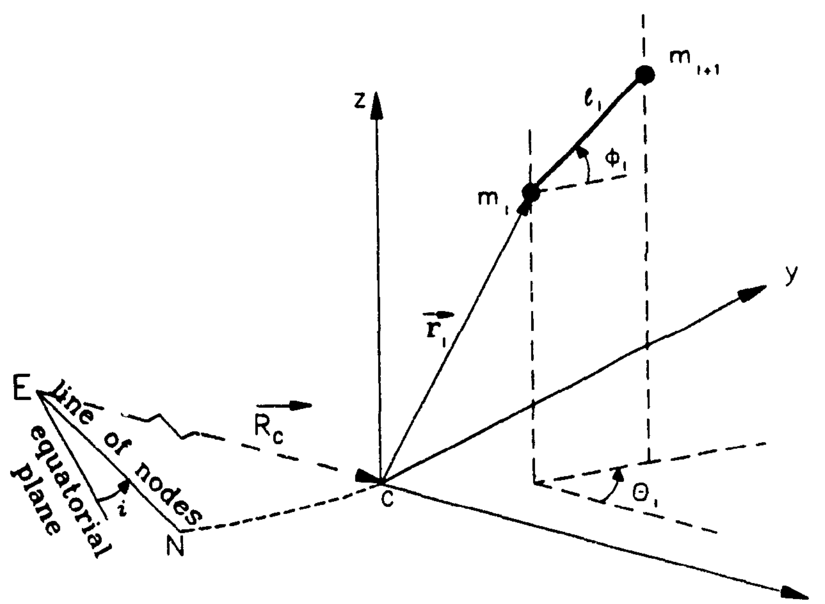

b) Definition of angles Θ_i and Φ_i

Fig. 2.1: Orientation and configuration of the system.

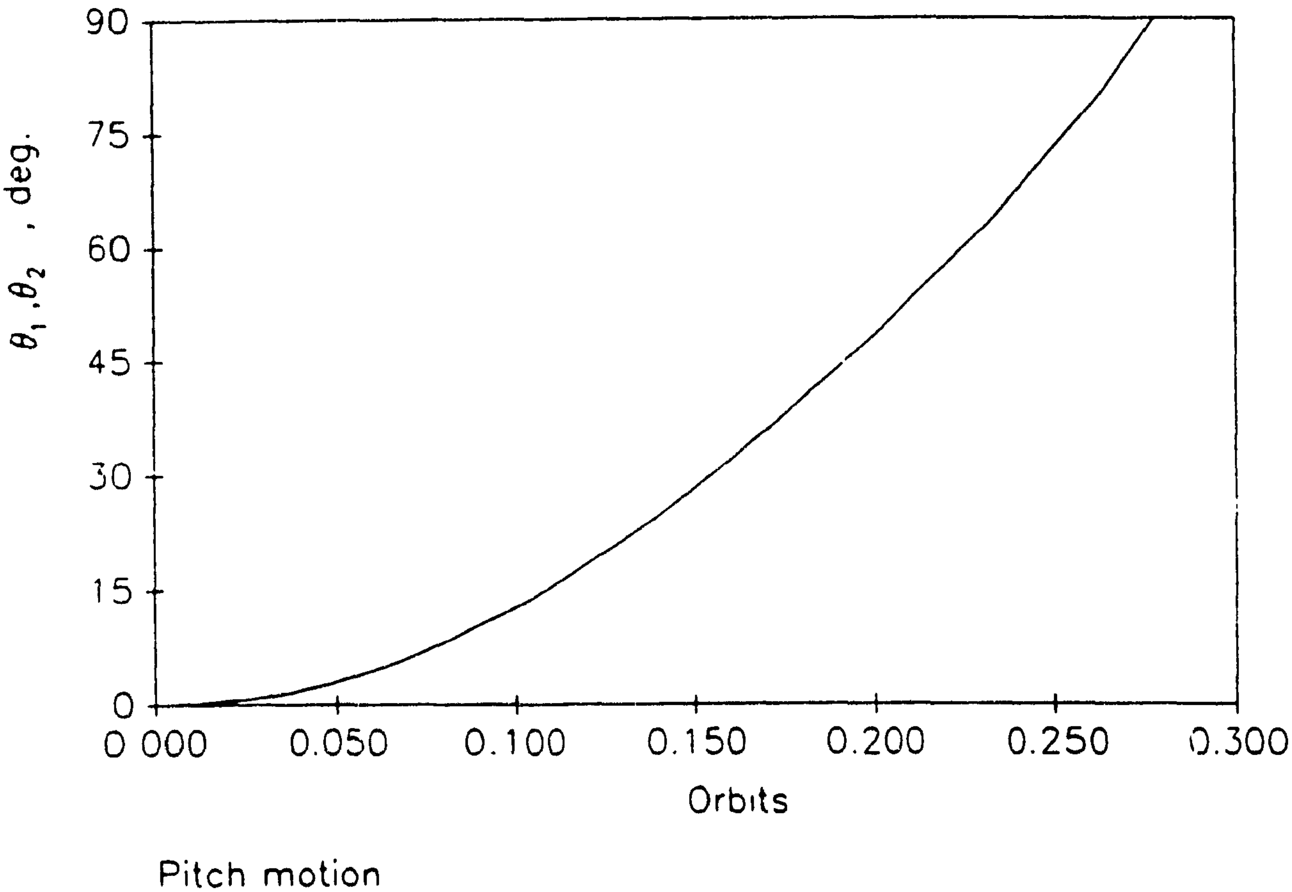

Fig. 3.1: Uncontrolled retrieval dynamics of a three-body system for the case of: $c_1 = c_2 = 0.5$, $m_1 = 1000$ kg, $m_2 = 100000$ kg, $m_3 = 2000$ kg, $\theta_1(0) = \theta_2(0) = 0.0$, $\phi_1(0) = \phi_2(0) = 0.1$, $\ell_1(0) = 10000.0$ m, $\ell_2(0) = 5000.0$ m, $\dot{\theta}_1(0) = \dot{\theta}_2(0) = \dot{\phi}_1(0) = \dot{\phi}_2(0) = 0.0$.

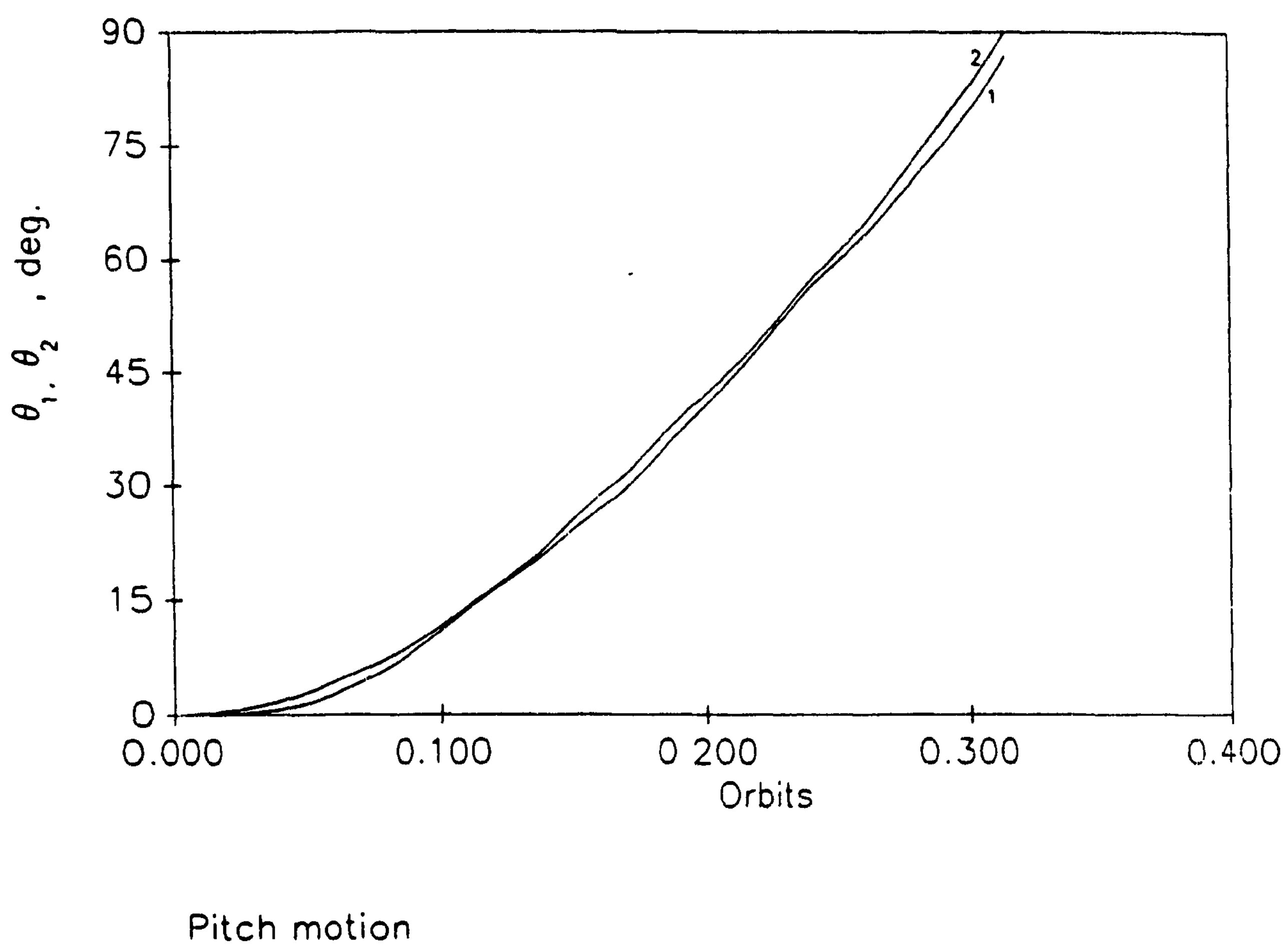

Fig. 3.2: Uncontrolled retrieval dynamics of a three-body system for the case of: $c_1 = 0.1$, $c_2 = 0.5$, $m_1 = 100000$ kg, $m_2 = 5000$ kg, $m_3 = 10000$ kg, $\theta_1(0) = \theta_2(0) = 0.0$, $\phi_1(0) = \phi_2(0) = 0.1$, $\ell_1(0) = 10000.0$ m, $\ell_2(0) = 100000.0$ m, $\dot{\theta}_1(0) = \dot{\theta}_2(0) = \dot{\phi}_1(0) = \dot{\phi}_2(0) = 0.0$.

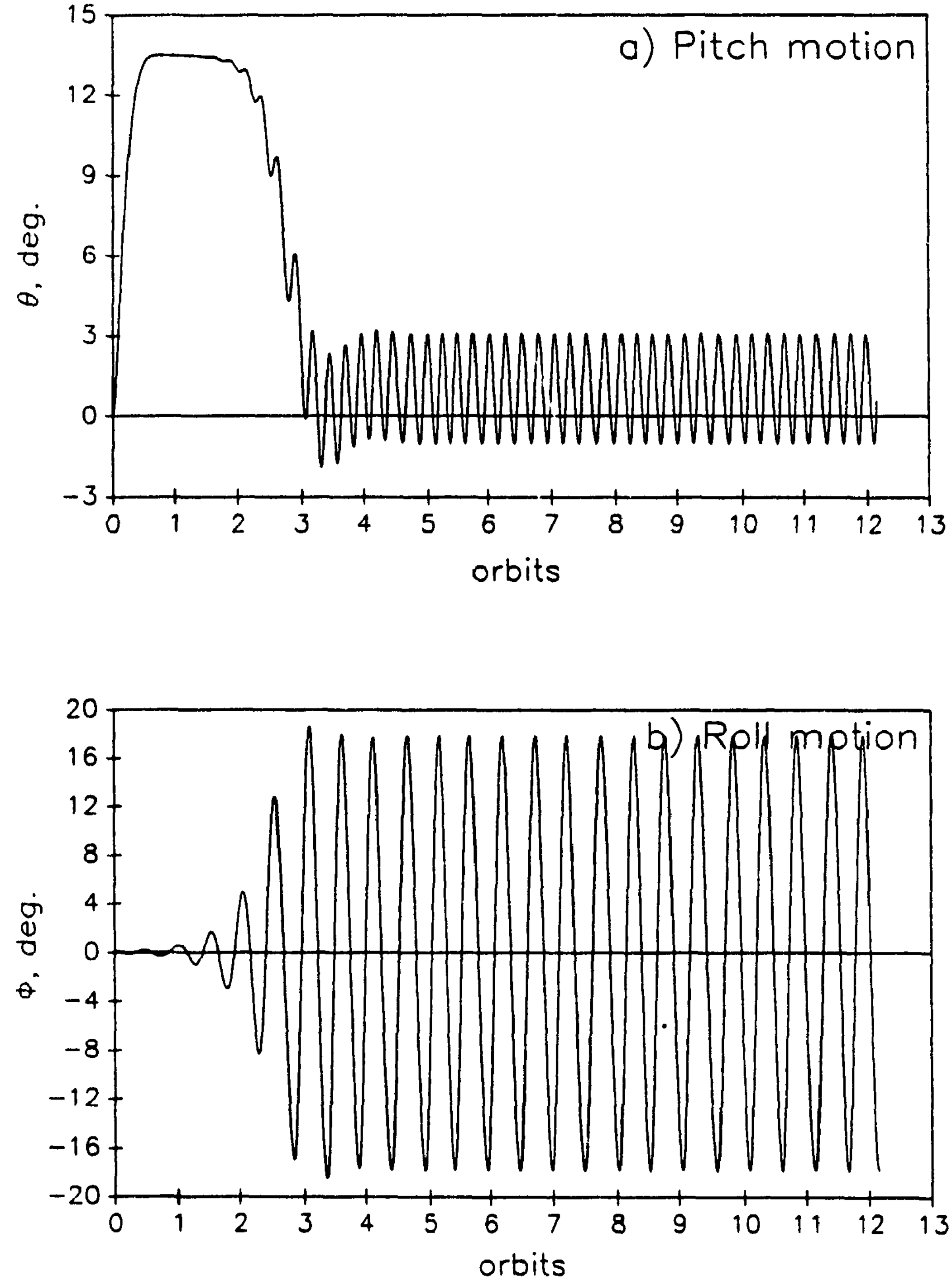

Fig. 3.3: Retrieval dynamics of a two-body system using the reel rate law of Eq. 3.18 for the case of: $c = 0.34$, $K = 5.0$, $m_2 = 150$ kg, $m_1 \gg m_2$, and $\theta(0) = 0.0$, $\phi(0) = 0.1$, $\ell(0) = 100.0$ km, $\dot{\theta}(0) = 0.0$, $\dot{\phi}(0) = 0.0$, $\ell_{\text{final}} = 0.1$ km.

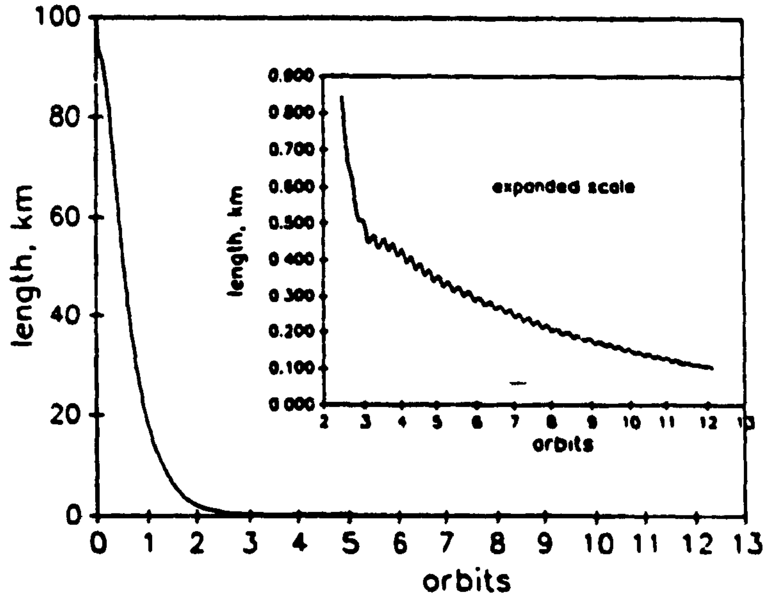

c)Variation of Length

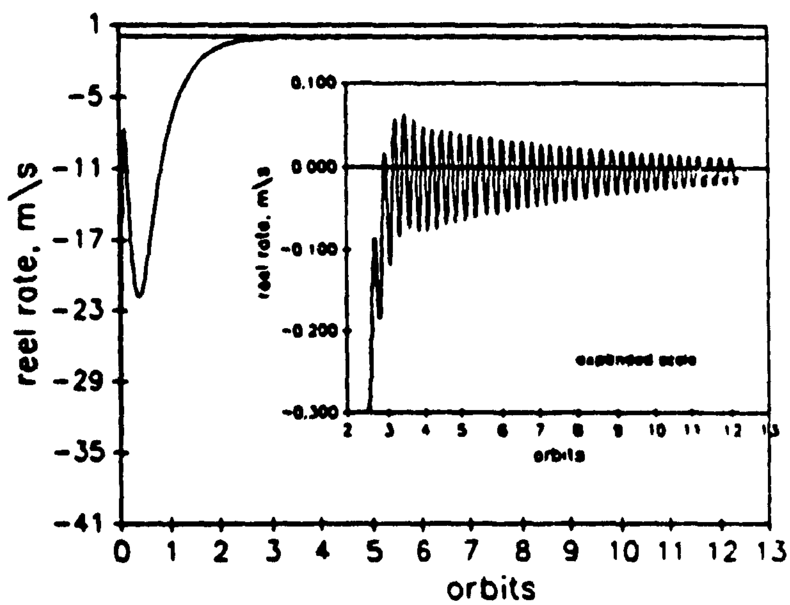

d) Variation of Reel Rate

Fig. 3.3 - Continued

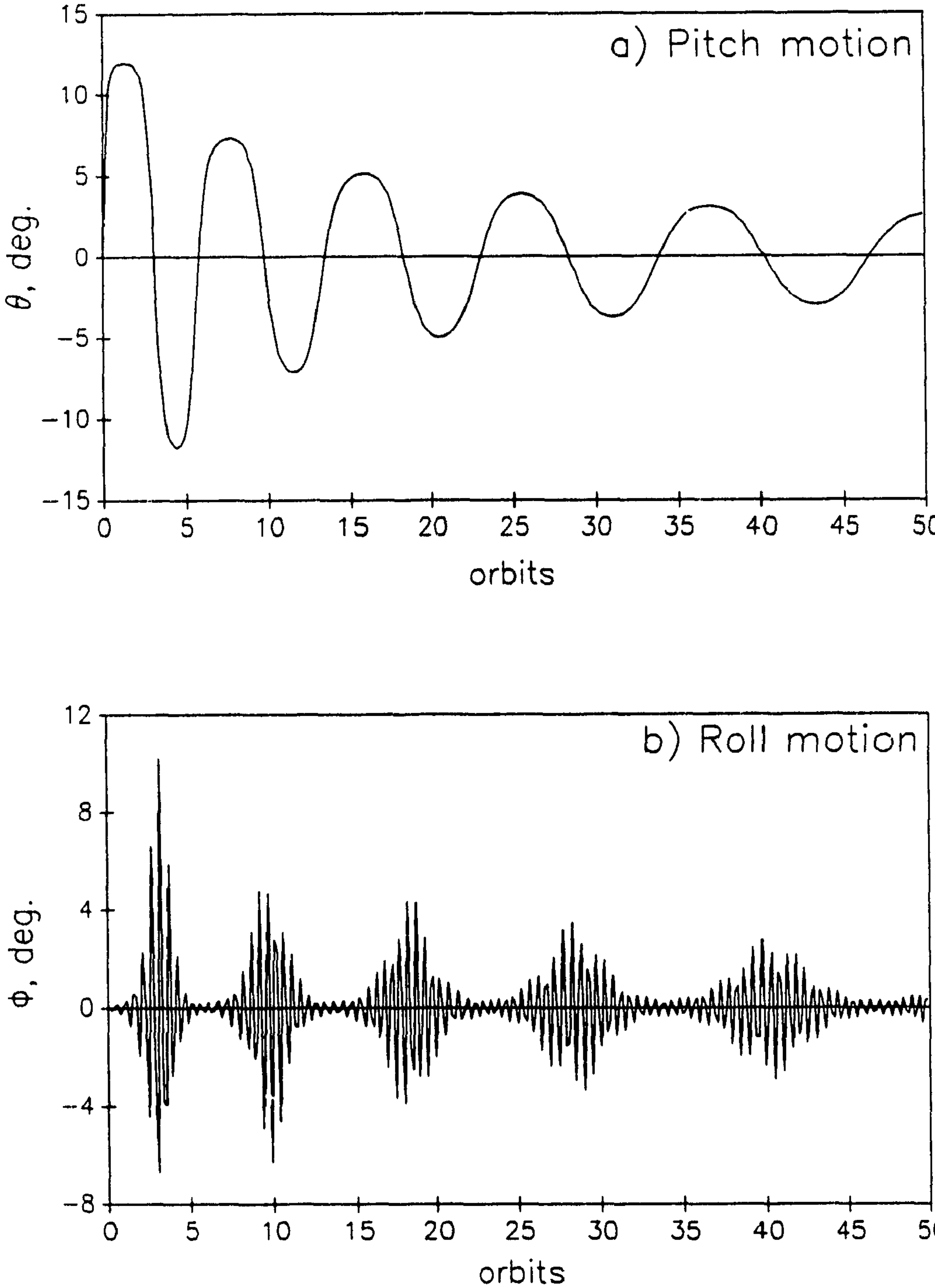

Fig. 3.4: Retrieval dynamics of a two-body system using the reel rate law of Eq. 3.20, proposed by Vadali and Kim [47]. The system parameters and initial conditions are the same as Fig. 3.3.

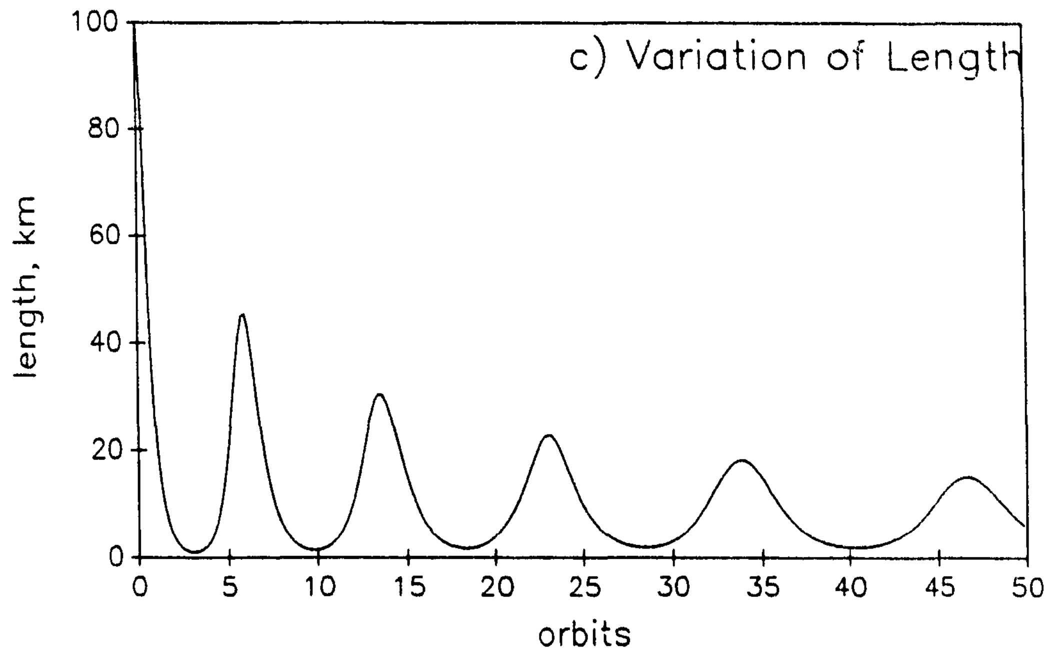

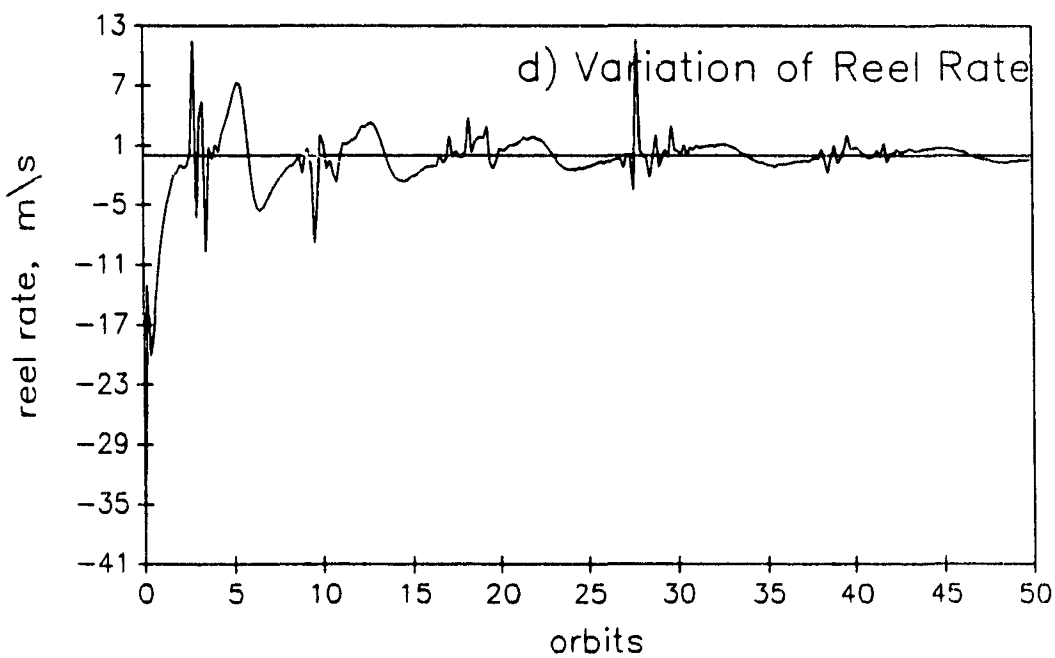

Fig. 3.4 - Continued

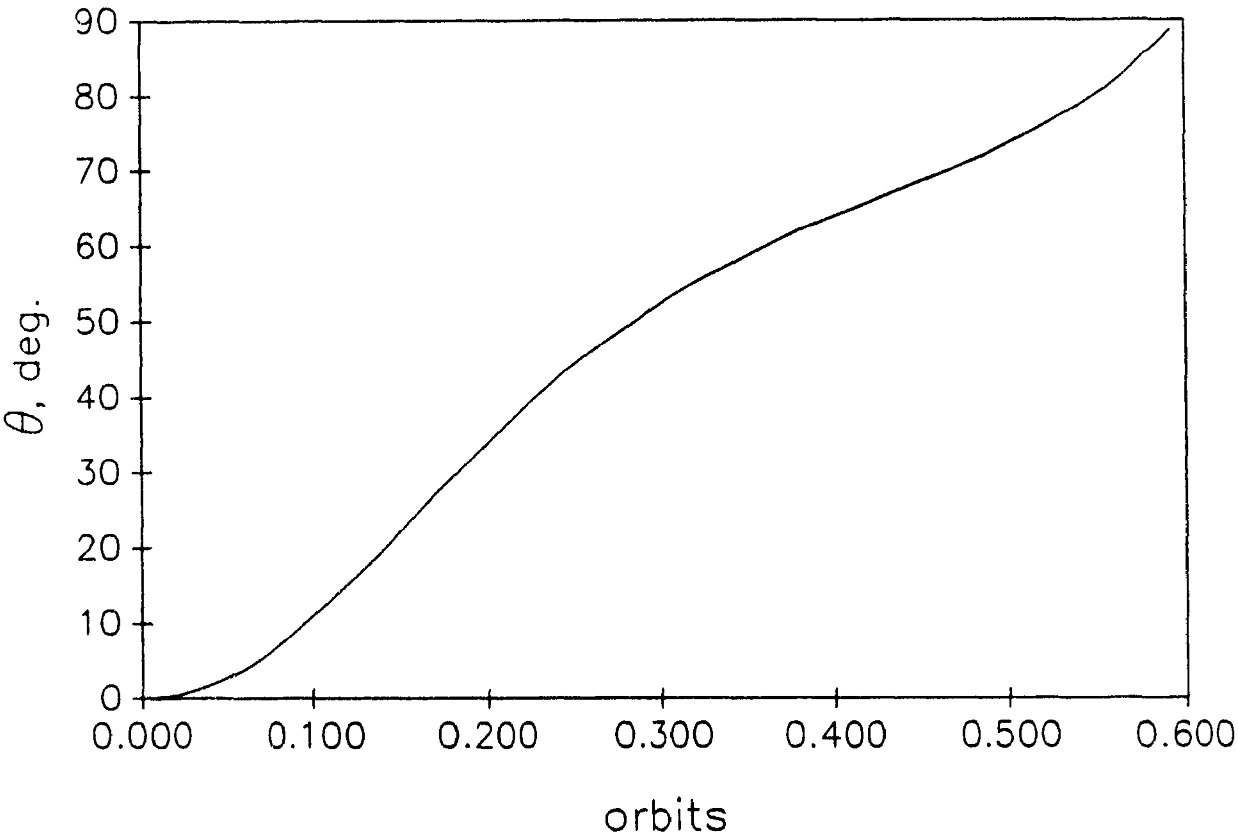

Fig. 4.1: Retrieval dynamics of a pure in-plane motion in the large (Eq. 4.37) with a linear feedback for the case of: $c = 0.5, \Longrightarrow \theta_e = 19.1^o \ K_\theta = 0.5$.

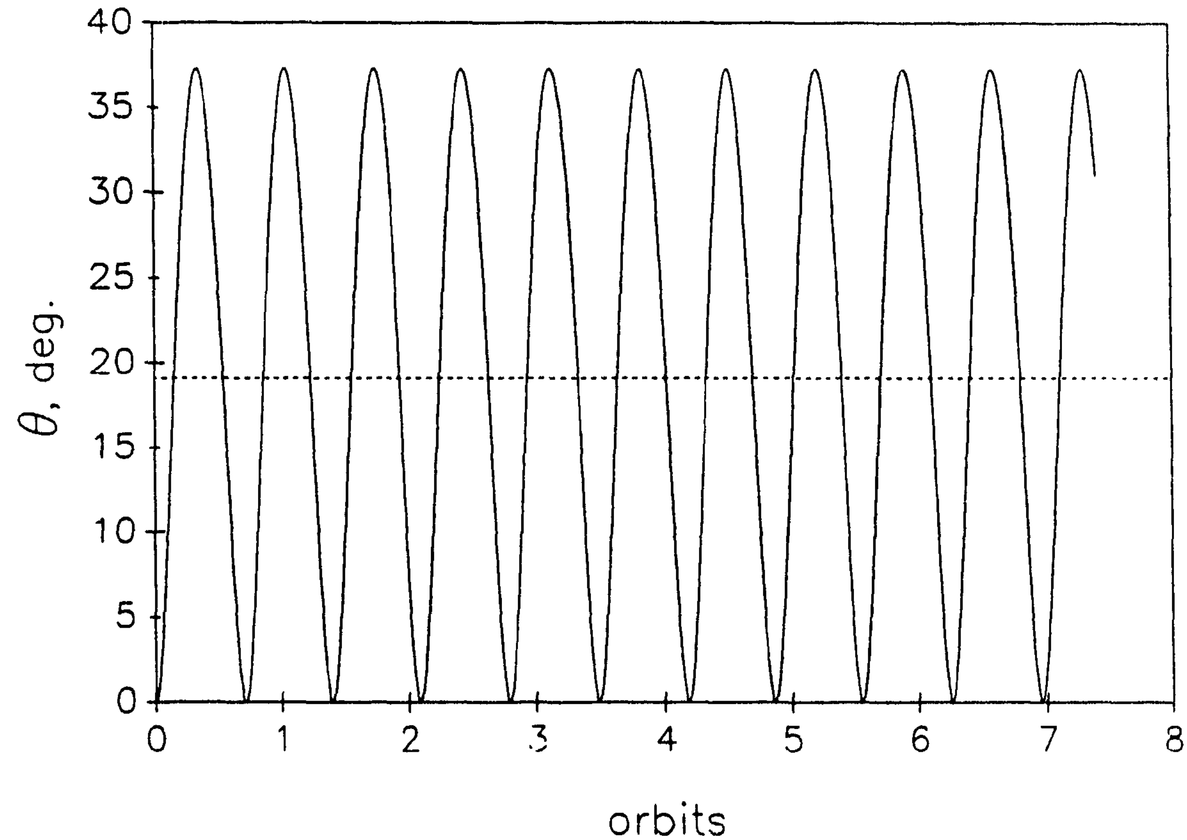

Fig. 4.2: Retrieval dynamics of a pure in-plane motion in the large (Eq. 4.37) with a linear feedback for the case of: $c = 0.5, \Longrightarrow \theta_e = 19.1^o \; K_\theta = 1.0$.

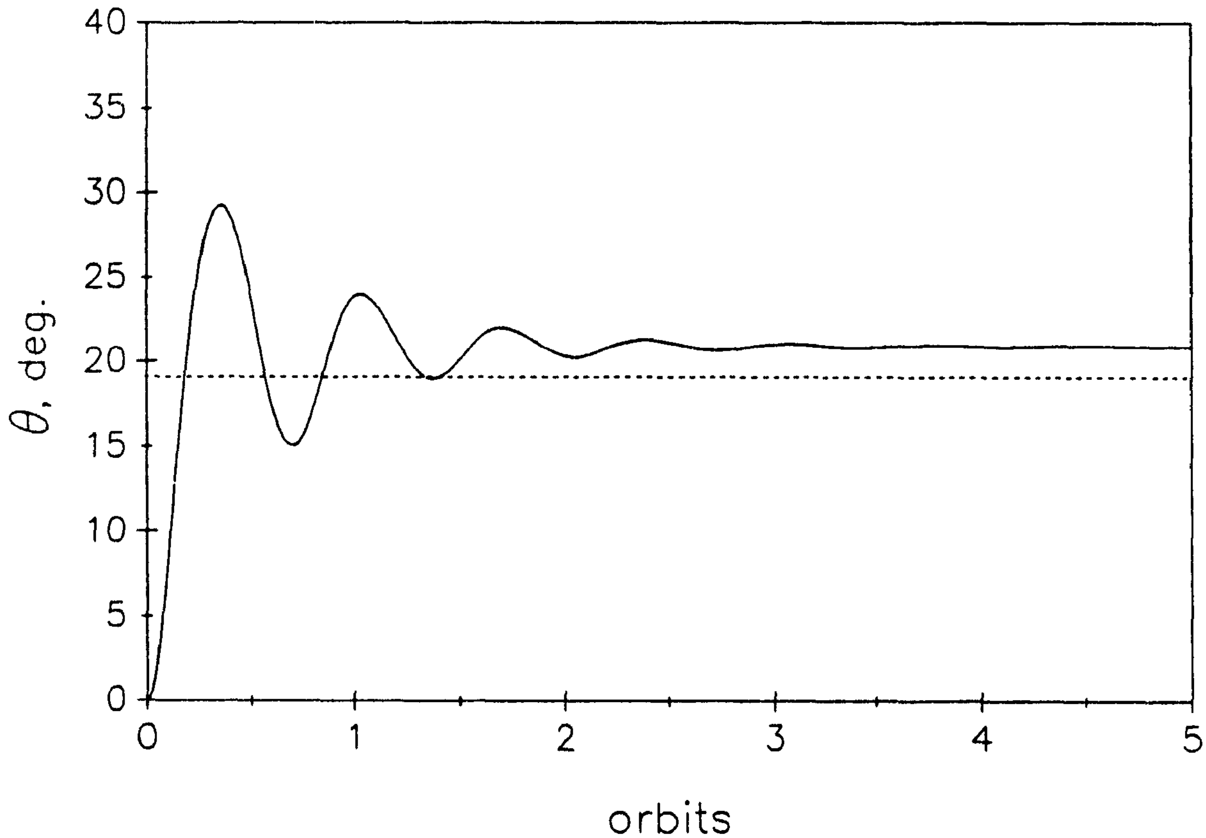

Fig. 4.3: Retrieval dynamics of a pure in-plane motion in the large (Eq. 4.37) with a linear feedback for the case of: $c = 0.5, \Longrightarrow \theta_e = 19.1^o \; K_\theta = 1.5$.

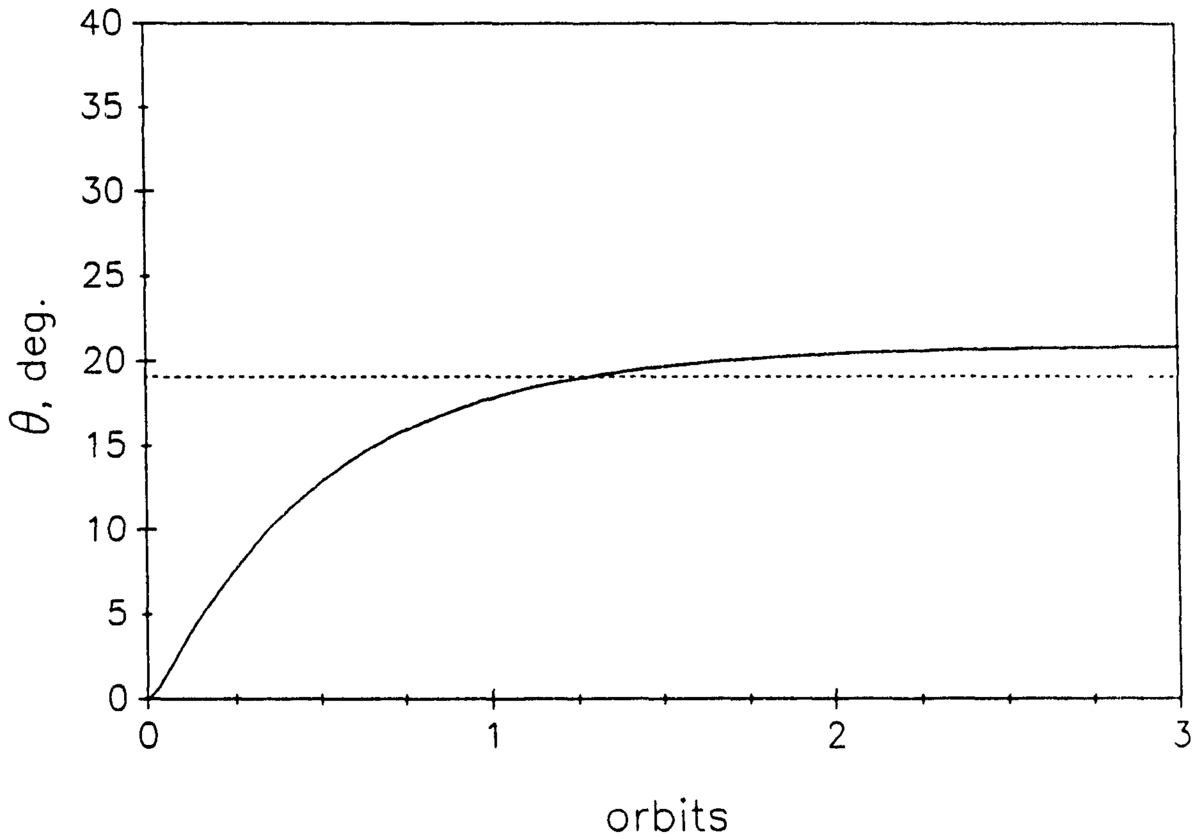

Fig. 4.4: Retrieval dynamics of a pure in-plane motion in the large (Eq. 4.37) with a linear feedback for the case of: $c = 0.5, \Longrightarrow \theta_e = 19.1^o \ K_\theta = 9.0$.

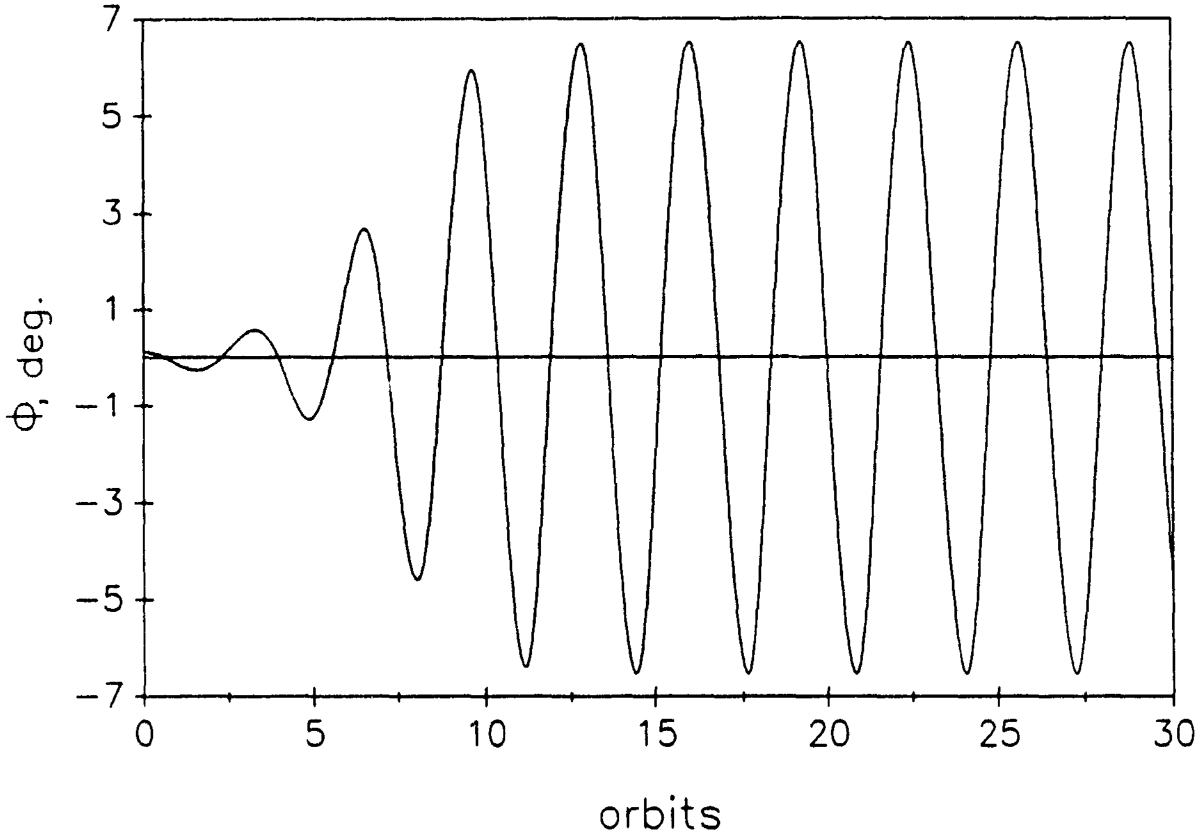

Fig. 4.5: Retrieval dynamics of a pure out-of-plane motion in the large (Eq. 4.43) with a quadratic feedback for the case of: $c = 0.5$, $K_\phi = 27.0$.

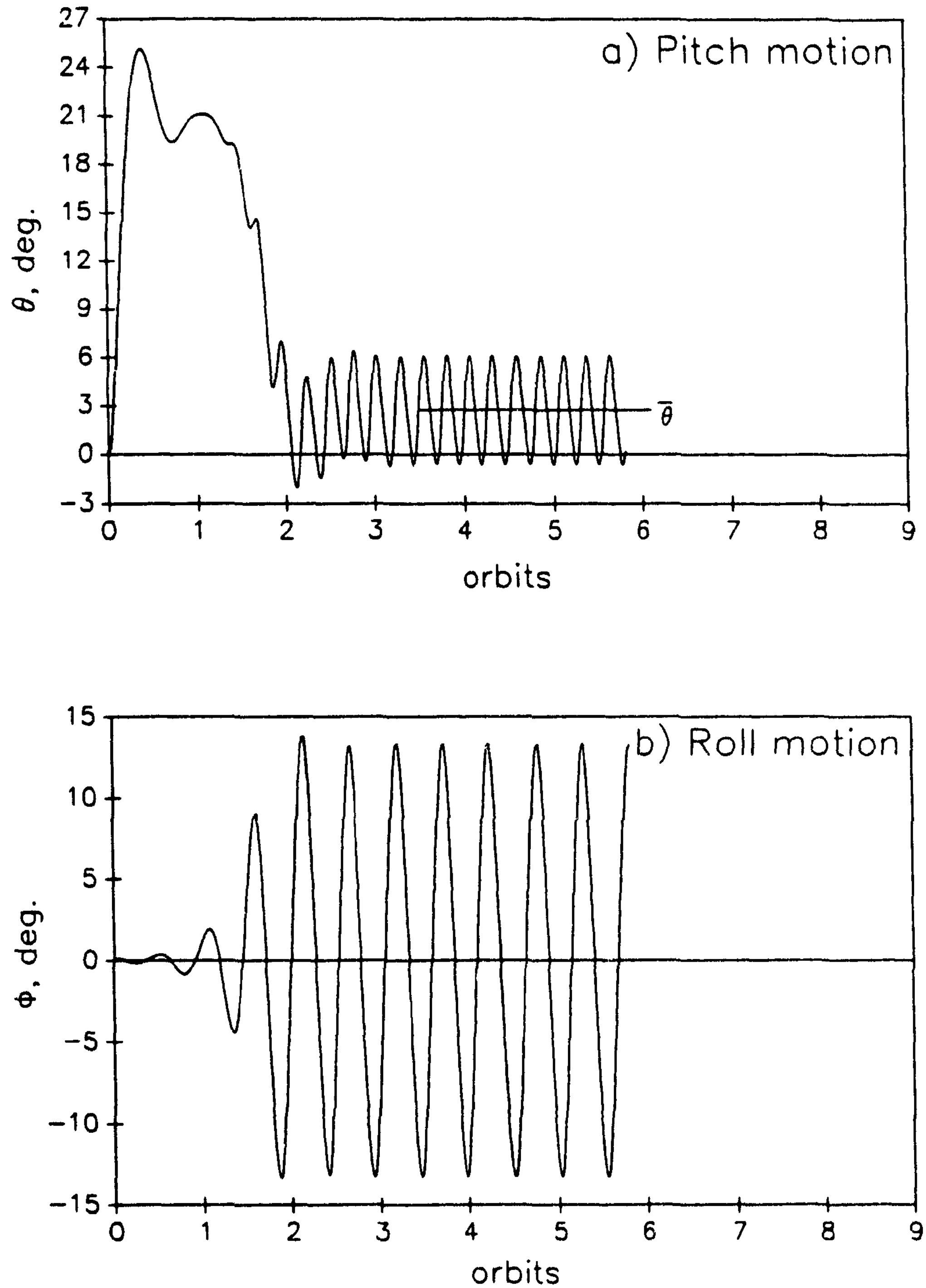

Fig. 4.6: Retrieval dynamics of a two-body system using the reel rate law of Eq. 4.25 for the case of: $c = 0.5$, $K_\theta = 2.0$, $K_\phi = 9.0$, and other system parameters and initial conditions the same as Fig. 3.3.

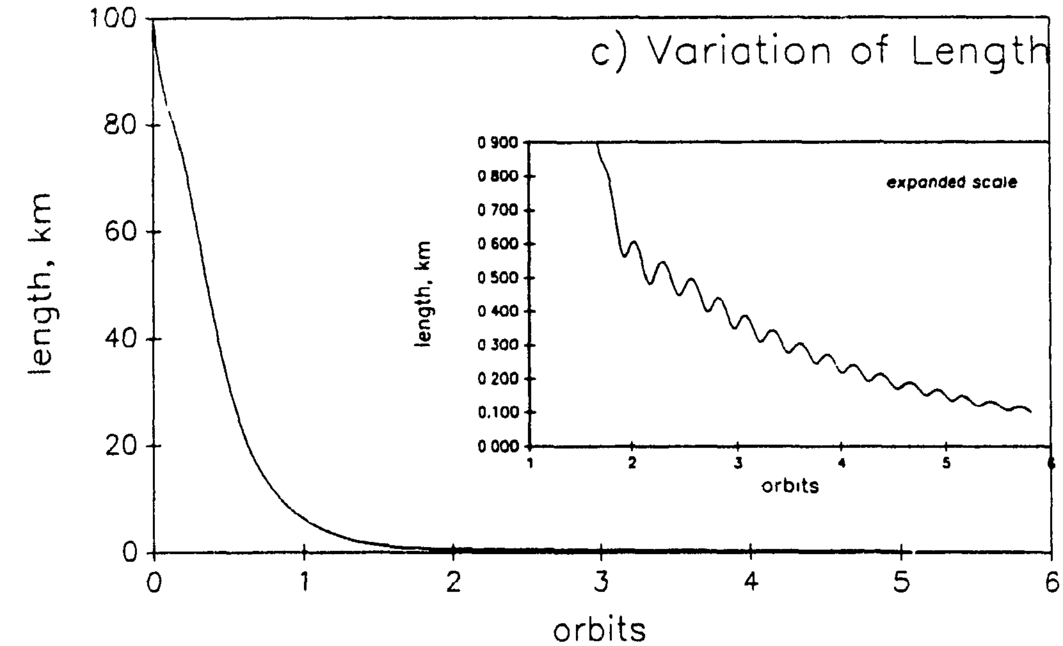

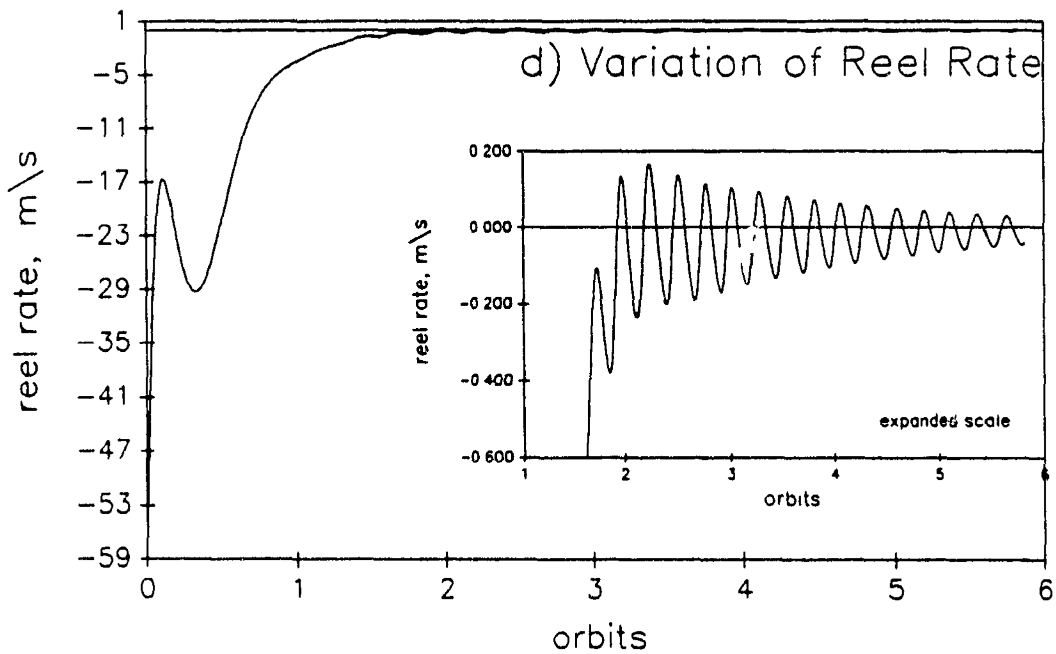

Fig. 4.6 - Continued

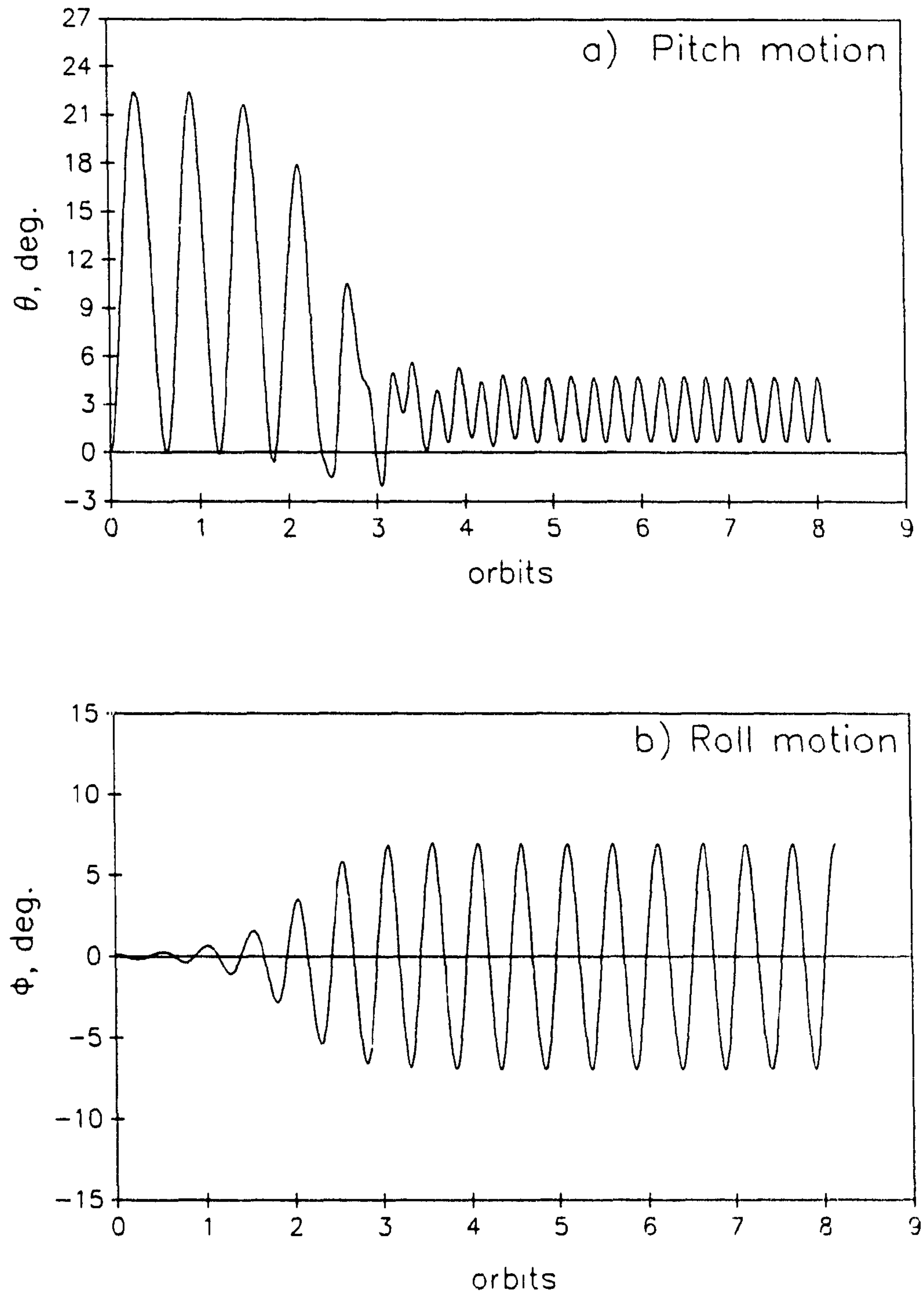

Fig. 4.7: Retrieval dynamics of a two-body system using the reel rate law of Eq. 4.25 for the case of: $c = 0.3$, $K_\theta = 1.0$, $K_\phi = 27.0$, and other system parameters and initial conditions the same as Fig. 4.6.

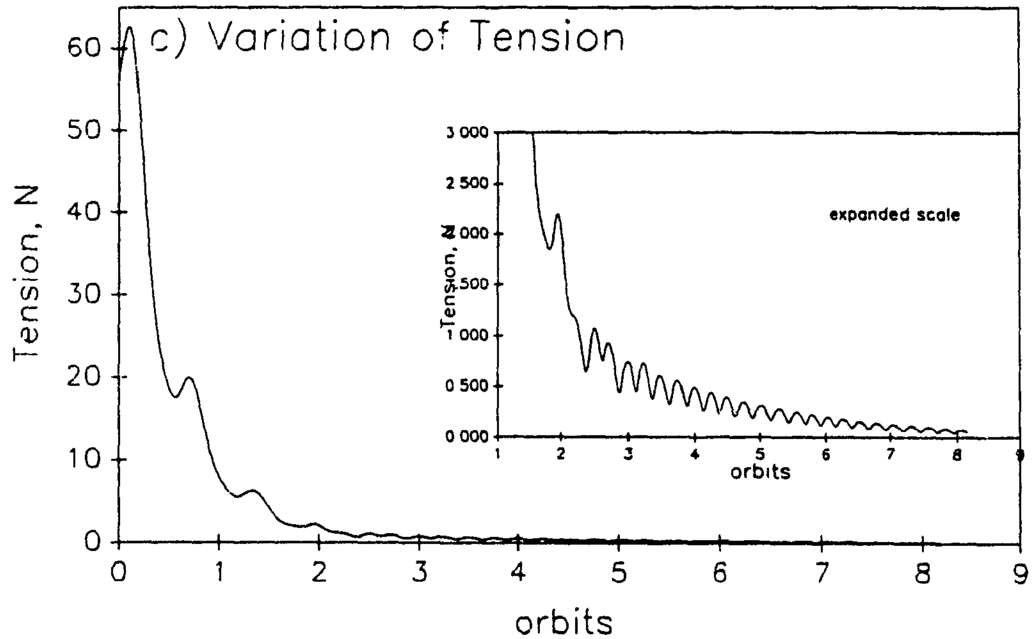

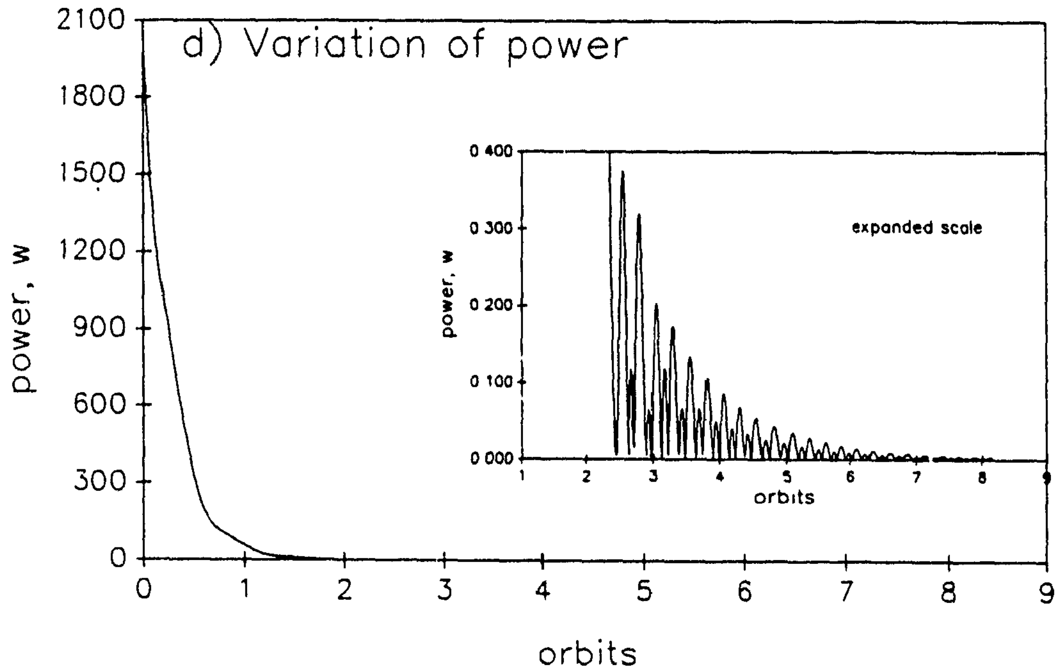

Fig. 4.7 - Continued

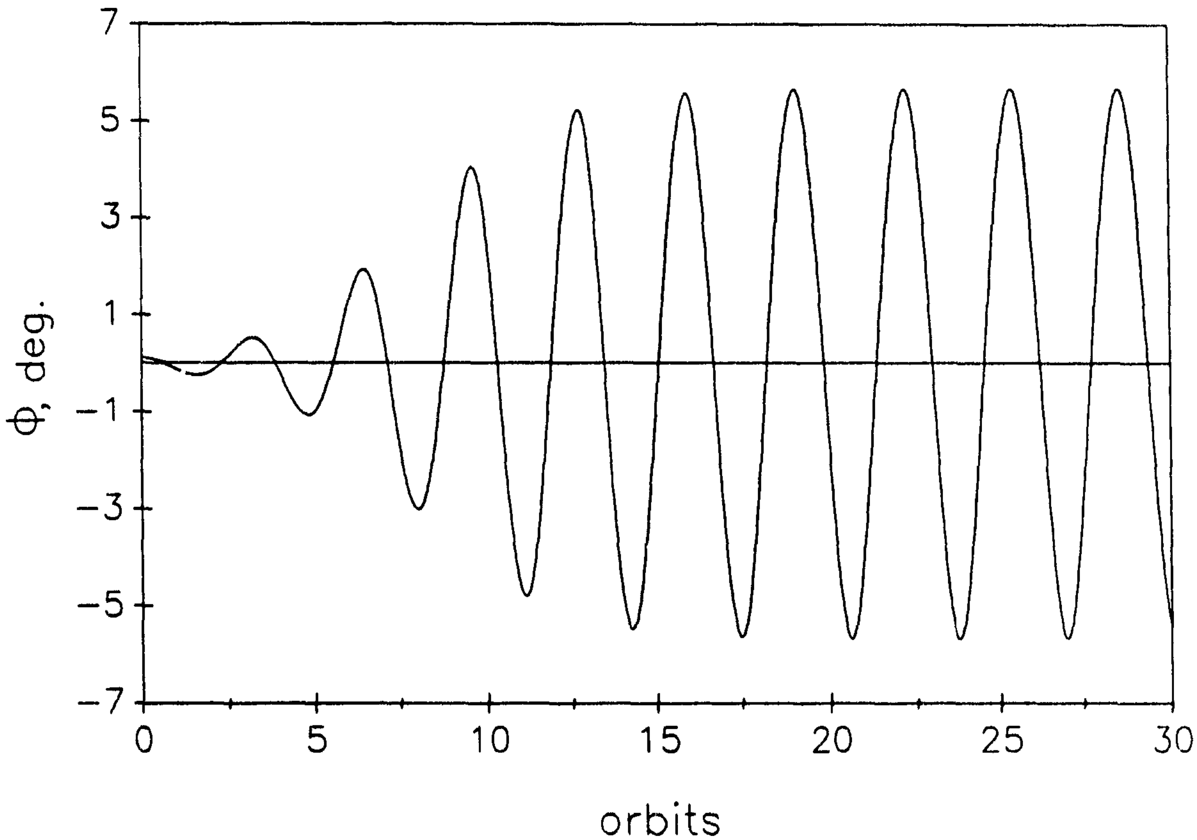

Fig. 4.8: Retrieval dynamics of a pure out-of-plane motion in the large (Eq. 4.59) with an absolute value feedback for the case of: $c = 0.5$, $K_\phi = 6.0$.

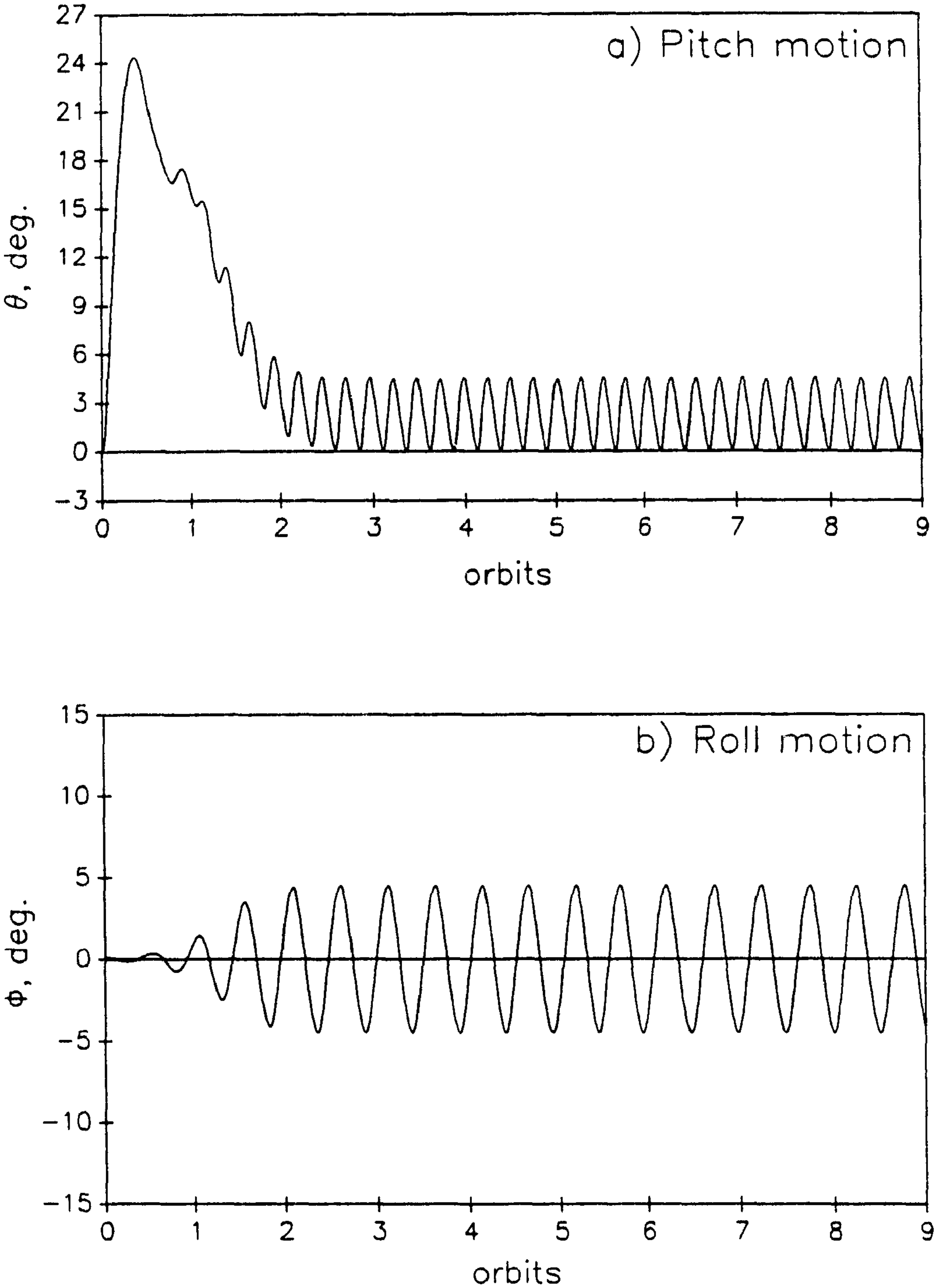

Fig. 4.9: Retrieval dynamics of a two-body system using the reel rate law of Eq. 4.53 for the case of: $c = 0.5$, $K_\theta = 2.0$, $K_\phi = 9.0$, and other system parameters and initial conditions the same as Fig. 4.6.

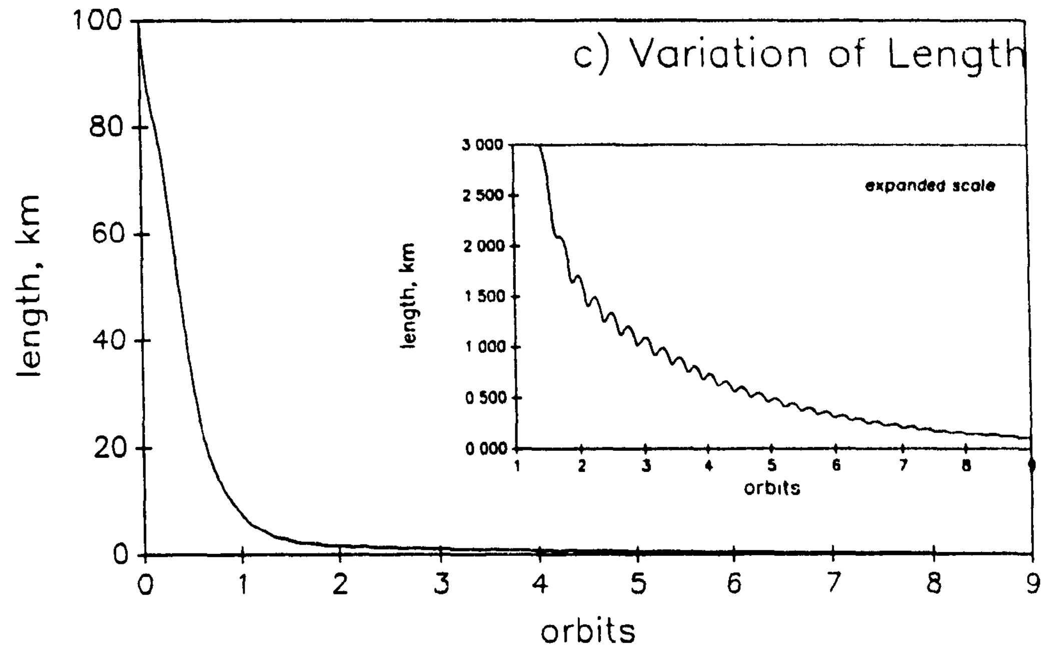

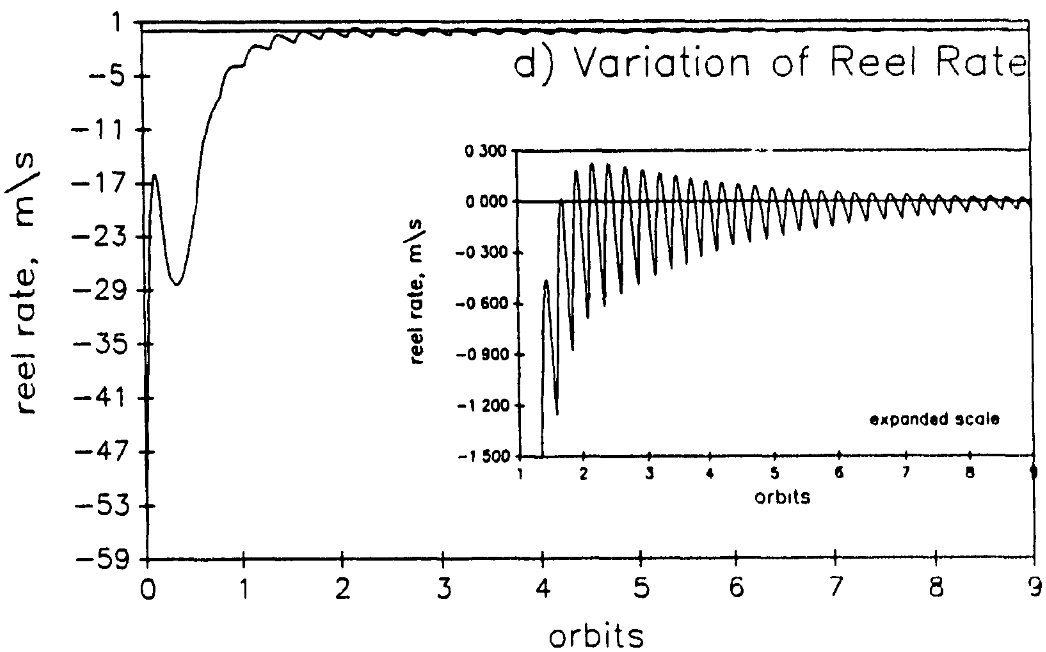

Fig. 4.9 - Continued

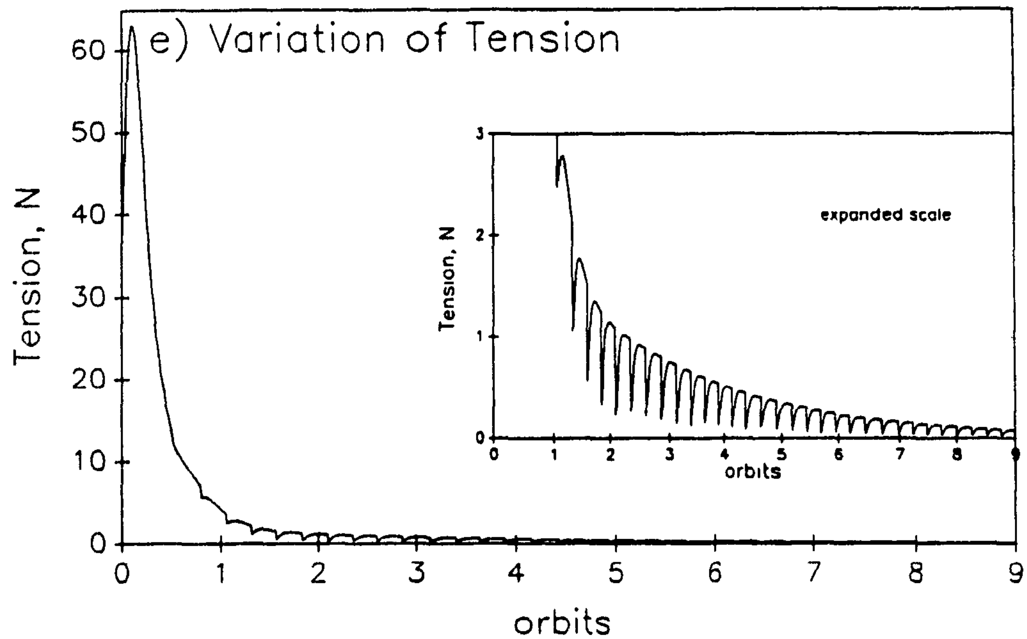

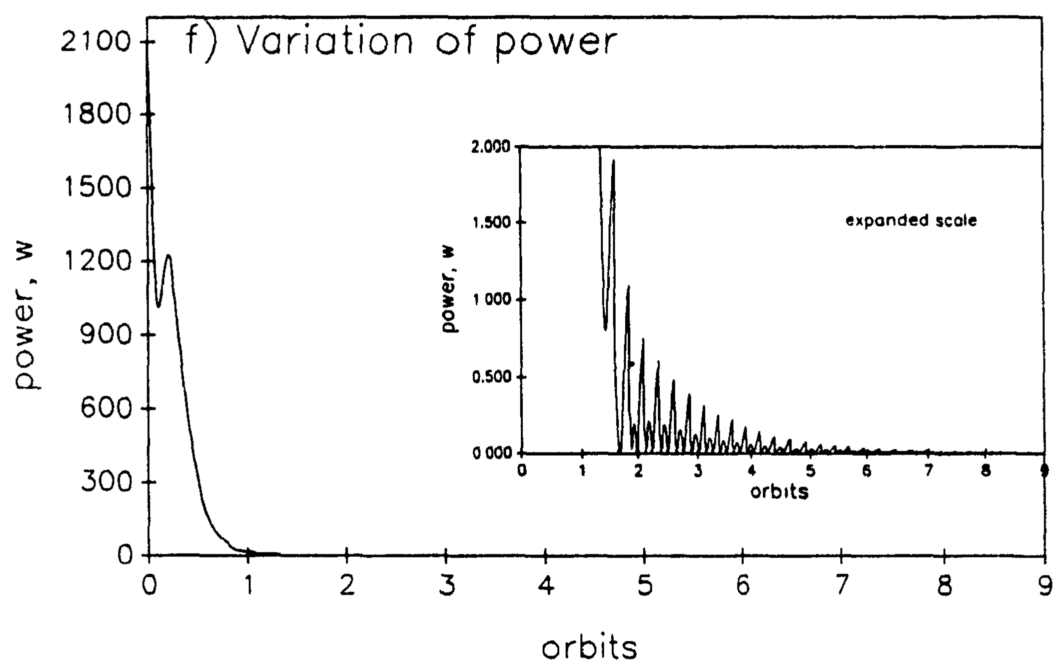

Fig. 4.9 - Continued

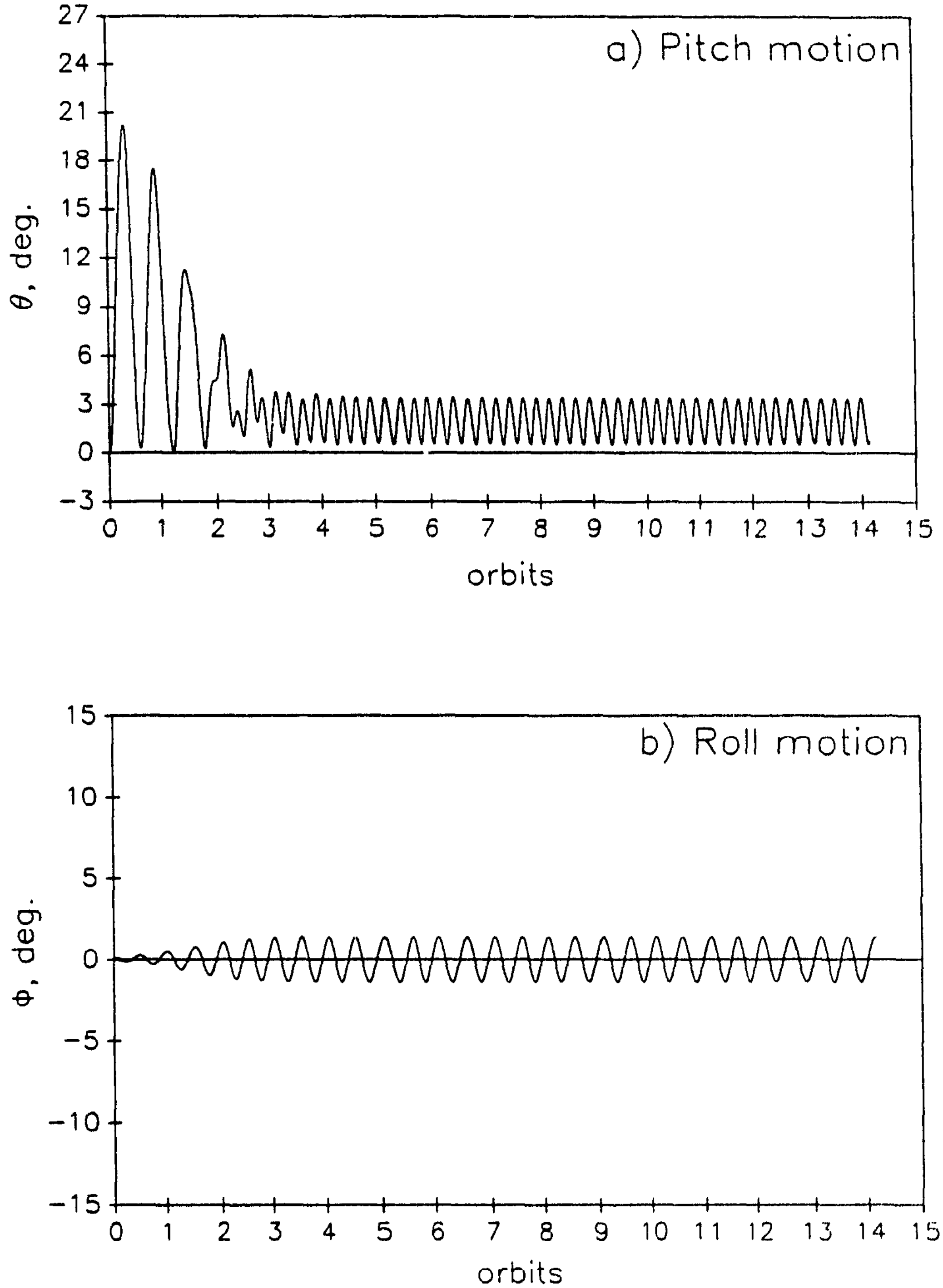

Fig. 4.10: Retrieval dynamics of a two-body system using the reel rate law of Eq. 4.53 for the case of: $c = 0.3$, $K_\theta = 1.0$, $K_\phi = 27.0$, and other system parameters and initial conditions the same as Fig. 4.6.

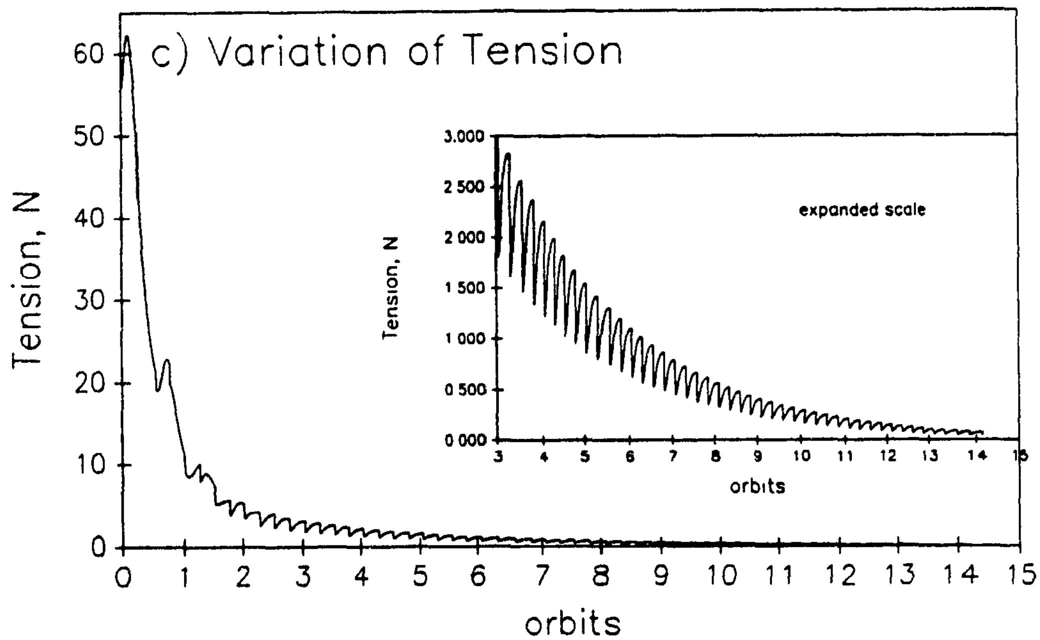

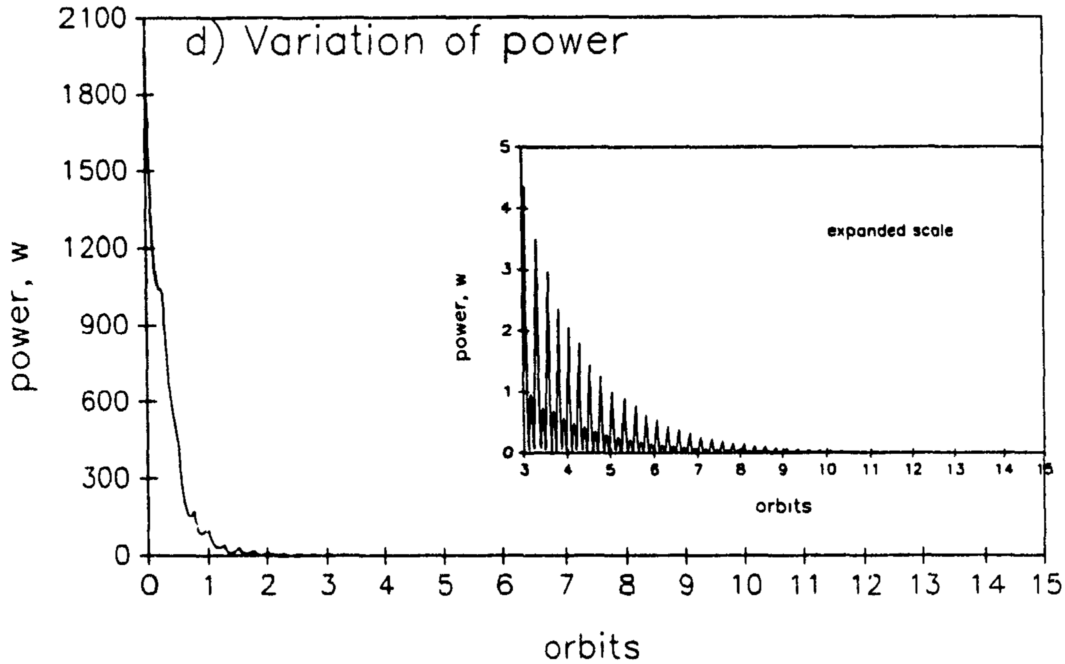

Fig. 4.10 - Continued

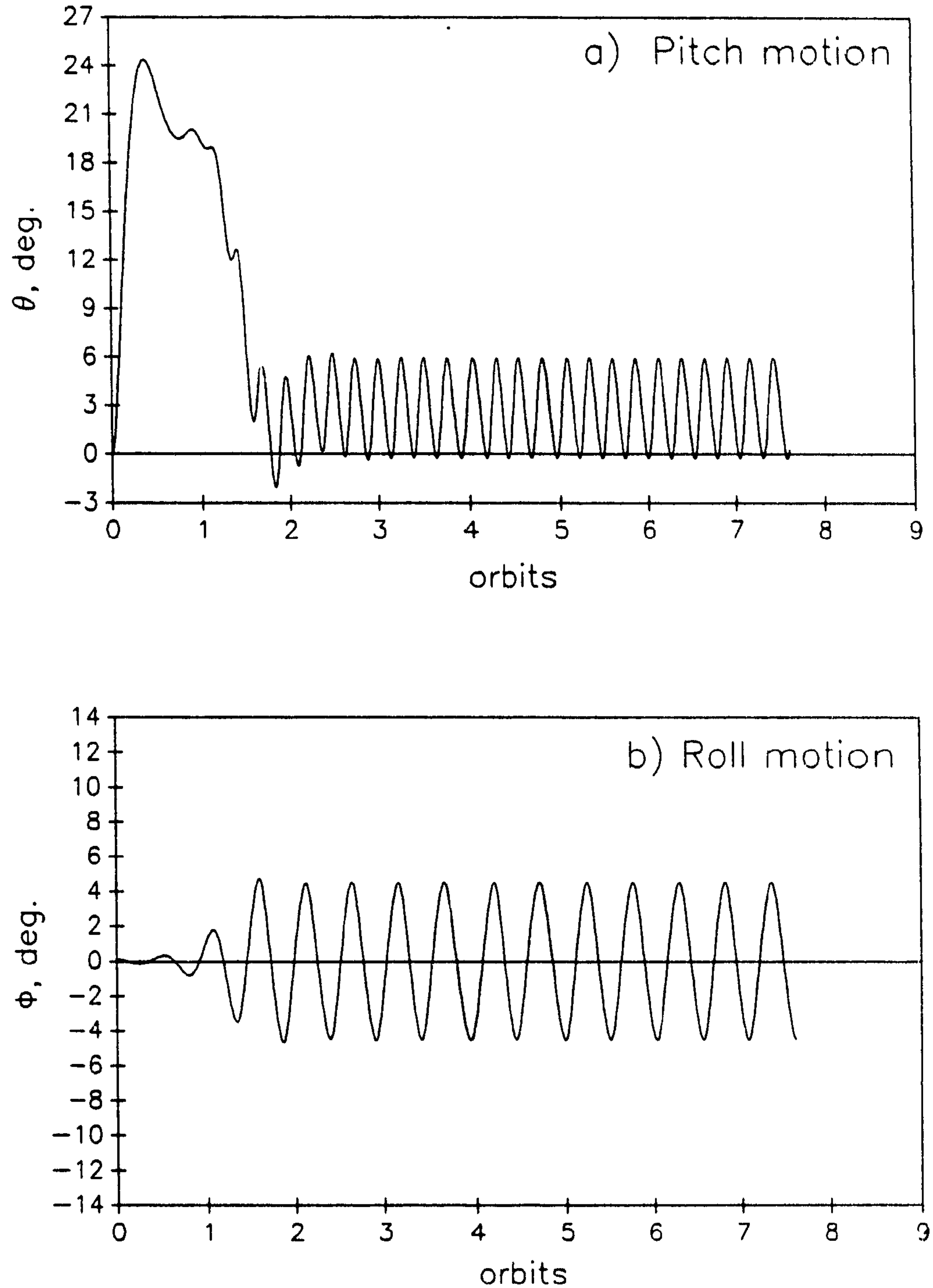

Fig. 4.11: Retrieval dynamics of a two-body system using the reel rate law of Eq. 4.25 for the case of: $c = 0.5$, $K_\theta = 2.13$, $K_\phi = 77.00$, and other system parameters and initial conditions the same as Fig. 4.6.

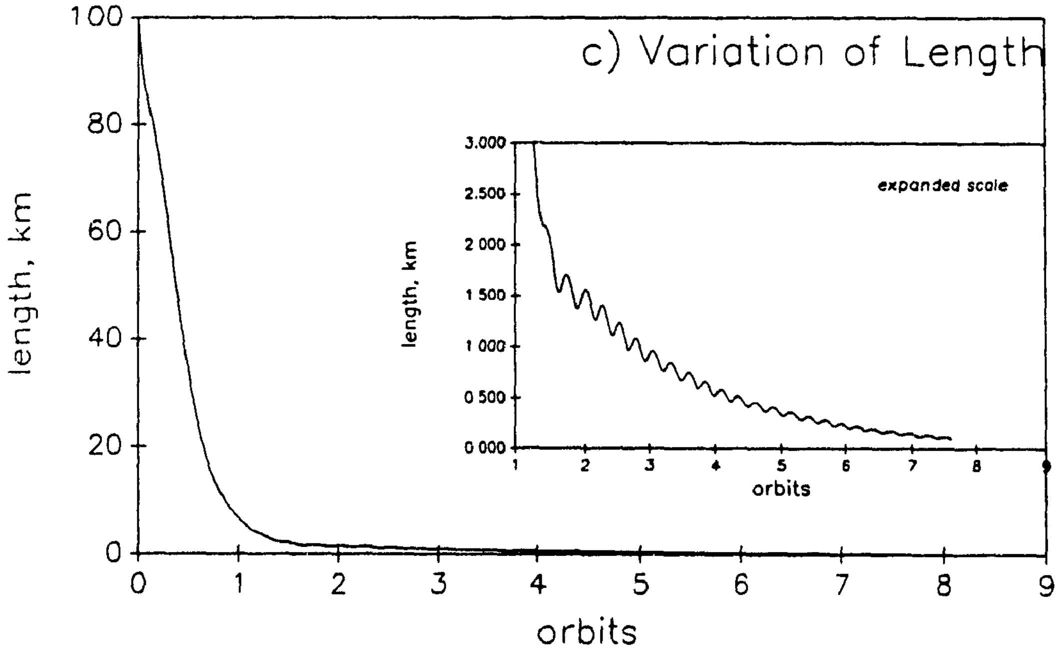

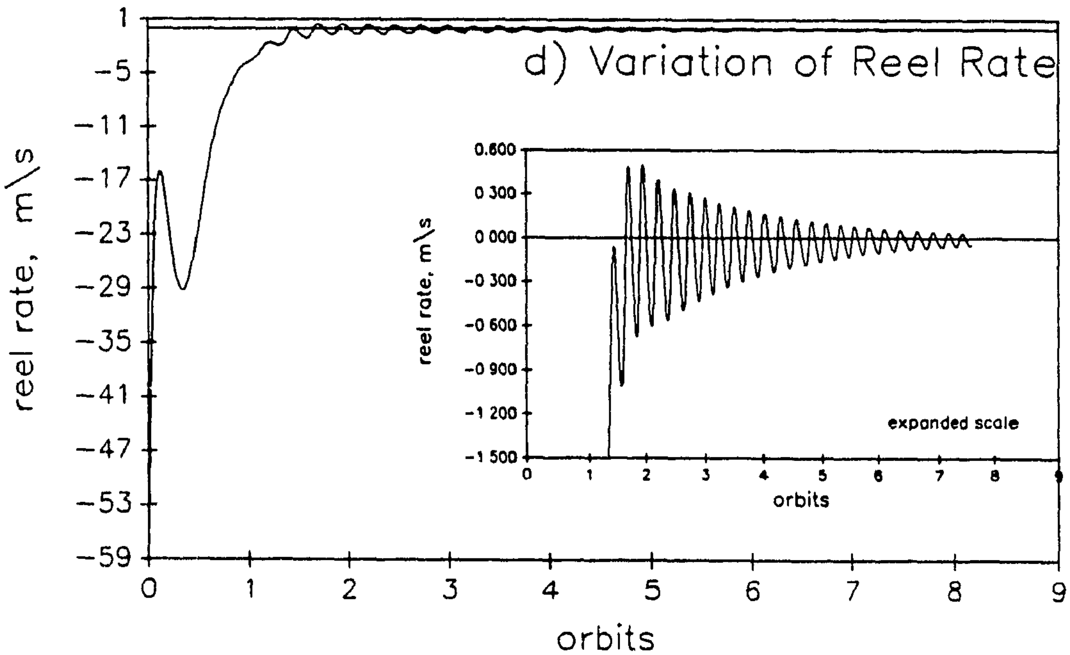

Fig. 4.11 - Continued

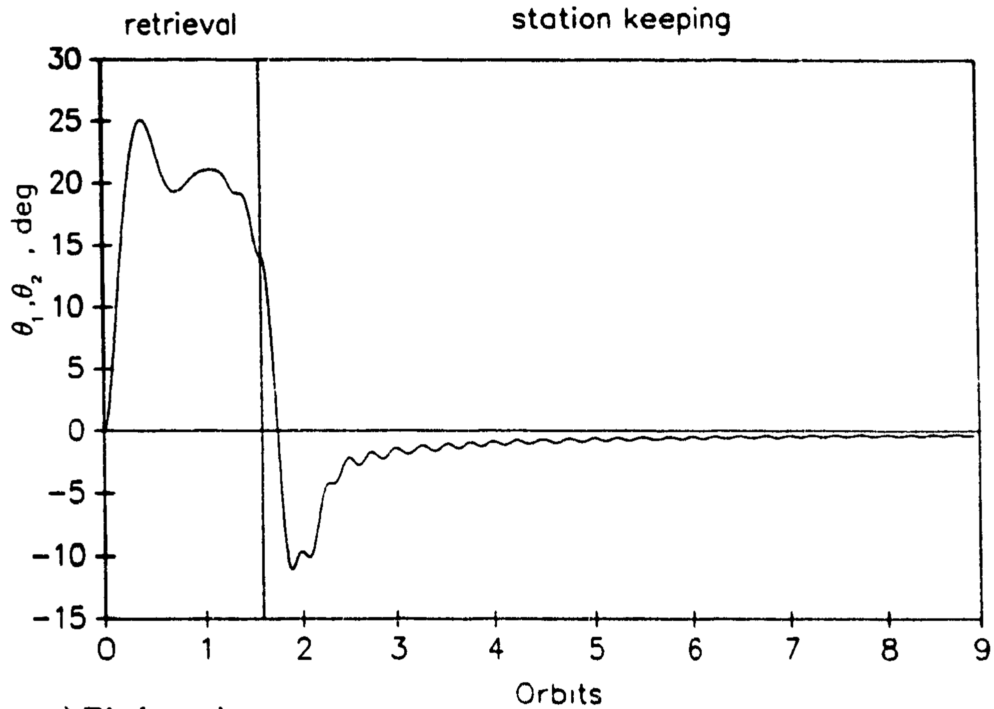

a) Pitch motion

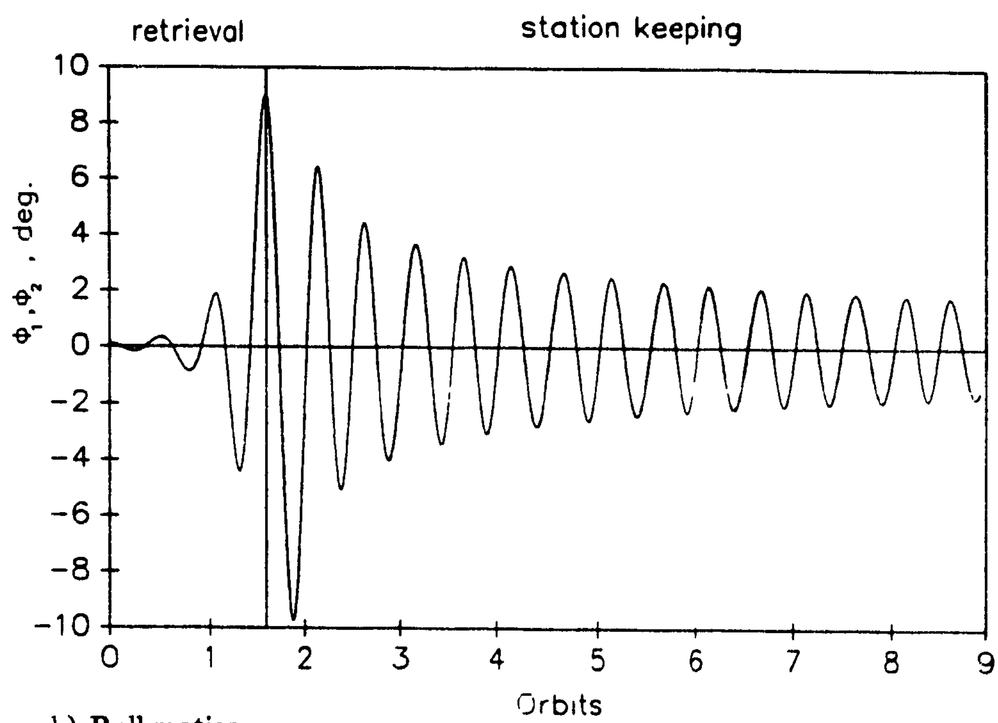

b) Roll motion

Fig. 4.12: Retrieval dynamics of a three-body system using the reel rate law of Eq. 4.63 for the case of: $K_{\theta_1} = K_{\theta_2} = 2.0$, $K_{\phi_1} = K_{\phi_2} = 9.0$, and other system parameters and initial conditions the same as Fig. 3.1.

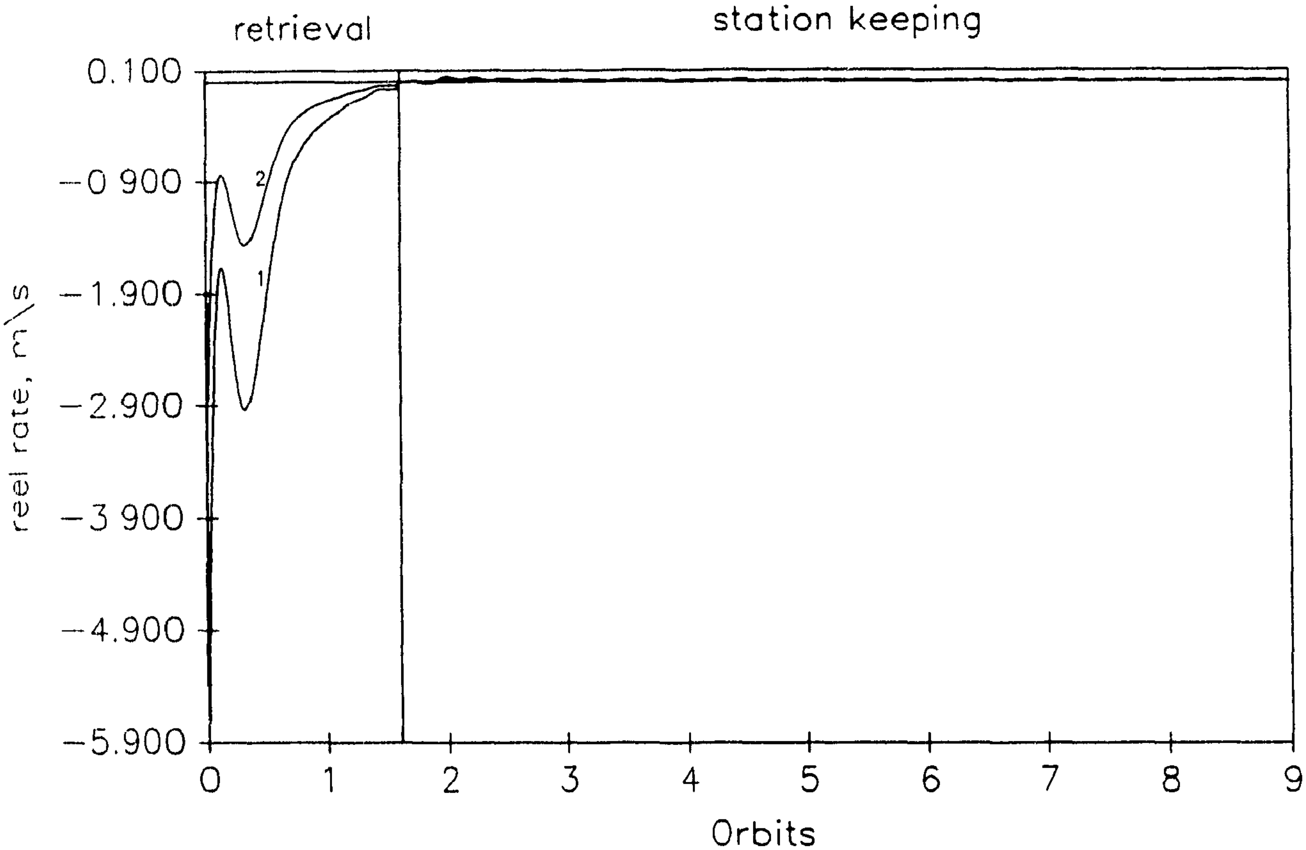

c) Variation of reel rate

Fig. 4.12 - Continued

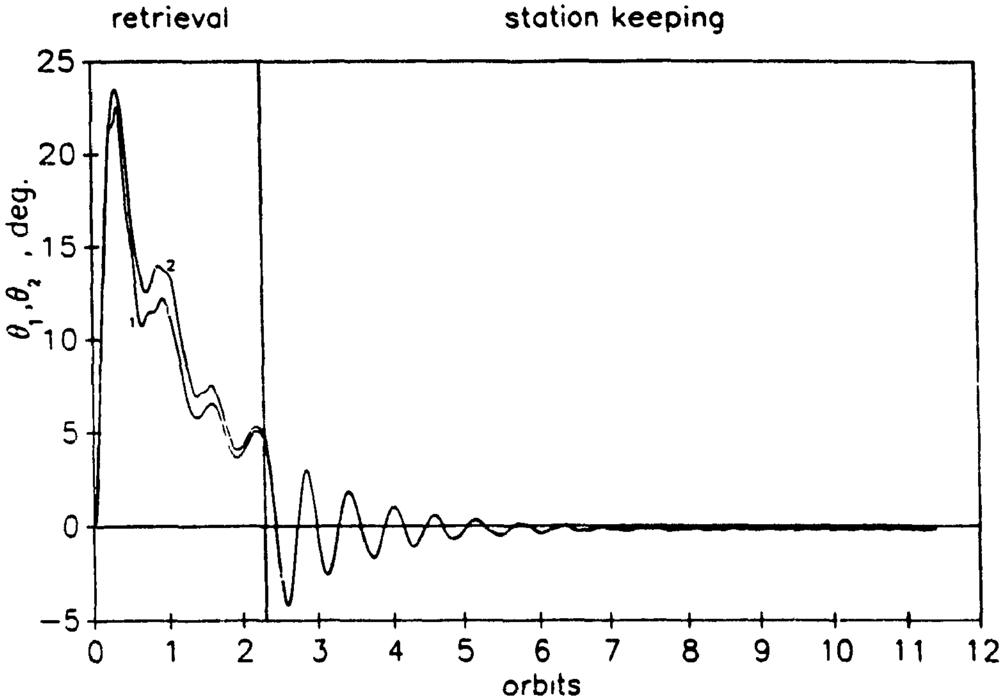

a) Pitch motion

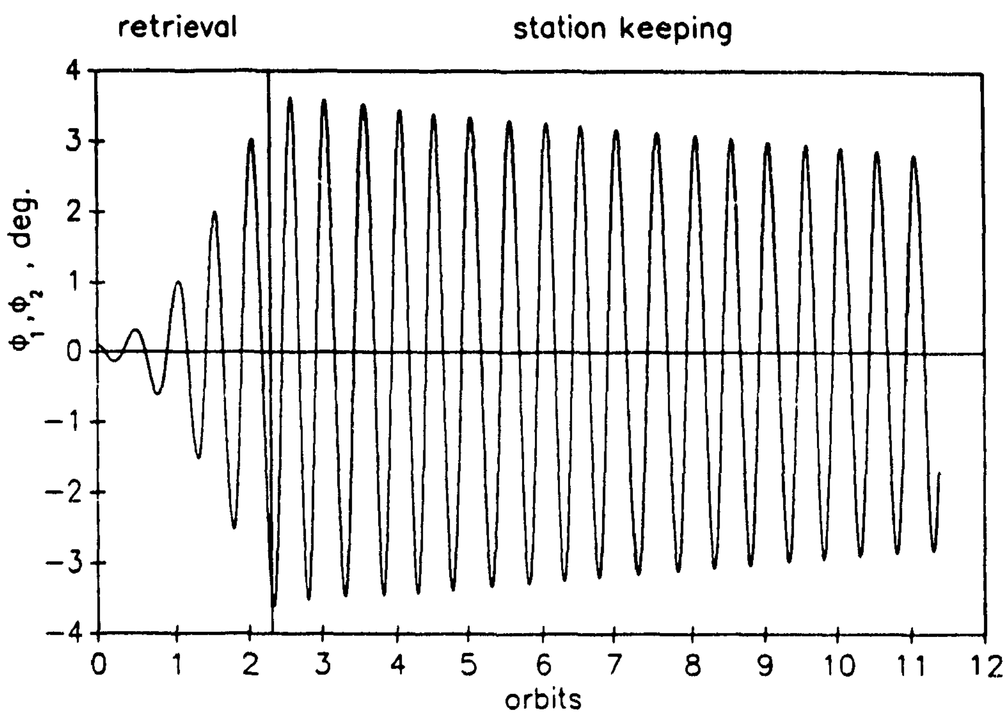

b) Roll motion

Fig. 4.13: Retrieval dynamics of a three-body system using the reel rate law of Eq. 4.63 for the case of: $K_{\theta_1} = 1.0$, $K_{\phi_1} = 3.0$, $K_{\theta_2} = 2.0$, $K_{\phi_2} = 9.0$, and other system parameters and initial conditions the same as Fig. 3.2.

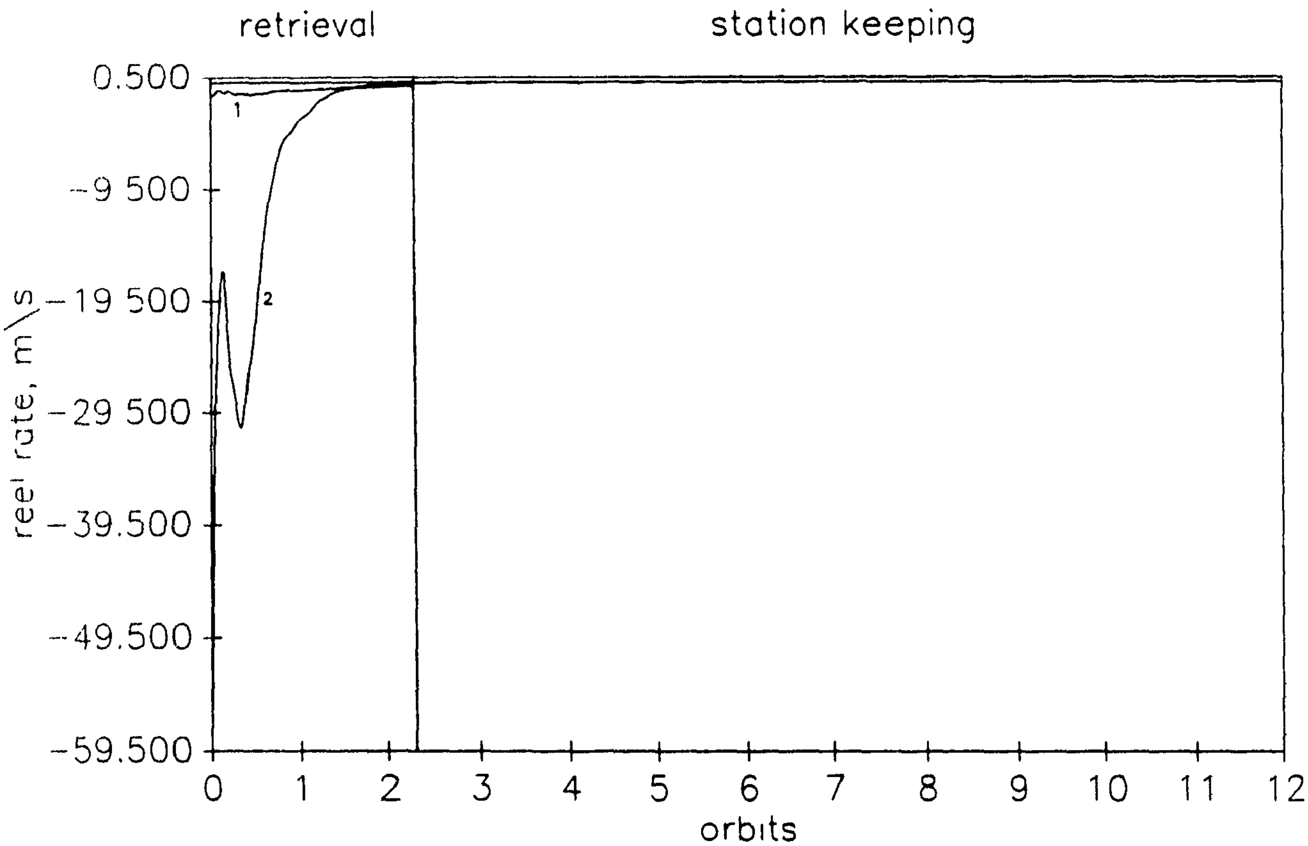

c) Variation of reel rate

Fig. 4.13 - Continued

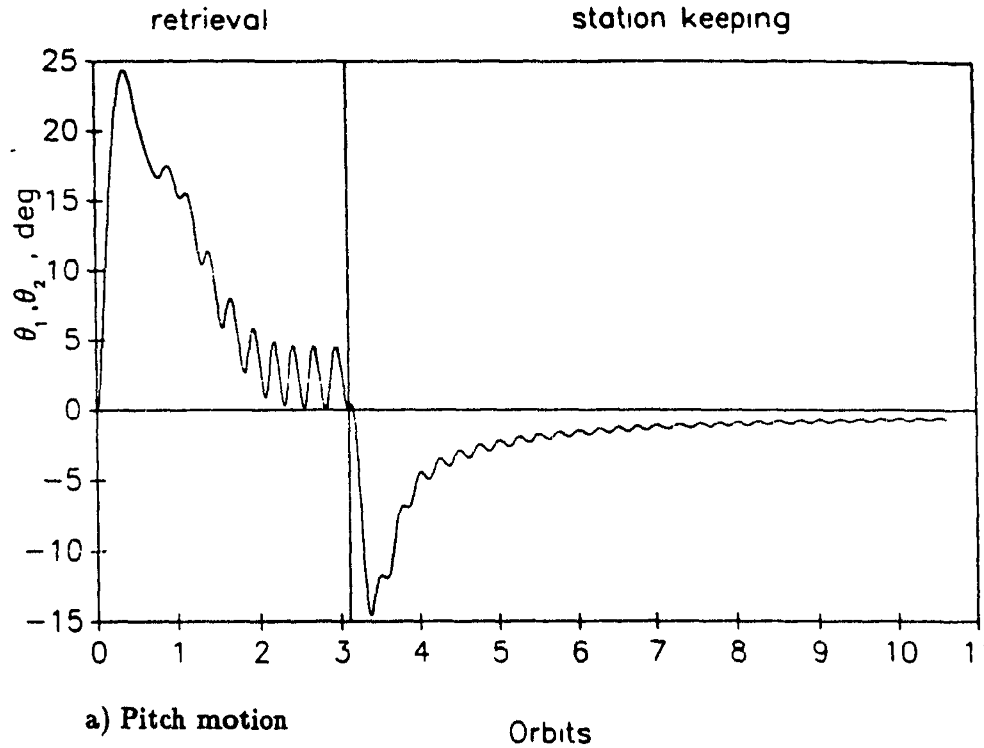

a) Pitch motion

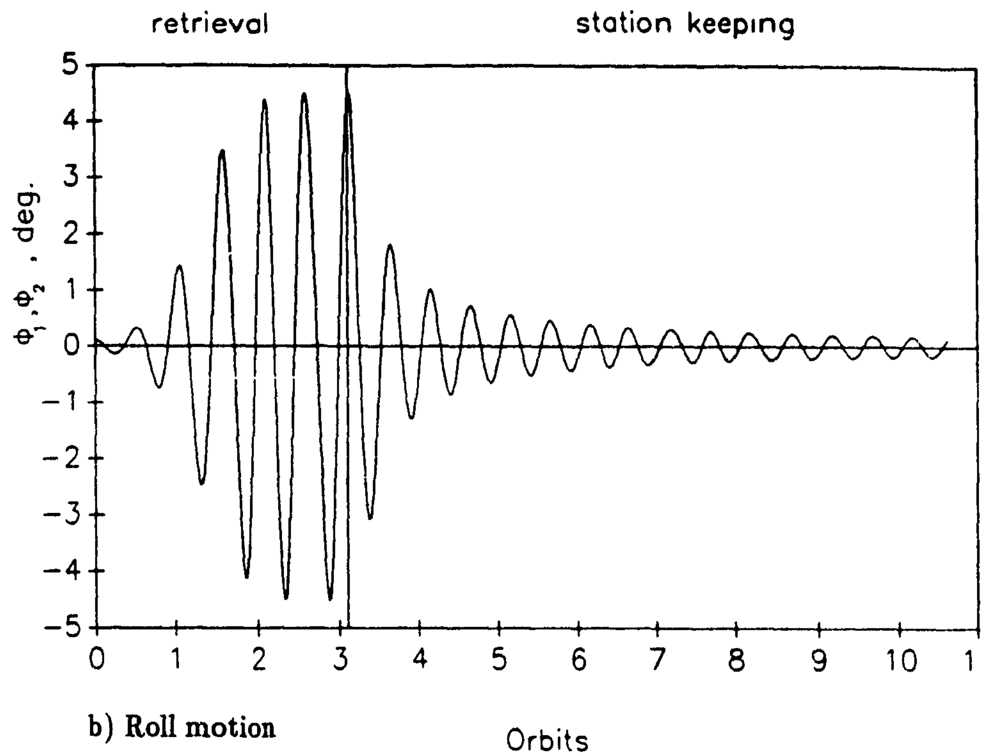

b) Roll motion

Fig. 4.14: Retrieval dynamics of a three-body system using the reel rate law of Eq. 4.64 and all system parameters and initial conditions the same as Fig. 4.12.

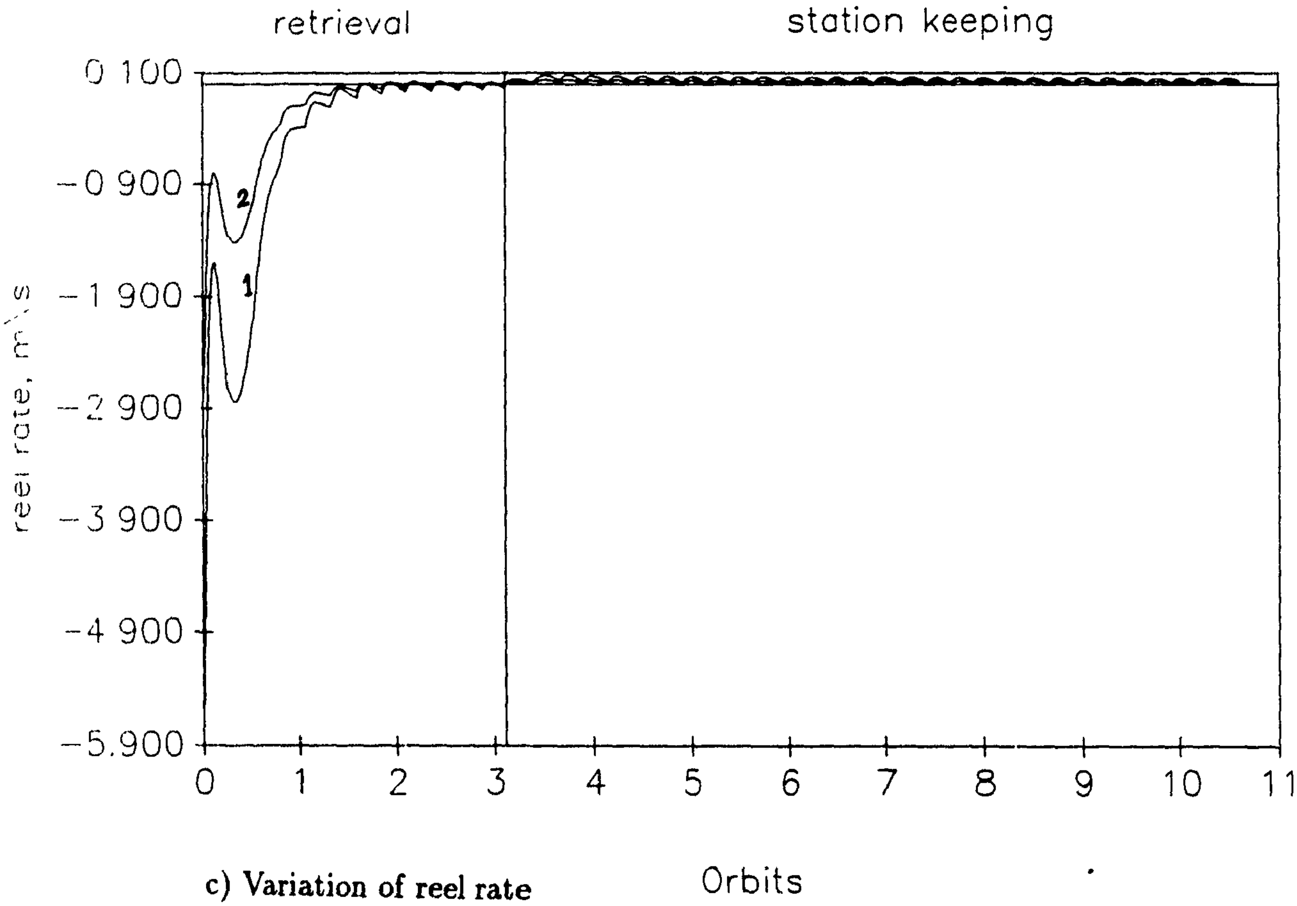

c) Variation of reel rate

Fig. 4.14 - Continued

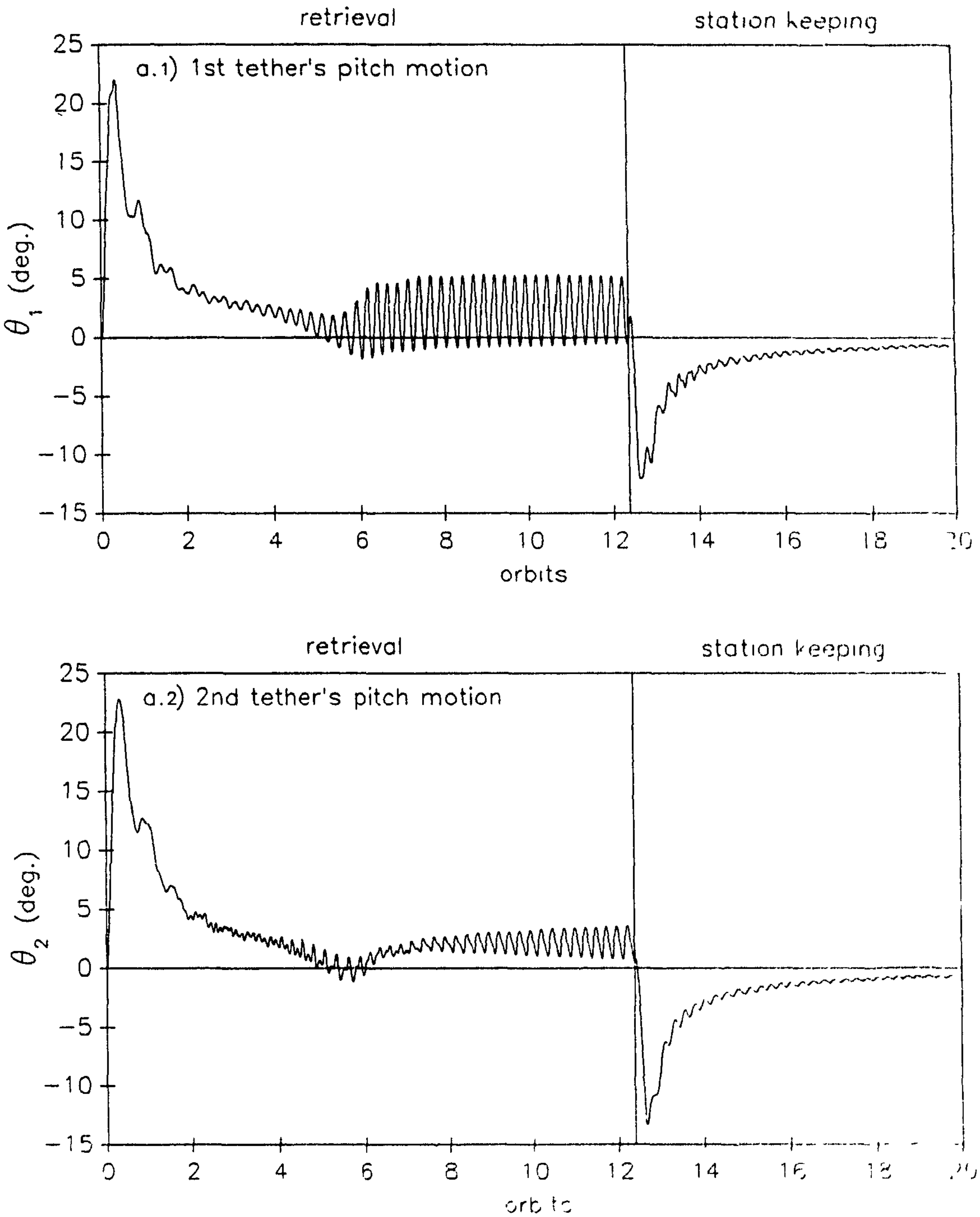

Fig. 4.15: Retrieval dynamics of a three-body system using the reel rate law of Eq. 4.64 and all system parameters and initial conditions the same as Fig. 4.13.

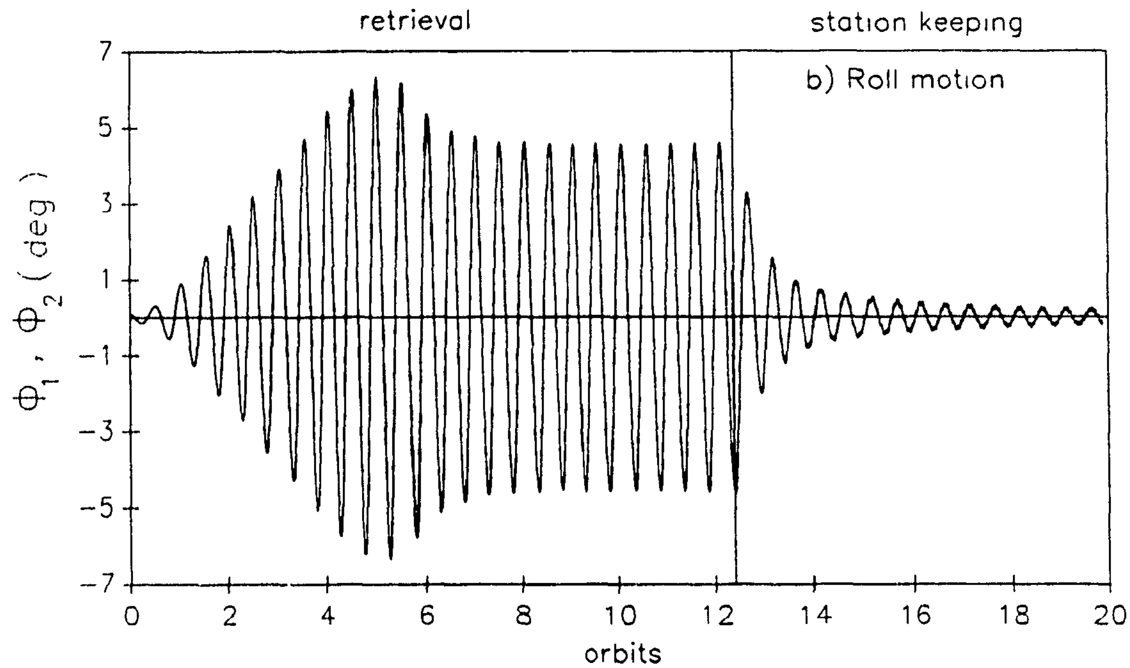

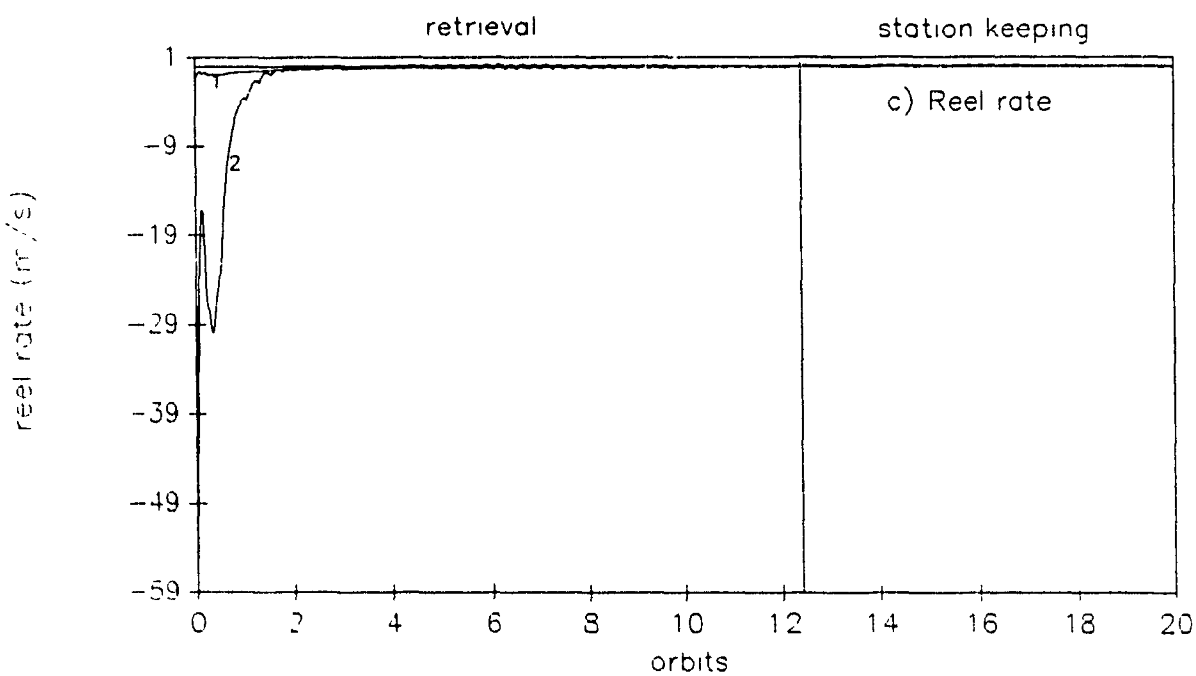

Fig. 4.15 - Continued

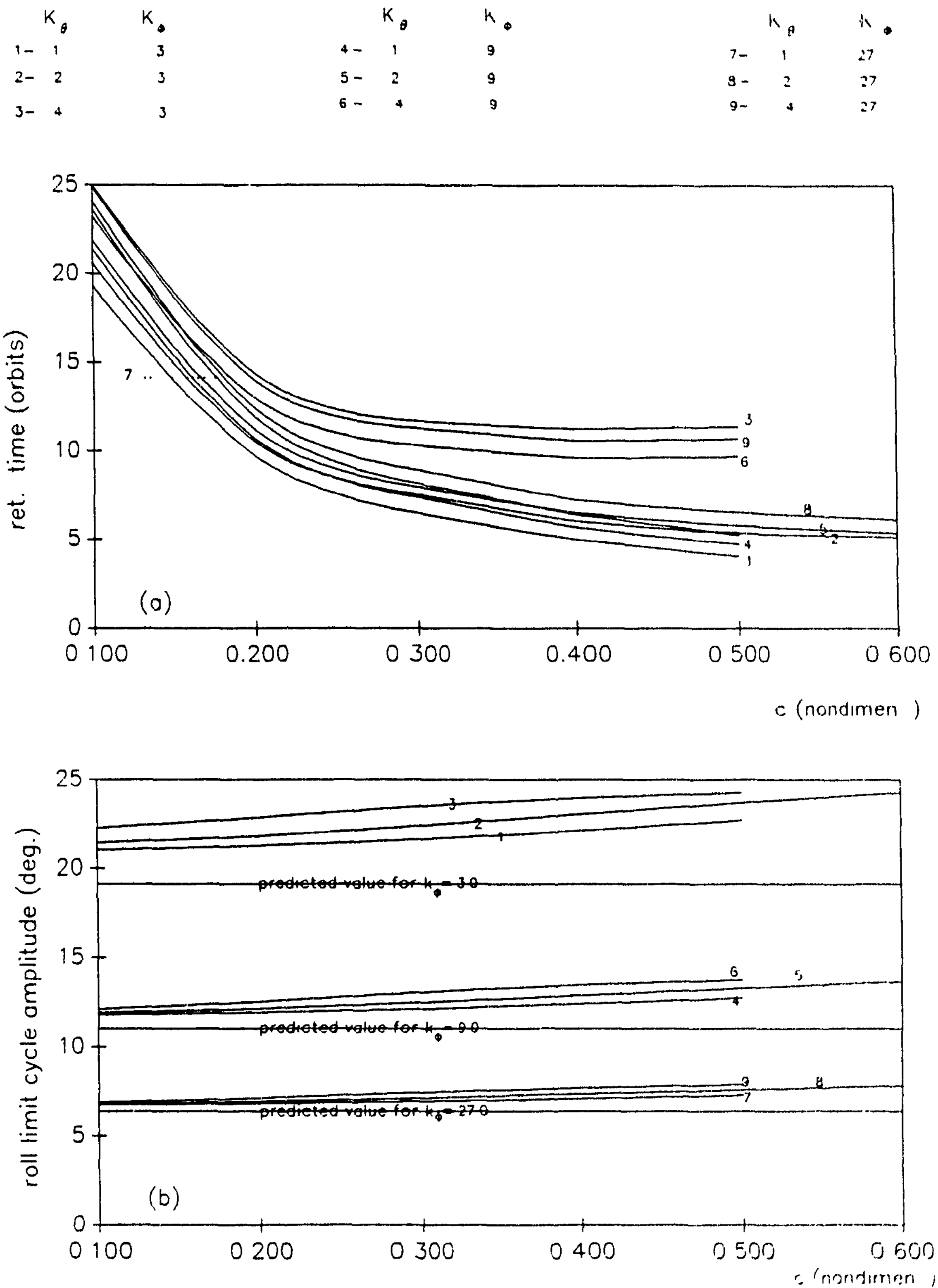

Fig. 4.16: The effect of retrieval constant c and control gains on the motion of a two-body system for the reel rate with quadratic roll rate feedback.

	K_θ	K_Φ		K_θ	K_Φ		K_θ	K_Φ
1-	1	3	4 -	1	9	7-	1	27
2-	2	3	5 -	2	9	8 -	2	27
3-	4	3	6 -	4	9	9-	4	27

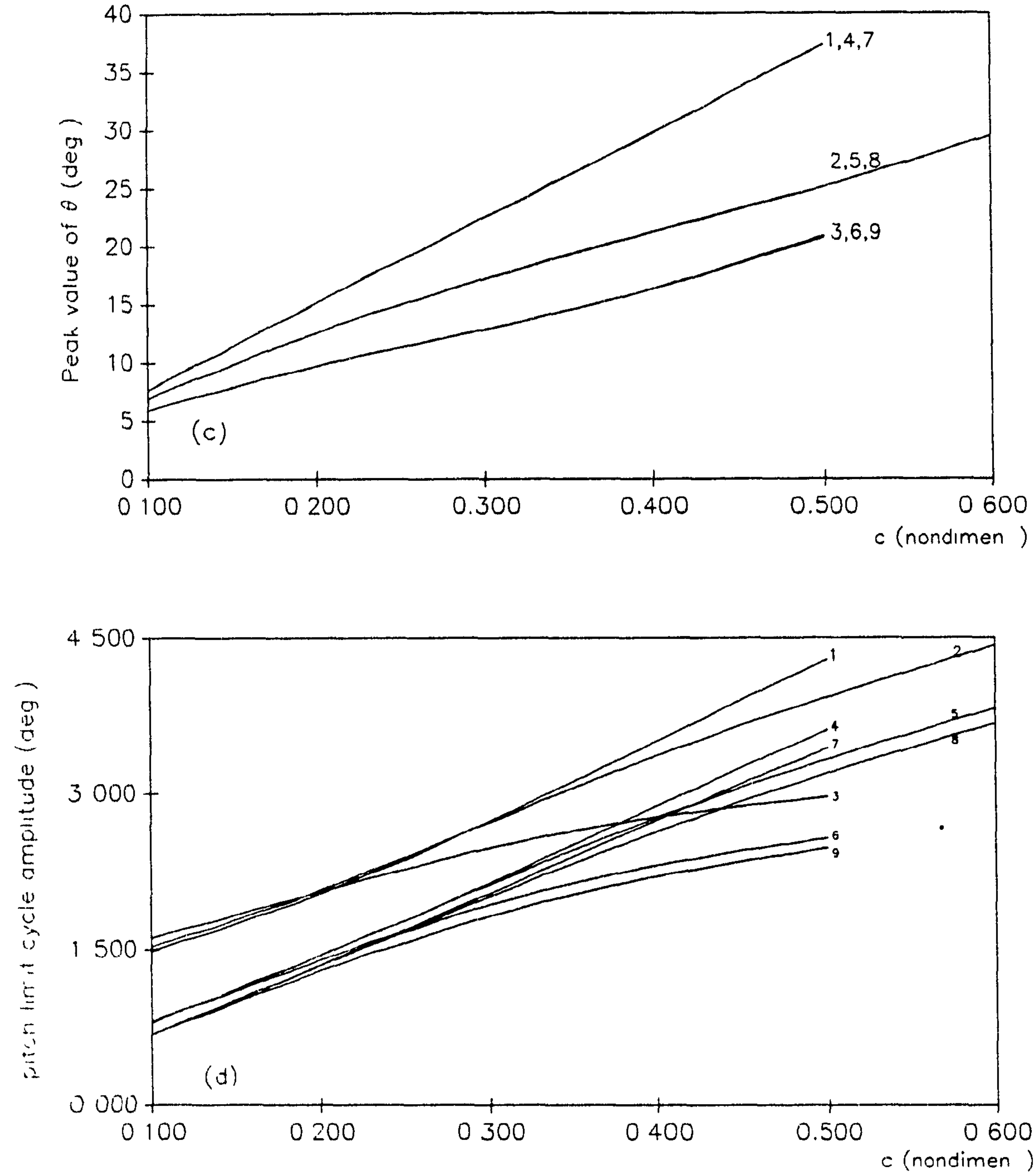

Fig. 4.16 - Continued

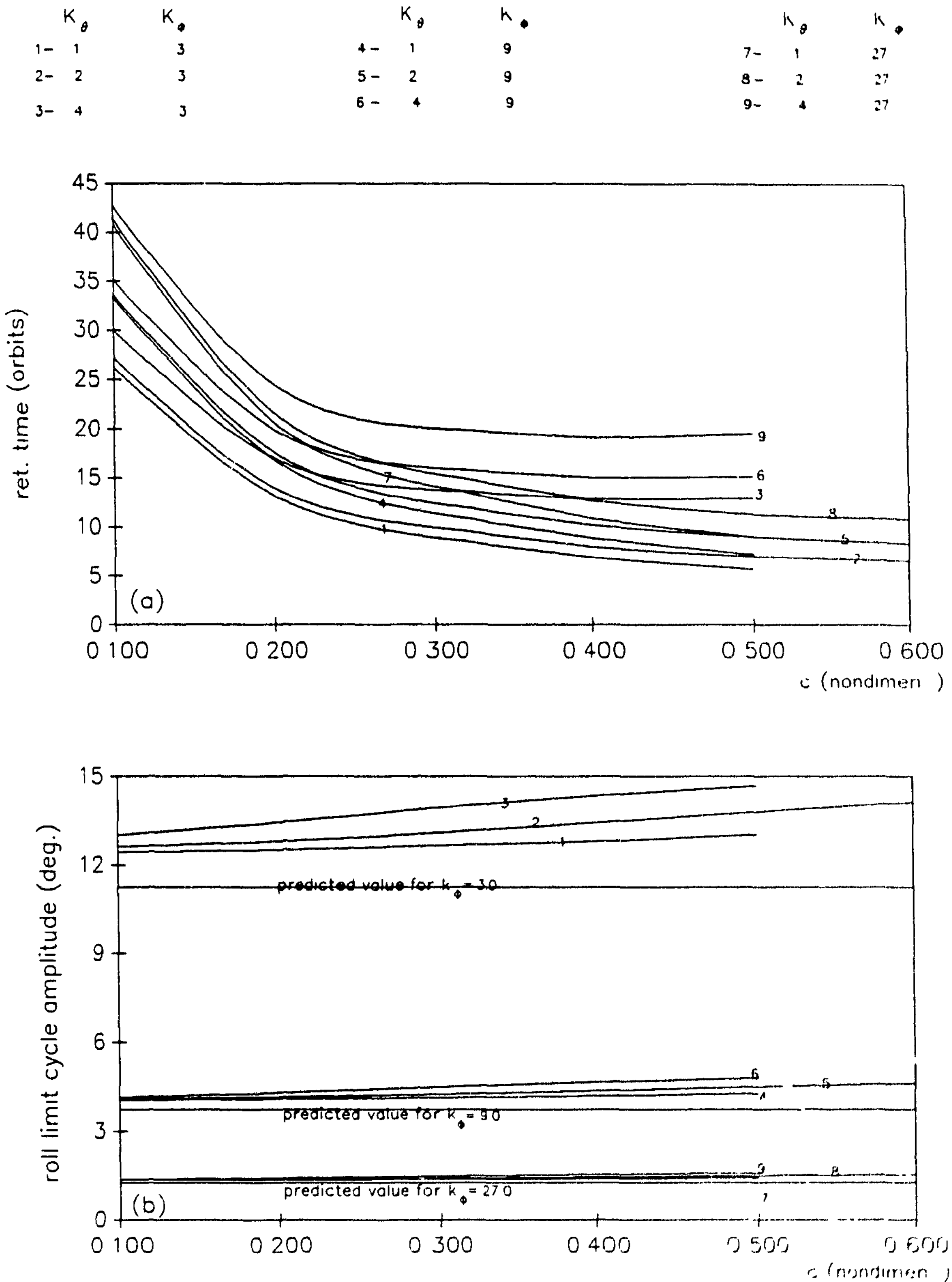

Fig. 4.17: The effect of retrieval constant c and control gains on the motion of a two-body system for the reel rate with absolute value roll rate feedback.

	K_θ	K_ϕ		K_θ	K_ϕ		K_θ	K_ϕ
1 –	1	3	4 –	1	9	7 –	1	27
2 –	2	3	5 –	2	9	8 –	2	27
3 –	4	3	6 –	4	9	9 –	4	27

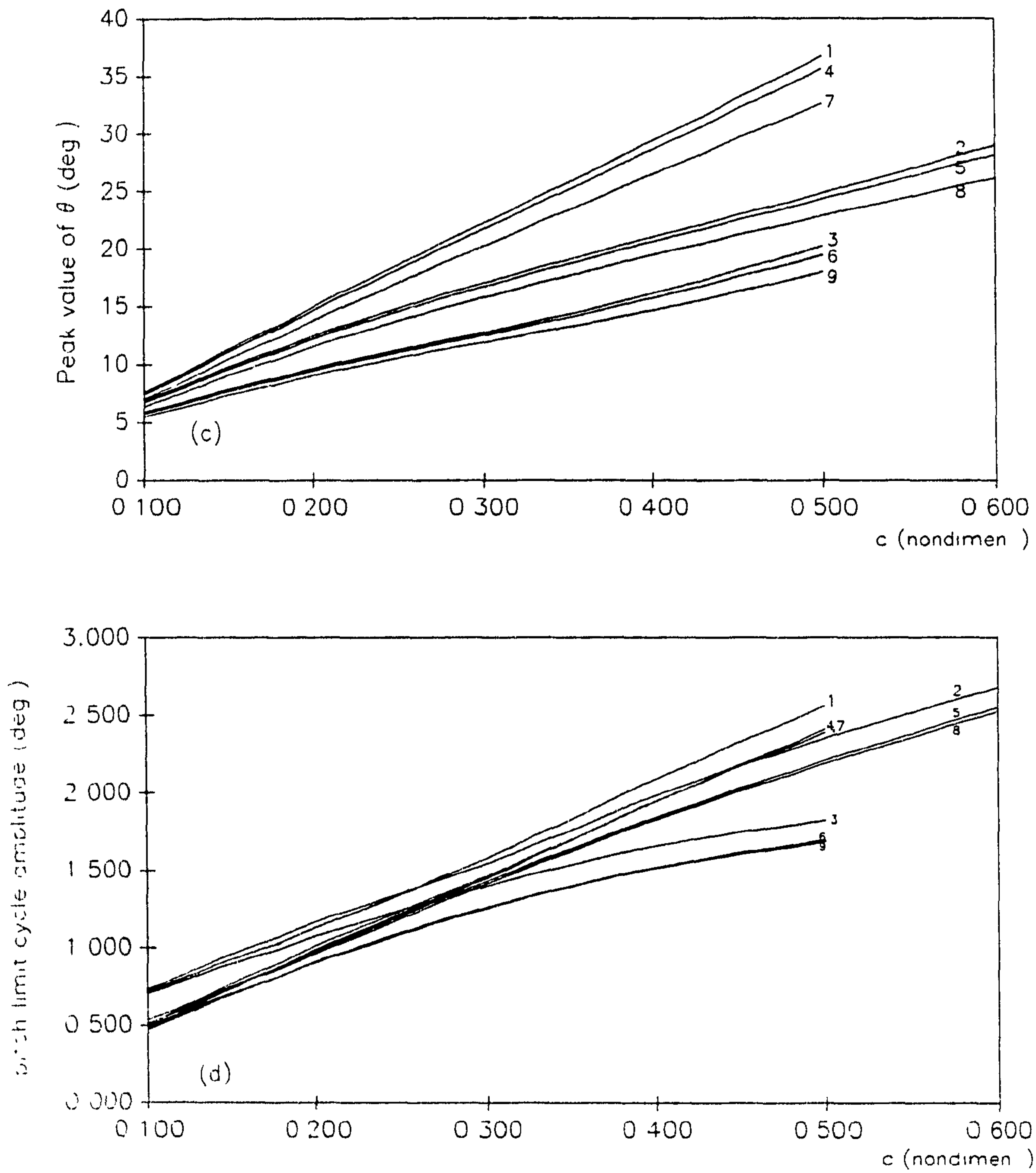

Fig. 4.17 - Continued

Appendix A

Applications of Tethered Satellite Systems

The applications of tethered satellites proposed by the early eighties have been documented by Bekey [1], and von Tiesenhausen [3]. In the second edition of the *Tethers In Space Handbook* [11], a rather recent and more complete up-date of these applications is available. Here we present a brief description of the important applications of the tethered satellites.[1]

A.1 Atmospheric and Aerodynamic Studies

The special advantage that can be mentioned for the applications of tethers in atmospheric studies is that orbiting the whole satellite inside the Earth's atmosphere will cause large drag forces and subsequently fast decay in the satellite altitude. But in the case of a tethered platform only the necessary parts will be sent to the atmosphere and most of the parts will be out of the Earth's atmo-

[1]The detailed explanation of the cases marked with * in this appendix was stated already in section 1.3 in the Introduction Chapter. They relate to multi-body tethered satellites.

sphere.

Applications of these tethered subsatellites for atmospheric and aerodynamic studies are listed below.

A.1.1 Shuttle connected hypersonic open wind tunnel

At an altitude of 250 km, the Shuttle orbits the Earth with the velocity of about 7755 m/sec . Consider a model tethered to the Shuttle and lowered to the altitude of 100–120 km . Then assuming that the atmosphere is rotating at the same angular velocity as the Earth, the relative velocity of the model to the atmosphere will be of the order of 7100 m/sec . This will result in a very high-velocity hypersonic flow around the model. The corresponding Mach number will be of the order of 26 (with velocity of sound about 276 m/sec at that altitude). At the same time very low Reynolds numbers are achievable, and this combination will make a very unique wind tunnel. If the necessary instruments for measuring different parameters like pressure, drag force, lift force, etc. be also deployed with the model we will have the Shuttle Continuous Open Wind Tunnel (SCOWT). In this way, the limitations that usually exist in ground-based wind tunnels will be eliminated, for example there will be no effect of the wall boundary layers.

A.1.2 Upper atmospheric measurements

Presently, atmospheric measurements in the region between 90 to 125 km altitudes can only be made with sounding rockets over small regions of area and time. By deploying a subsatellite tethered to the Shuttle very valuable research can be performed in this region. These subsatellites could also be tethered to the Space Station, but since the operational altitude of the Space Station is likely to be 500 km, the necessary tether will be rather lengthy. Thus, Shuttle-based tethered systems are preferable for atmospheric studies.

Some of the projects which are being studied include TSS–2 (Tethered Satellite Systems–2) and STARFAC (*Shuttle Tethered Aerothermodynamic Research Facility*) [11]. The Figure on page 37 of [11] can be considered as a general scheme for a Shuttle-based tethered system for atmospheric studies. *Collecting data at different locations simultaneously* is one the examples.

Gathering cosmic dust by sending a tethered subsatellite to the upper atmosphere from the Shuttle is also under consideration. The surface of the subsatellite contains numerous small collecting elements which would document the impact of cosmic dust or actually retain the particles for analysis back on the Earth.

A.2 Transportation Uses

A.2.1 Momentum exchange

Some applications in this area are described below:

One of the interesting ideas in this regard is to benefit from the momentum captured in a rocket spent stages. After one stage of a rocket reaches the end, before the start of the next stage, its center of gravity will follow a central force orbital motion (usually an elliptic orbit). If in this interval the spent stage be separated and tethered to the rest of the rocket and deployed down toward the Earth, since the center of gravity will maintain the same orbit as before, the rest of the rocket will move outward from the Earth. In this manner, the spent stage will lose some angular momentum and the rest of the rocket will gain it. When the deployment terminates the tether will be under tension. At the proper time the tether is disconnected which causes a deboost in the spent stage and a boost in the other parts of the rocket. This concept is practical only if the spent stage has a mass comparable to the mass of the rest of the rocket. The same principle can also be implemented to the Shuttle external tank.

The reverse situation is also considered in some cases. Boosting a satellite or platform or payload (generally an end mass) from the Shuttle to orbits higher than the orbit of the Orbiter itself. An end mass is deployed along a tether upward (away from the Earth) from the Shuttle. Librational motion begins and momentum is transferred from the Shuttle to the end mass; as a result, the end mass ascends and the Shuttle descends. Then the end mass will be released and placed into a higher orbit which simultaneously will give a deboost to the Orbiter. This process should be done at the end of the mission where the deboost in the Orbiter actually will be useful for its deorbiting to the Earth. In this way less fuel will be used both for the deployment of the satellite and deorbit of the Shuttle.

Now we concentrate on another application in the category of Transportation:

A.2.2 Tether assisted rendezvous

Maintenance of the previously deployed satellites from the Shuttle, can be mentioned in this category. A permanent tether attached to the Shuttle Orbiter is used to rendezvous with a decaying or defective satellite. A decaying satellite will be reboosted into a higher orbit and a defective satellite will be retrieved, repaired by the Shuttle crewmen, and reboosted to its initial orbit. This would eliminate the need to launch a replacement for defective or decaying satellite and decrease some of the expenses, but the project itself seems costly and it is under investigation. The Shuttle docking to and deorbit from the Space Station is also another example. The main point that can be mentioned for this project is that instead of coming back to the Earth's surface for the necessary services, the Shuttle can dock to the Space Station.

A.3 Gravity Related Applications

With the help of tethers one can create all kinds of artificial gravity laboratories and other gravity related facilities necessary for today's scientific and commercial studies. Some of the suggested designs are listed below

A.3.1 Wide range variable gravity laboratory

It is a tethered platform composed of two structures connected by a variable length tether. One end includes the solar arrays, related subsystems, and tether reel mechanism. The other includes two manned modules and a propellant motor. For generating the artificial gravity the tether will be extended, and then the whole system will be rotated about its center of mass by firing the motor. The solar panels should be de-spun. By changing the tether length one can get different gravity levels: from low gravity levels e.g. 0.08 g through 0.16 g simulating the gravity on the Moon, 0.38 g for Mars, g for Earth, and up to 2 g. The manned module can be a habitation module, for studying the long term effects of various artificial gravity levels on the human body and its feasibility for the interplanetary missions, or it can be a laboratory for scientific experiments. The coupling between the two structures could be done by a rigid linkage but the tethered connection is superior: firstly because the distance can be changed for getting different gravity levels; secondly, since we can set the length to very large values, with a less rotational rate we can get the desired g level and then the inconvenient side effects like Coriolis force would be less.

There are two designs associated with the Space Station explained in the following two subsections.

A.3.2 Microgravity laboratory*

A.3.3 Variable low-gravity laboratory*

A.3.4 Gravity wave detector*

A.4 Electrodynamic Applications

A.4.1 Power and thrust generation

DC electrical power can be generated at the expense of a spacecraft orbital energy. An insulated conducting tether, terminated at the ends by plasma contactors, is connected to the spacecraft (the Shuttle or any other spacecraft). The plasma contactors are for collecting electrons from the surrounding environment at one end and discharging them at the other end (for getting a better image, figure on page 53 of [11] may be consulted). Motion through the geomagnetic field induces a voltage in the tether. This voltage can be used to drive a DC electrical current in the tether. A force of the magnitude ($i\ell B$) will act as a drag force on the system. In this relation, i is the tether current, ℓ is the tether length, and B is the Earth's magnetic field flux density. Electrical power is generated at a rate equal to the loss in spacecraft orbital energy due to this induced drag. This project can be used also with spacecraft that are travelling to the planets with atmosphere and magnetic field such as Jupiter or Saturn.

If the process in the previous application is reversed, instead of the drag force we will have a thrust force which increases the orbital energy at the expense of primary on-board electric power.

This system can be used with combination of the two applications as a power storage. During the daytime the current from the on-board solar array power system is fed into the tether to generate a propulsive force. This thrust boosts the orbital altitude of the spacecraft. In the darkness periods, the system will act as a generator and DC electrical power is generated by reduction in the orbital altitude. This energy storage system has higher efficiency than a system involving charging and discharging of batteries. It will also reduce the size of arrays by 10% but the main reduction will be in the required batteries, which will make the weight of this supplementary system about 40% of the weight of conventional arrays and batteries system with similar performance. The heat rejection produced in power processing would also be reduced by 60 %.

A.4.2 Tether communications antenna*

A.5 Orbital Parameters Modification

A.5.1 Changing the orbital inclination

The inclination of the Shuttle's orbit (or of any other spacecraft's orbit near the Earth's atmosphere) can be changed by tethering a hypersonic lifting body below the Shuttle and sending it down to the atmosphere (tether length about 100 km). By shifting the body from one orientation to another a side force is generated which can be used to modify the inclination of the system's orbit.

A.5.2 Lowering the orbit of a planetary probe

Conventional planetary probes carry substantial propellant to establish low orbits about a celestial body of interest. With the help of tethers, for the case when the planet possesses an atmosphere, an alternate method reduces the necessary propellant to the amount required only to achieve a highly elliptical capture orbit. After achieving the elliptical orbit, a suspended body is deployed to the local vertical from the probe, using a small diameter tether. At each successive periapsis pass, the suspended body and the lower region of the tether experiences rarefied flow which creates drag on the system including the probe and reduces gradually the apoapsis until eventually the orbit is circularized. The suspended body could contain an instrument package for gathering data during the atmospheric passes.

A.5.3 Altering the orbit eccentricity

The necessity of a propulsion system for changing the eccentricity of the Space Station or a platform can be eliminated by applying a tethered system. An end mass is tethered to the Space Station or the platform. The length of the tether is changed in phase with the natural libration of the tether. If this sequential retrieval and deployment of the tether, which is known as *libration pumping*, is performed with proper timing, it can create the necessary change in eccentricity.

Appendix B

The Orbital Center of a Tethered Satellite System

In this Appendix we try to develop an expression for the location of the orbital center in tethered satellite systems. For the sake of simplicity we consider a circular orbit, but the same principle operates for non-circular orbits. As mentioned in the beginning of Chapter 2, the orbital center is the point where the resultant of the gravitational and centrifugal forces is zero. If the system consists only of one satellite modeled as a point mass, the point mass itself is the orbital center. For this orbiting body the amount of gravitational force is equal to

$$F_g = -\mathrm{GM}_e m/r^2 \quad , \tag{B.1}$$

where GM_e is the gravitational constant of the Earth, m the mass of the body, and r its distance from the center of the Earth. The centrifugal force on the body is

$$F_c = mr\Omega^2 \quad , \tag{B.2}$$

where Ω is the orbital angular velocity. The total force in the x direction (refer to definition of axes in Chapter 2) will be

$$F_x = F_g + F_c \quad . \tag{B.3}$$

If the body's orbit is a circle, this total force in the x direction should be zero, i.e., [52]

$$mr\Omega^2 - \mathrm{GM}_e m/r^2 = 0 \quad ,$$

or

$$\Omega^2 = \mathrm{GM}_e/r^3 \quad . \tag{B.4}$$

For a multi-body tethered system, all of the points have the same orbital angular velocity. By noticing Eqs. B.1 and B.2 we can see that the masses which are closer to the Earth are subjected to more downward gravitational force than the outer masses, and the situation is reverse for the centrifugal forces. As a result, for the lower masses there is a net force toward the Earth and for the outer masses there will be an outward net force. These result in the tethers being under tension. The magnitude of the angular velocity Ω which maintains a circular orbit is such that the resultant of the total gravitational and centrifugal forces acting on the system should be zero. Then ignoring the tethers masses we should get

$$\sum_{i=1}^{N} F_{g_i} = \sum_{i=1}^{N} F_{c_i} \quad , \tag{B.5}$$

or

$$\frac{GM_e m_1}{r_1^2} + \frac{GM_e m_2}{r_2^2} + \cdots + \frac{GM_e m_N}{r_N^2} = m_1 r_1 \Omega^2 + m_2 r_2 \Omega^2 + \cdots + m_N r_N \Omega^2 \quad . \quad \text{(B.6)}$$

This yields

$$\Omega^2 = GM_e \left(\frac{\sum_{i=1}^{N} m_i / r_i^2}{\sum_{i=1}^{N} m_i r_i} \right) \quad . \quad \text{(B.7)}$$

Now the orbital center is the point where, if the whole mass of the system was concentrated, the resultant of the forces acting would be zero. Therefore referring to Eq. B.4 if we call the $R_{O.C.}$ as the radius of orbital center, the orbital angular velocity will be equal to

$$\Omega^2 = GM_e / R_{O.C.}^3 \quad . \quad \text{(B.8)}$$

From Eqs. B.7 and B.8 one gets

$$R_{O.C.} = \left(\frac{\sum_{i=1}^{N} m_i r_i}{\sum_{i=1}^{N} m_i / r_i^2} \right)^{1/3} \quad . \quad \text{(B.9)}$$

This equation expresses the location of the orbital center for a tethered satellite system with N number of bodies.